

Universidade Federal de Juiz de Fora  
Engenharia Elétrica  
Programa de Pós-Graduação em Engenharia Elétrica

**Victor Fernandes**

**Analyses of a Low-Bit Rate Hybrid PLC-Wireless Single-Relay Channel**

Juiz de Fora  
2017

Ficha catalográfica elaborada através do Modelo Latex do CDC da  
UFJF com os dados fornecidos pelo(a) autor(a)

Fernandes, Victor.

Analyses of a Low-Bit Rate Hybrid PLC-Wireless Single-Relay Channel / Victor Fernandes. – 2017.

84 f. : il.

Orientador: Moisés Vidal Ribeiro

Dissertação de Mestrado – Universidade Federal de Juiz de Fora, Engenharia Elétrica. Programa de Pós-Graduação em Engenharia Elétrica, 2017.

1. Comunicação via rede de energia elétrica. 2. Comunicação sem fio. 3. Híbrido. 4. Taxa de dados. I. Vidal Ribeiro, Moisés, orient. II. Título.

**Victor Fernandes**

**Analyses of a Low-Bit Rate Hybrid PLC-Wireless Single-Relay Channel**

Dissertação de mestrado apresentada ao Programa de Pós-Graduação em Engenharia Elétrica da Universidade Federal de Juiz de Fora, na área de concentração em sistemas eletrônicos, como requisito parcial para obtenção do título de Mestre em Engenharia Elétrica.

Orientador: Moisés Vidal Ribeiro

Juiz de Fora

2017

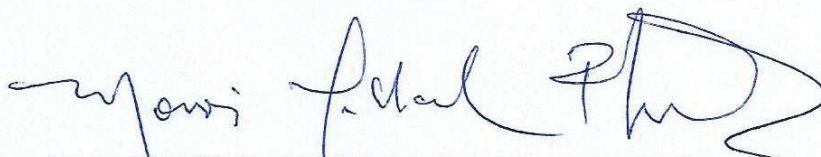
Victor Fernandes

Analyses of a Low-Bit Rate Hybrid PLC-Wireless Single-Relay Channel

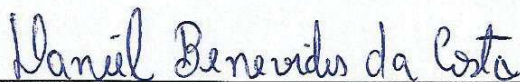
Dissertação de mestrado apresentada ao Programa de Pós-Graduação em Engenharia Elétrica da Universidade Federal de Juiz de Fora, na área de concentração em sistemas eletrônicos, como requisito parcial para obtenção do título de Mestre em Engenharia Elétrica.

Aprovada em: 23/02/17

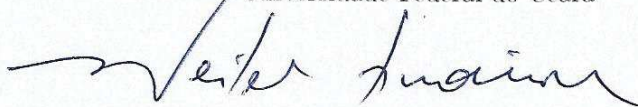
BANCA EXAMINADORA



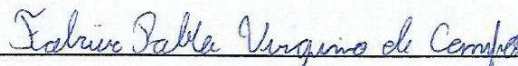
Prof. Dr. Moisés Vidal Ribeiro - Orientador  
Universidade Federal de Juiz de Fora



Prof. Dr. Daniel Benevides da Costa  
Universidade Federal do Ceará



Prof. Dr. Weiler Alves Finamore  
Universidade Federal de Juiz de Fora



Prof. Dr. Fabrício Pablo Virgínio de Campos  
Universidade Federal de Juiz de Fora

*Dedico este trabalho aos meus pais Sebastião e Maria Helena, aos meus irmãos Thiago e Diogo e a minha namorada Máxime*

## AGRADECIMENTOS

Agradeço primeiro a Deus, por sempre estar comigo.

Aos meus pais Sebastião Fernandes da Silva Neto e Maria Helena dos Santos Fernandes, pelo exemplo e apoio incondicional que sempre me deram.

Aos meus irmãos Thiago Fernandes e Diogo Fernandes, por todo suporte e companheirismo.

A minha amada Máxime Teixeira Rezende, pelo amor, carinho, amizade e apoio incondicionais.

Ao professor Moisés Vidal Ribeiro, por todo suporte, orientação e incentivo.

Ao professor Weiler Alves Finamore, pela orientação e apoio.

Aos colegas de laboratório, pelas longas conversas de muito aprendizado.

“A fool thinks himself to be wise, but a wise man knows himself to be a fool.”  
(William Shakespeare)

## RESUMO

Essa dissertação tem por objetivo mostrar os benefícios em termos de desempenho e confiabilidade de um modelo de canal híbrido de baixa taxa de dados que pode ser aplicado a *smart grids* e internet das coisas. Esse modelo é chamado de *hybrid power line communication-wireless single-relay channel* (HSRC), que consiste do uso paralelo e mútuo dos modelos *single-relay channel* baseado em transmissão de dados via rede elétrica e sem fio. Para mostrar os benefícios do mesmo, foi considerado que a posição do nó de retransmissão é variável, também foi assumida alocação de potência uniforme e ótima sob restrição de potência, bem como o uso de dois protocolos de cooperação: *amplify-and-forward* (AF) e *decode-and-forward* (DF). Além disso, essa dissertação discute o modelo HSRC incompleto, que é caracterizado pela perda de um enlace de comunicação de dados ou uma interface de comunicação de um nó no modelo HSRC. Primeiramente, foi apresentada a formulação matemática no que tange a taxa de dados ergódica e probabilidade de *outage* dos dois modelos mencionados. Em seguida, foi realizada a análise numérica dos mesmos. Por fim, os resultados numéricos foram analisados e mostraram que tanto o HSRC quanto o HSRC incompleto têm performance melhores do que o *single-relay channel* baseado em transmissão de dados via rede elétrica ou sem fio para todas as posições do nó de retransmissão e protocolos de cooperação considerados. Também, os resultados mostraram que a posição relativa entre os nós de fonte, destino e de retransmissão impactam significativamente na taxa de dados ergódica bem como na probabilidade de *outage*. Ainda, foi mostrado o impacto da perda de cada enlace de comunicação de dados ou interface de comunicação de um nó (HSRC incompleto) quando a posição relativa do nó de retransmissão muda. Por último, é mostrado que a diferença de desempenho entre os protocolos de cooperação AF e DF reduz quando o modelo HSRC é utilizado e que a melhor posição para o nó de retransmissão é entre os nós fonte e destino em termos de taxa de dados ergódica.

Palavras-chave: Comunicação via rede de energia elétrica. Comunicação sem fio. Modelo de canal híbrido. Taxa de dados ergódica. Probabilidade de *outage*.

## ABSTRACT

This dissertation aims at discussing improvements of performance and reliability of low-bit rate data communication technologies applied to smart grids and internet of things. In this regard, a comprehensive analysis of the ergodic achievable data rate and the outage probability of the so-called low-bit rate hybrid power line communication-wireless single-relay channel (HSRC) model, which jointly and in parallel uses power line and wireless channels for data transmission, is presented. In order to highlight the benefits of such hybrid channel model for the target applications when the relative position of relay node changes, optimal and uniform power allocations under sum power constraint, amplify-and-forward (AF) and decode-and-forward (DF) cooperative protocols are taken into account. Moreover, this dissertation discusses the so-called incomplete HSRC which is characterized by the loss of one data communication link or node communication interface in a HSRC. Numerical results show that the HSRC and incomplete HSRC remarkably outperform power line or wireless single-relay channels for all considered positions of the relay node and the chosen cooperative protocols. Furthermore, these results show that the relative distances among source, relay and destination nodes significantly impact the achievable data rate and outage probabilities. In addition, the impact of each missing data communication link or node communication interface (incomplete HSRC) when the relay position, relative to source and destination nodes, changes is quantified. Finally, but not the least, it is shown that the performance difference between AF and DF protocols reduces when the HSRC model is taken into account and that the best relay position is in the middle between source and destination nodes.

Key-words: power line communication, wireless communication, hybrid channel model, achievable data rate, outage probability.

## LIST OF FIGURES

Figure 1 – Hybrid PLC-wireless single-relay channel model. . . . .	19
Figure 2 – The HSRC without $SD^q$ , for (a) $q = P$ and (b) $q = W$ . . . . .	30
Figure 3 – The HSRC without $SR^q$ , for (a) $q = P$ and (b) $q = W$ . . . . .	30
Figure 4 – The HSRC without $RD^q$ , for (a) $q = P$ and (b) $q = W$ . . . . .	31
Figure 5 – The HSRC without $S^q$ , for (a) $q = P$ and (b) $q = W$ . . . . .	32
Figure 6 – The HSRC without $R^q$ , for (a) $q = P$ and (b) $q = W$ . . . . .	32
Figure 7 – The HSRC without $D^q$ , for (a) $q = P$ and (b) $q = W$ . . . . .	33
Figure 8 – The R node position regions varying $\alpha$ and $\beta$ . . . . .	41
Figure 9 – The R node position varying parameters $\alpha$ and $\beta$ . . . . .	44
Figure 10 – case #1: $\rho_a^b$ vs $\alpha$ , in which $a$ and $b$ are (a) $b$ in the legend, $P = 1$ mW (-- ) and $P = 100$ mW (—). . . . .	45
Figure 11 – case #2: $\rho_a^b$ vs $\alpha$ , in which $a$ and $b$ are (a) $b$ in the legend, $P = 1$ mW (-- ) and $P = 100$ mW (—). . . . .	46
Figure 12 – case #3: $\rho_a^b$ vs $\alpha$ , in which $a$ and $b$ are (a) $b$ in the legend, $P = 1$ mW (-- ) and $P = 100$ mW (—). . . . .	47
Figure 13 – $\rho_a^b$ vs $P$ , in which $a$ and $b$ are (a) $b$ in the legend, when assuming optimal power allocation (OA). . . . .	49
Figure 14 – Outage probability for the HSRC when $\alpha = 1$ , case #1 ( $\beta = 1$ ). UA (top) and OA (bottom) are adopted. Also, the values of total transmis- sion power ( $P$ ) are highlighted. . . . .	50
Figure 15 – Outage probability for the HSRC when $\alpha = 1$ , case #2 ( $\beta = 10$ ). UA (top) and OA (bottom) are adopted. Also, the values of total transmission power ( $P$ ) are highlighted. . . . .	51
Figure 16 – Outage probability for the HSRC when $\alpha = 1$ , case #3 ( $\beta = 1/10$ ). UA (top) and OA (bottom) are adopted. Also, the values of total transmission power ( $P$ ) are highlighted. . . . .	52
Figure 17 – $\varrho_{AF}^b$ vs $\alpha$ for the HSRC without a link, PSRC, and WSRC. . . . .	54
Figure 18 – $\varrho_{DF}^b$ vs $\alpha$ for the HSRC without a link, PSRC, and WSRC. . . . .	57
Figure 19 – $\varrho_{AF}^b$ vs $\alpha$ for the HSRC without a node communication interface, PSRC, and WSRC. . . . .	59
Figure 20 – $\varrho_{DF}^b$ vs $\alpha$ for the HSRC without a node communication interface, PSRC, and WSRC. . . . .	61
Figure 21 – Outage probability for the HSRC without a link when $\alpha = 1$ . . . . .	63
Figure 22 – Outage probability for the HSRC without a node communication inter- face when $\alpha = 1$ . . . . .	64
Figure 23 – The HSRC without $SD^q$ , for (a) $q = P$ and (b) $q = W$ . . . . .	72
Figure 24 – The HSRC without $SR^q$ , for (a) $q = P$ and (b) $q = W$ . . . . .	74
Figure 25 – The HSRC without $RD^q$ , for (a) $q = P$ and (b) $q = W$ . . . . .	76

Figure 26 – The HSRC without $S^q$ , for (a) $q = P$ and (b) $q = W$ . . . . .	78
Figure 27 – The HSRC without $R^q$ , for (a) $q = P$ and (b) $q = W$ . . . . .	80
Figure 28 – The HSRC without $D^q$ , for (a) $q = P$ and (b) $q = W$ . . . . .	82

## LIST OF TABLES

Table 1 – Adopted values of the parameters used in the NB-PLC channel model. . 39

Table 2 – Adopted values of the parameters used in LP-RF wireless channel model. 41

## ACRONYMS

<b>2WSRC</b>	two LP-RF wireless SRC
<b>AF</b>	amplify-and-forward
<b>BER</b>	bit error rate
<b>CIR</b>	channel impulse response
<b>CSI</b>	channel state information
<b>DF</b>	decode-and-forward
<b>HSRC</b>	hybrid PLC-wireless single-relay channel
<b>IoT</b>	internet of things
<b>LGRC</b>	linear Gaussian relay channel
<b>LP-RF</b>	low-power radio frequency
<b>NB</b>	narrowband
<b>nSNR</b>	normalized signal-to-noise ratio
<b><i>N</i>-CGRC</b>	<i>N</i> -block memoryless circular Gaussian relay channel
<b><i>N</i>-LGRC</b>	<i>N</i> -block LGRC
<b>OA</b>	optimal power allocation
<b>OFDM</b>	orthogonal frequency division multiplexing
<b>pdf</b>	probability density function
<b>PLC</b>	power line communication
<b>PSD</b>	power spectral density
<b>PSRC</b>	PLC SRC
<b>r.v.</b>	random variable
<b>SG</b>	smart grid
<b>SRC</b>	single-relay channel
<b>UA</b>	uniform power allocation
<b>WF</b>	water filling
<b>WSRC</b>	wireless SRC

# CONTENTS

<b>1</b>	<b>Introduction . . . . .</b>	<b>14</b>
1.1	Objectives . . . . .	16
1.2	Dissertation outline . . . . .	16
<b>2</b>	<b>Hybrid PLC-Wireless Single-Relay Channel Model . . . . .</b>	<b>18</b>
2.1	The Hybrid Single-Relay Channel . . . . .	18
2.1.1	The Achievable Data Rate . . . . .	21
2.1.2	Limit Analyses of HSRC, PSRC, and WSRC . . . . .	24
2.1.3	The Outage Probability . . . . .	28
2.2	The Incomplete Hybrid Single-Relay Channel . . . . .	29
2.2.1	The Incomplete HSRC: Achievable Data Rate . . . . .	29
2.2.1.1	The HSRC without a link . . . . .	30
2.2.1.2	The HSRC without one node communication interface . . . . .	31
2.2.2	Limit Analyses of the Incomplete HSRC . . . . .	33
2.2.3	The Outage Probability . . . . .	35
2.2.3.1	The HSRC without a link . . . . .	36
2.2.3.2	The HSRC without one communication interface . . . . .	36
<b>3</b>	<b>Numerical Results . . . . .</b>	<b>38</b>
3.1	The HSRC model . . . . .	41
3.1.1	The Achievable Data Rate . . . . .	43
3.1.2	The Outage Probability . . . . .	49
3.2	The Incomplete HSRC . . . . .	51
3.2.1	The Achievable Data Rate . . . . .	52
3.2.1.1	The Incomplete HSRC: The HSRC without a link . . . . .	53
3.2.1.2	The Incomplete HSRC: The HSRC without one node communication interface . . . . .	58
3.2.2	The Outage Probability . . . . .	62
3.2.2.1	The Incomplete HSRC: The HSRC without a link . . . . .	62
3.2.2.2	The Incomplete HSRC: The HSRC without one node communication interface . . . . .	62
<b>4</b>	<b>Conclusion . . . . .</b>	<b>65</b>
4.1	Future Works . . . . .	66

REFERENCES . . . . .	68
Appendix A – Achievable Data Rate: The HSRC without $SD^q$	72
Appendix B – Achievable Data Rate: The HSRC without $SR^q$	74
Appendix C – Achievable Data Rate: The HSRC without $RD^q$	76
Appendix D – Achievable Data Rate: The HSRC without $S^q$	78
Appendix E – Achievable Data Rate: The HSRC without $R^q$	80
Appendix F – Achievable Data Rate: The HSRC without $D^q$	82
Appendix G – Publications . . . . .	84

## 1 Introduction

The recent worldwide interest in turning the electric power grids into a smart grid (SG) has been leading investigations to improve the performance of power line communication (PLC) systems, which are one of the main data communications technology for accomplishing this aim [1]. On the other hand, one may say that the wireless communications are a more established alternative for this purpose. However, it is widely recognized that the SG will be supported by a heterogeneous set of networking technologies, as no single solution fits all scenarios [2]. As PLC technology is the only one that has deployment cost comparable to that of wireless since no new infrastructure is needed, narrowband, or low-bit rate, PLC (NB-PLC) and unlicensed wireless communications are considered as the two leading data communication technologies for SG applications [3] as well as internet of things (IoT) [4].

Regarding PLC, it can be stated that electric power grids are a challenging data communication media because they were designed to maximize energy delivery [5]. As a consequence, the propagation of signal carrying information can be severely degraded due to dynamic of loads, impedance mismatching, signal attenuation, power line breaks, unshielded power lines, and high power impulsive noise presence [6–9]. Therefore, to avoid these issues the PLC data communication is preferably realized using orthogonal frequency division multiplexing (OFDM) technique [10]. To characterize the impact of such medium over transmitted information, several measurement setups and methodologies are being developed to estimate time and frequency behavior of PLC channels and to statistically characterize the additive noise [11–17].

On the other hand, it is well-known that in the wireless communication the transmitted signal suffers three different propagation effects: *reflection*, *scattering*, and *diffraction* [18]. The first effect appears when the propagation wave meets a very large object in comparison to its wavelength. On the contrary, scattering happens when the propagation wave meets a very small object in comparison to its wavelength. Lastly, diffraction occurs when the signal passes through a sharpened object and it is responsible for making possible the non-line-of-sight (NLOS) communications. Besides the distortions introduced by the aforementioned propagation, the transmitted signal through wireless channel suffers interference, which is primarily generated from uncoordinated transmissions [19].

In order to overcome the problems experienced in the wireless communication and to fulfill the increasing demand for higher data rate, coverage, and reliability, the investigation of advanced techniques that remarkably increase the efficient use of the available bandwidths is a challenging issue to be pursued. In this regard, cooperative communication was introduced [20]. Initially, cooperative communication was addressed in the wireless communication field to achieve diversity and to improve reliability [21–

23]. Currently, cooperative communication is being investigated to improve PLC system performance, in which the focus is more related to the physical layer [24–27] than the link layer [28]. In relation to cooperative communication, some main advantages of using it are the performance gains, infrastructure-less deployment, and reduced costs. On the opposite, the main disadvantages of cooperation are related to complex synchronization process between the nodes of the system, extra relay traffic, increased interference and channel estimations [29]. Although reliability improvement on the power line and wireless communications is attained with the use of cooperative protocols, the exploitation of the existing diversity between both power line and wireless channels [3, 19, 30] can benefit SG and IoT applications.

Concerning the exploitation of the existing diversity between both power line and wireless channels, [31] briefly discussed advantages and disadvantages of NB-PLC and low-power radio frequency (LP-RF) wireless for the European, American, and Latin-American electric power grids. Moreover, it showed that, unlike European and American electric power grids, the Latin-American one has a number of consumers connected to a distribution transformer that is economically reasonable considering the number of equipment (e.g., electricity meters) on the field and consumers served. Also, it concluded that the hybrid point-to-point transmission can have either a lower bit error rate (BER) while maintaining the same total transmission power or a lower total transmission power while maintaining the same BER in comparison to not hybrid systems. Furthermore, [32] showed that PLC enhances the capacity of wireless networks even using very low transmission power. Additionally, [33] stated that PLC is a promising candidate to enhance wireless relaying schemes. In addition, [34] considered an ideal multi-channel (PLC and wireless) receiver to show that relevant performance improvement may be achieved by mutually using these two data communication channels. Moreover, [35] and [36] used link throughput analysis to show that existing diversity between PLC and wireless can be useful to minimize the likelihood of low throughput links and that coding diversity has the potential to offer very high throughput over PLC-wireless links, respectively. Furthermore, [37] showed that the parallel use of PLC and wireless with multihop relaying enhances performance in comparison to the separate use of relays in the PLC and wireless channels. Additionally, [38] briefly discussed that the hybrid PLC-wireless scheme can improve the achievable data rate for a point-to-point data communication in comparison to the sole use of PLC or wireless medium. Finally, [18] showed an extensive study of the power line and wireless channels for smart grid applications and [39, 40] studied the characteristics of a hybrid PLC-wireless channel.

After a careful review of the literature related to the hybrid PLC-wireless channel, it could be noticed that there is a scarcity of works which treat the hybrid channel model composed of PLC and wireless channels, in parallel, for low-bit rate data communication and their performance analysis in theoretical terms. In this regard, this dissertation tries

to cover this gap in this promising area and to expand the knowledge on this issue for extracting the benefits and defining limitations of the parallel use of PLC and wireless channels.

### 1.1 Objectives

Aiming to increase the understanding of hybrid PLC-wireless channels and their usefulness for improving data communication, this work discusses the so-called hybrid PLC-wireless single-relay channel (HSRC) model. Also, in order to analyze the HSRC behavior in terms of achievable data rate, when it misses a data communication link (power line is broken or the wireless path is physically limited, for example, due to the growth of a tree or the construction of a building) or node communication interface (hardware failure, i.e., the communication node only uses PLC or wireless interface in the region between the source and destination nodes), the so-called incomplete HSRC is introduced and analyzed. Note that, the term incomplete refers to the HSRC without a (PLC or wireless) data communication link or a node communication interface. Moreover, the investigation is carried out at the frequency bandwidth which covers low-bit rate applications, such as IoT, machine-to-machine, and smart metering. To be precise, the dissertation objectives are as follows:

- To present mathematical formulation of the so-called HSRC and incomplete HSRC together with their ergodic achievable data rates and outage probabilities. In this regard, amplify-and-forward (AF) and decode-and-forward (DF) cooperative protocols are taken into account, the relay (R) node is located in the midway between source (S) and destination (D) nodes (case #1), closer to the S than D node (case #2), closer to the D than S node (case #3), and far from both S and D nodes (case #4). All analyses takes into account NB-PLC channel models and LP-RF wireless ones.
- To show comparative results among HSRC, incomplete HSRC, PLC single-relay channel (SRC), and wireless SRC in terms of ergodic achievable data rates and outage probabilities when the R node is located in the midway between S and D nodes (case #1), closer to the S than D node (case #2), closer to the D than S node (case #3), and far from both S and D nodes (case #4). All analyses takes into account NB-PLC channel models and LP-RF wireless ones.

### 1.2 Dissertation outline

The rest of the document is organized as follows:

- Chapter 2 covers the mathematical formulation of the HSRC and incomplete HSRC ergodic achievable data rates and outage probabilities assuming AF and DF cooperative protocols.
- Chapter 3 discusses the adopted channels and additive noises models as well as numerical results and analyses of the HSRC and incomplete HSRC ergodic achievable data rates and outage probabilities.
- Chapter 4 states the concluding remarks of this dissertation.

## 2 Hybrid PLC-Wireless Single-Relay Channel Model

The HSRC model is composed of three hybrid nodes (source - S, relay - R and destination - D). The term hybrid refers to the use of PLC and wireless data communication interfaces by a node. It means that each node makes use of two data communication links to communicate with other node within the model, resulting that it contains two communication interfaces in each node, labeled as  $S^P$ ,  $R^P$ , and  $D^P$  for PLC just as  $S^W$ ,  $R^W$ , and  $D^W$  for wireless. In this model, there are six data communication links: PLC  $SD$ ,  $SR$ , and  $RD$  links (namely  $SD^P$ ,  $SR^P$ , and  $RD^P$ , respectively) as well as wireless  $SD$ ,  $SR$ , and  $RD$  links (namely  $SD^W$ ,  $SR^W$ , and  $RD^W$ , respectively). Moreover, the loss of one data communication link (for short, link) or one node communication interface characterizes the so-called incompleteness of the HSRC. Furthermore, the R node is used in order to support the data transmission between S and D nodes which is accomplished with a cooperative protocol. The considered cooperative protocols at this dissertation are AF and DF. Therefore, in order to increase the knowledge and understanding of usefulness of HSRC regarding achievable data rate and outage probability metrics for low-bit rate applications, this chapter introduces the HSRC and incomplete HSRC models.

This chapter is organized as follows: Section 2.1 focused on the mathematical formulation of the HSRC model. More specifically, Subsection 2.1.1 demonstrates the ergodic achievable data rate calculation of the HSRC model assuming AF and DF cooperative protocols, respectively, while Subsection 2.1.2 addresses the adopted assumptions about the channel energy, power allocation, power of the additive noise, and limit analyses of HSRC. Furthermore, Subsection 2.1.3 shows the outage probability of HSRC. In the sequel, Section 2.2 addresses the mathematical formulation of the incomplete HSRC model. More precisely, Subsections 2.2.1 and 2.1.2 express the way to get the ergodic achievable data rate and the limit analyses of the incomplete HSRC, respectively, with AF and DF cooperative protocols. Finally, the outage probability calculation of the incomplete HSRC is shown in Subsection 2.2.3.

### 2.1 The Hybrid Single-Relay Channel

In this section, closed-form expressions of ergodic achievable data rates and outage probabilities of the HSRC are derived. Two cooperative protocols are considered in this work: AF and DF [20–25]. Also, it is demonstrated the limit analyses concerning the achievable data rate of HSRC.

The HSRC model is shown in Figure 1. It is constituted by PLC and wireless SRC models operating in parallel. In this model, each node makes use of PLC and wireless communication interfaces to transmit signals among the S, R and D nodes. The R node operates in half-duplex mode and does not apply any combining technique over the signals

received through the PLC and wireless interfaces of R node.

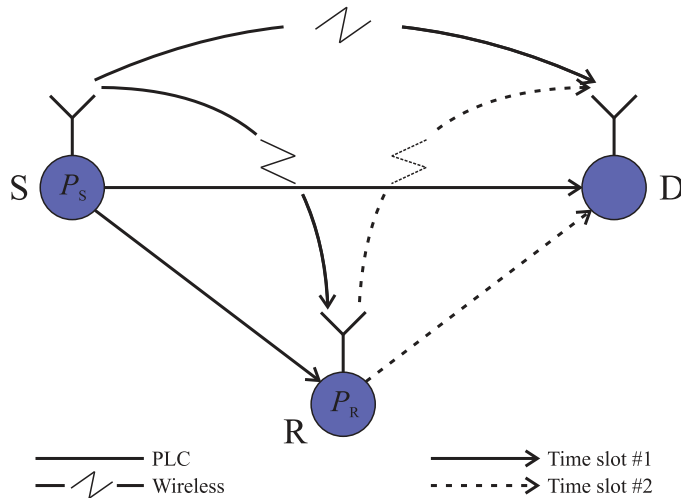


Figure 1: Hybrid PLC-wireless single-relay channel model.

According to Figure 1, in HSRC, the S node broadcasts the same copy of the source information to R and D nodes through the wireless and power line channels during the first time slot. In the second time slot, the R node forwards the detected information to the D node. It is assumed that  $P_t^q$  is the transmission power allocated to the  $q^{\text{th}}$  communication medium in the  $t^{\text{th}}$  time slot, where  $q \in \{P, W\}$  refers to PLC or wireless medium and  $t \in \{0, 1\}$  denotes the first and second time slots, respectively. Note that  $P = P_S + P_R$  is the total transmission power allocated to HSRC during the two time slots, in which  $P_S = P_0^P + P_0^W$  and  $P_R = P_1^P + P_1^W$  are the transmission powers allocated to the S and R nodes, respectively.

In this model, PLC and wireless channels are linear and time varying (LTV) and both of them are invariant during one symbol period. In this regard, let  $\{x[n]\}$  and  $\{\hat{x}_R^q[n]\}$  be the symbols sequence which is transmitted by node S during the first time slot and an estimate of the detected symbol sequence by the R node that is associated with the  $q^{\text{th}}$  medium, respectively. Additionally, the discrete-time representations of channel impulse responses (CIRs) are denoted by  $\{h_\ell^q[m, n]\}$ , in which  $\ell \in \{SD, SR, RD\}$  denotes  $SD$ ,  $SR$  and  $RD$  links, respectively. Also,  $\{v_\ell^q[n]\}$  refers to the additive noise for the  $\ell^{\text{th}}$  link associated with the  $q^{\text{th}}$  communication medium. Therefore, the discrete-time signals received by the  $M_R^{\text{th}}$  node from the  $M_T^{\text{th}}$  node, through the  $q^{\text{th}}$  medium and  $\ell^{\text{th}}$  link, are given by

$$y_{M_T, M_R}^q[n] = \sum_{m=-\infty}^{\infty} h_\ell^q[m, n] \hat{x}[m] + v_\ell^q[n], \quad (2.1)$$

where  $\{M_T, M_R\} \in \{\{S, D\}, \{S, R\}, \{R, D\}\}$  and

$$\hat{x}[n] = \begin{cases} \hat{x}_R^q[n], & \text{if } \{M_T, M_R\} = \{R, D\} \\ x[n], & \text{otherwise.} \end{cases} \quad (2.2)$$

The PLC and wireless channels are considered to be LTV. However, both of them remain constant during one time slot and completely independent and changed between two different time slots. In other words, the discrete-time representations of CIRs for a given time slot are denoted by  $\{h_\ell^q[n]\}_{n=0}^{L_\ell^q-1}$ , in which  $L_\ell^q$  are their lengths. Therefore, for a given common memory length for the PLC channel,  $\max_\ell\{L_\ell^P\} \leq L_{\max}$ ,  $\forall \ell$ , the PLC SRC is assumed to be a linear Gaussian relay channel (LGRC) with finite memory ( $L_{\max} \in \mathbb{N}$ ) during one symbol period (see [41]). As the same assumption can be made for the wireless SRC, we propose to model the HSRC as two parallel LGRC. In this regard and similar to [42], the  $N$ -block memoryless channel is defined as the channel in which the outputs over any  $N$ -block transmission are independent of channel inputs and noise samples from previous or subsequent  $N$ -block transmissions, for  $N > L_{\max}$ . Finally, the  $N$ -block memoryless circular Gaussian relay channel ( $N$ -CGRC) is defined as the  $N$ -block LGRC ( $N$ -LGRC) switching the linear convolution operation in (2.1) to the circular convolution. Now, and most important, as [41] states, the direct computation of the channel capacity of the  $N$ -LGRC is challenged by the presence of inter-block interference due to the fact that the CIRs have memory and noises are correlated. As addressed in [42], the capacity of the  $N$ -LGRC can be computed as the same of the  $N$ -CGRC, as  $N \rightarrow \infty$ . Dealing with the  $N$ -CGRC model avoids inter-block interference by converting the linear convolution of an  $N$ -LGRC into a circular convolution.

Based on the aforementioned adoptions, let the discrete-time vectorial representation of the CIR of the  $q^{\text{th}}$  channel associated with the  $\ell^{\text{th}}$  link during one symbol period be  $\mathbf{h}_\ell^q = [h_\ell^q[0], h_\ell^q[1], \dots, h_\ell^q[L_\ell^q - 1]]^T$ , then  $\mathbf{H}_\ell^q = [H_\ell^q[0], H_\ell^q[1], \dots, H_\ell^q[N - 1]]^T$  is the  $N$ -length discrete Fourier transform (DFT) of the CIR of PLC or wireless channels such that  $\mathbf{H}_\ell^q = \mathcal{F}[\mathbf{h}_\ell^q, \mathbf{0}_{N-L_\ell^q}]^T$ , in which  $\mathcal{F}$  is  $N$ -size DFT matrix,  $\mathbf{0}_N$  is an  $N$ -length column vector constituted by zeros, and  $N$  is the number of subchannels. Also, diagonal matrices are defined as

$$\mathcal{H}_\ell^q \triangleq \mathbf{diag} \{H_\ell^q[0], H_\ell^q[1], \dots, H_\ell^q[N - 1]\} \quad (2.3)$$

and

$$\mathbf{\Lambda}_{|\mathcal{H}_\ell^q|^2} \triangleq \mathbf{diag} \{ |H_\ell^q[0]|^2, |H_\ell^q[1]|^2, \dots, |H_\ell^q[N - 1]|^2 \}, \quad (2.4)$$

for further use. Moreover, the joint probability  $p(|H_\ell^q[0]|^2, |H_\ell^q[1]|^2, \dots, |H_\ell^q[N - 1]|^2) = p(|H_\ell^q[0]|^2)p(|H_\ell^q[1]|^2) \dots p(|H_\ell^q[N - 1]|^2)$  because it is assumed that  $H_\ell^q[i]$  and  $H_\ell^q[j]$ ,  $\forall i \neq j$ , are independent random variables (r.v.s).

The vectorial representation of a symbol, after digital modulation in the frequency domain, is given by  $\mathbf{X} \in \mathbb{C}^{N \times 1}$ , while  $\mathbf{V}_\ell^P \in \mathbb{C}^{N \times 1}$  and  $\mathbf{V}_\ell^W \in \mathbb{C}^{N \times 1}$  are the vectorial representation of the additive noise in the frequency domain for PLC and wireless channels, respectively. Moreover, it is considered that  $\mathbb{E}\{\mathbf{X}\} = \mathbf{0}$ ,  $\mathbb{E}\{\mathbf{X}\mathbf{X}^\dagger\} = \mathbf{\Lambda}_{\sigma_{\mathbf{X}}^2} = \mathbf{I}_N$ , in which  $\mathbf{I}_N$  denotes the  $N \times N$  identity matrix,  $\mathbb{E}\{\cdot\}$  is the expectation operator and  $\dagger$  is the

conjugate transpose operator. Also,  $\mathbb{E}\{\mathbf{V}_\ell^q\} = 0$  and  $\mathbb{E}\{\mathbf{V}_\ell^q \mathbf{V}_\ell^{q\dagger}\} = \mathbf{\Lambda}_{\sigma_{\mathbf{V}_\ell^q}^2}$ , where

$$\mathbf{\Lambda}_{\sigma_{\mathbf{V}_\ell^q}^2} = \mathbf{diag} \left\{ \sigma_{\mathbf{V}_\ell^q}^2[0], \sigma_{\mathbf{V}_\ell^q}^2[1], \dots, \sigma_{\mathbf{V}_\ell^q}^2[N-1] \right\}. \quad (2.5)$$

In addition, let us assume that the diagonal matrix,

$$\mathbf{\Lambda}_{P_t^q} = \mathbf{diag} \left\{ P_{t,0}^q, P_{t,1}^q, \dots, P_{t,N-1}^q \right\}, \quad (2.6)$$

is the matrix representation of the transmission power allocated to the  $q^{th}$  medium and during the  $t^{th}$  time slot, so that  $\text{Tr}(\mathbf{\Lambda}_{P_t^q}) = P_t^q$ , where  $\text{Tr}(\cdot)$  denotes the trace operator. Therefore,

$$\mathbf{\Lambda}_{\sqrt{P_t^q}} = \mathbf{diag} \left\{ \sqrt{P_{t,0}^q}, \sqrt{P_{t,1}^q}, \dots, \sqrt{P_{t,N-1}^q} \right\} \quad (2.7)$$

denotes the amplitude, in the frequency domain, of the symbol that is transmitted through the  $q^{th}$  medium at the  $t^{th}$  time slot.

Now, it can be stated that the frequency domain vectorial representation of a symbol at the output of the  $q^{th}$  medium, which is associated with the  $\ell^{th}$  link during one symbol period, is given by

$$\mathbf{Y}_\ell^q = \mathbf{\Lambda}_{\sqrt{P_t^q}} \mathcal{H}_\ell^q \tilde{\mathbf{X}} + \mathbf{V}_\ell^q, \quad (2.8)$$

where

$$\tilde{\mathbf{X}} = \begin{cases} \mathbf{X}_R^q, & \text{if } t = 1 \\ \mathbf{X}, & \text{otherwise,} \end{cases} \quad (2.9)$$

and  $\mathbf{X}_R^q \in \mathbb{C}^{N \times 1}$  is the frequency domain vectorial representation of the estimated symbol that is received at the output of the  $q^{th}$  medium at the R node.

### 2.1.1 The Achievable Data Rate

*Amplify-and-Forward:* The AF protocol retransmits the received symbol on node R using a scale factor, which is related to the power allocated to the R node at the second time slot. Essentially, when the AF protocol is applied, the R node simply forwards an amplified version of its received symbol to the D node. Mathematically, the vectorial frequency domain representation of the symbol at the output of the  $q^{th}$  medium associated with the *SRD* link, using AF protocol, is given by

$$\mathbf{Y}_{SRD,AF}^q = \mathbf{\Lambda}_{\sqrt{P_1^q}} \mathcal{H}_{RD}^q \mathbf{X}_R^q + \mathbf{V}_{RD}^q, \quad (2.10)$$

in which  $\mathbf{X}_R^q = \mathbf{\Lambda}_{\sigma_{\mathbf{Y}_{SR}^q}^2}^{-1} \mathbf{Y}_{SR}^q$  is the symbol transmitted to the D node by the R node and [24, 25]

$$\begin{aligned} \mathbf{\Lambda}_{\sigma_{\mathbf{Y}_{SR}^q}^2} &= \mathbb{E}\{\mathbf{Y}_{SR}^q \mathbf{Y}_{SR}^{q\dagger}\} \\ &= \mathbf{\Lambda}_{P_0^q} \mathbf{\Lambda}_{|\mathcal{H}_{SR}^q|^2} \mathbf{\Lambda}_{\sigma_{\mathbf{X}}^2} + \mathbf{\Lambda}_{\sigma_{\mathbf{V}_{SR}^q}^2}. \end{aligned} \quad (2.11)$$

From (2.8) and (2.10), the received symbol at the output of HSRC when AF is used, can be expressed by

$$\begin{aligned}
\mathbf{Y} &= [\mathbf{Y}_{SD}^P, \mathbf{Y}_{SRD,AF}^P, \mathbf{Y}_{SD}^W, \mathbf{Y}_{SRD,AF}^W]^T \\
&= \begin{bmatrix} \mathcal{H}_{SD}^P & 0 & 0 & 0 \\ 0 & \mathcal{H}_{SR}^P \mathcal{H}_{RD}^P & 0 & 0 \\ 0 & 0 & \mathcal{H}_{SD}^W & 0 \\ 0 & 0 & 0 & \mathcal{H}_{SR}^W \mathcal{H}_{RD}^W \end{bmatrix} \begin{bmatrix} \Lambda \sqrt{P_0^P} \\ \Lambda \sqrt{P_0^P} \Lambda \sqrt{P_1^P} \Lambda^{-1} \sigma_{\mathbf{Y}_{SR}^P} \\ \Lambda \sqrt{P_0^W} \\ \Lambda \sqrt{P_0^W} \Lambda \sqrt{P_1^W} \Lambda^{-1} \sigma_{\mathbf{Y}_{SR}^W} \end{bmatrix} \mathbf{X} + \\
&\quad \begin{bmatrix} \mathbf{V}_{SD}^P \\ \Lambda \sqrt{P_1^P} \mathcal{H}_{RD}^P \Lambda^{-1} \sigma_{\mathbf{Y}_{SR}^P} \mathbf{V}_{SR}^P + \mathbf{V}_{RD}^P \\ \mathbf{V}_{SD}^W \\ \Lambda \sqrt{P_1^W} \mathcal{H}_{RD}^W \Lambda^{-1} \sigma_{\mathbf{Y}_{SR}^W} \mathbf{V}_{SR}^W + \mathbf{V}_{RD}^W \end{bmatrix} \\
&= \begin{bmatrix} \mathcal{H}_{SD}^P \Lambda \sqrt{P_0^P} \\ \mathcal{H}_{SR}^P \mathcal{H}_{RD}^P \Lambda \sqrt{P_0^P} \Lambda \sqrt{P_1^P} \Lambda^{-1} \sigma_{\mathbf{Y}_{SR}^P} \\ \mathcal{H}_{SD}^W \Lambda \sqrt{P_0^W} \\ \mathcal{H}_{SR}^W \mathcal{H}_{RD}^W \Lambda \sqrt{P_0^W} \Lambda \sqrt{P_1^W} \Lambda^{-1} \sigma_{\mathbf{Y}_{SR}^W} \end{bmatrix} \mathbf{X} + \\
&\quad \begin{bmatrix} \mathbf{I}_N & 0 & 0 & 0 & 0 & 0 \\ 0 & \Lambda \sqrt{P_1^P} \mathcal{H}_{RD}^P \Lambda^{-1} \sigma_{\mathbf{Y}_{SR}^P} & \mathbf{I}_N & 0 & 0 & 0 \\ 0 & 0 & 0 & \mathbf{I}_N & 0 & 0 \\ 0 & 0 & 0 & 0 & \Lambda \sqrt{P_1^W} \mathcal{H}_{RD}^W \Lambda^{-1} \sigma_{\mathbf{Y}_{SR}^W} & \mathbf{I}_N \end{bmatrix} \mathbf{V} \\
&= \mathbf{A}\mathbf{X} + \mathbf{B}\mathbf{V},
\end{aligned} \tag{2.12}$$

where  $\mathbf{V} = [\mathbf{V}_{SD}^P, \mathbf{V}_{SR}^P, \mathbf{V}_{RD}^P, \mathbf{V}_{SD}^W, \mathbf{V}_{SR}^W, \mathbf{V}_{RD}^W]^T$ .

Now, let  $f(\mathbf{Z})$  be the entropy of a random vector  $\mathbf{Z}$  and  $\mathbf{Y} \in \mathbb{C}^{4N \times 1}$  the representation of the received symbol in the D node after the two time slots occurs. Then, the mutual information between the transmitted and received symbols is [22, 24, 25]

$$\begin{aligned}
I(\mathbf{X}, \mathbf{Y}) &= f(\mathbf{Y}) - f(\mathbf{Y}|\mathbf{X}) \\
&= f(\mathbf{Y}) - (f(\mathbf{A}\mathbf{X}|\mathbf{X}) + f(\mathbf{B}\mathbf{V}|\mathbf{X})) \\
&= f(\mathbf{Y}) - f(\mathbf{B}\mathbf{V}).
\end{aligned} \tag{2.13}$$

Based on the adopted assumptions, the entropy of  $\mathbf{Y}$  is given by [43]

$$f(\mathbf{Y}) = \log_2[(\pi e)^{4N} \det(\mathbf{R}_{\mathbf{Y}\mathbf{Y}})], \tag{2.14}$$

and, due to the Gaussianity of the additive noise, it is obtained that

$$f(\mathbf{B}\mathbf{V}) = \log_2[(\pi e)^{4N} \det(\mathbf{B}\mathbf{R}_{\mathbf{V}\mathbf{V}}\mathbf{B}^\dagger)], \tag{2.15}$$

where  $\mathbf{R}_{\mathbf{Y}\mathbf{Y}} = \mathbb{E}\{\mathbf{Y}\mathbf{Y}^\dagger\} = \mathbf{A}\mathbf{R}_{\mathbf{X}\mathbf{X}}\mathbf{A}^\dagger + \mathbf{B}\mathbf{R}_{\mathbf{V}\mathbf{V}}\mathbf{B}^\dagger$ ,  $\mathbf{R}_{\mathbf{X}\mathbf{X}} = \mathbb{E}\{\mathbf{X}\mathbf{X}^\dagger\} = \mathbf{I}_N$ , and  $\mathbf{R}_{\mathbf{V}\mathbf{V}} = \mathbb{E}\{\mathbf{V}\mathbf{V}^\dagger\}$ . Making  $\mathbf{C}_{AF} = \mathbf{A}\mathbf{R}_{\mathbf{X}\mathbf{X}}\mathbf{A}^\dagger$  and  $\mathbf{D}_{AF} = \mathbf{B}\mathbf{R}_{\mathbf{V}\mathbf{V}}\mathbf{B}^\dagger$ , in which  $\mathbf{C}_{AF}$  and  $\mathbf{D}_{AF}$  are given by (2.18) and (2.19), respectively. From (2.13), the mutual information is

$$I(\mathbf{X}, \mathbf{Y}) = \log_2 [\det(\mathbf{I}_{4N} + \mathbf{C}_{AF}\mathbf{D}_{AF}^{-1})]. \quad (2.16)$$

As a result, the ergodic achievable data rate of an HSRC using AF is given by

$$C_{AF}^{\text{HSRC}} = \mathbb{E}_{\mathbf{H}_\ell^P, \mathbf{H}_\ell^W} \left\{ \max_{\Lambda_P} \frac{B_W}{N} \log_2 [\det(\mathbf{I}_{4N} + \mathbf{C}_{AF}\mathbf{D}_{AF}^{-1})] \right\} \quad (2.17)$$

subject to  $\text{Tr}(\Lambda_P) \leq P$ , where  $\Lambda_P = \text{diag}\{\Lambda_{P_0^P}, \Lambda_{P_0^W}, \Lambda_{P_1^P}, \Lambda_{P_1^W}\}$ ,  $B_W$  and  $\mathbb{E}_{\mathbf{H}_\ell^P, \mathbf{H}_\ell^W}\{\cdot\}$  are the frequency bandwidth and the expectation operation related to both power line and wireless channels, respectively.

$$\mathbf{C}_{AF} = \begin{bmatrix} \Lambda_{P_0^P} \Lambda_{|\mathcal{H}_{SD}^P|^2} & 0 & 0 & 0 \\ 0 & \Lambda_{P_0^P} \Lambda_{P_1^P} \Lambda_{\sigma_{\mathbf{Y}^{SR}}^2}^{-1} & \Lambda_{|\mathcal{H}_{SR}^P|^2} \Lambda_{|\mathcal{H}_{RD}^P|^2} & 0 \\ 0 & 0 & 0 & \Lambda_{P_0^W} \Lambda_{|\mathcal{H}_{SD}^W|^2} \\ 0 & 0 & 0 & \Lambda_{P_0^W} \Lambda_{P_1^W} \Lambda_{\sigma_{\mathbf{Y}^{SR}}^2}^{-1} \Lambda_{|\mathcal{H}_{SR}^W|^2} \Lambda_{|\mathcal{H}_{RD}^W|^2} \end{bmatrix}. \quad (2.18)$$

$$\mathbf{D}_{AF} = \begin{bmatrix} \Lambda_{\sigma_{\mathbf{V}^{SD}}^2} & 0 & 0 & 0 \\ 0 & \Lambda_{|\mathcal{H}_{RD}^P|^2} \Lambda_{P_1^P} \Lambda_{\sigma_{\mathbf{V}^{SR}}^2}^{-1} \Lambda_{\sigma_{\mathbf{V}^{SR}}^2} + \Lambda_{\sigma_{\mathbf{V}^{RD}}^2} & 0 & 0 \\ 0 & 0 & \Lambda_{\sigma_{\mathbf{V}^{SD}}^2} & 0 \\ 0 & 0 & 0 & \Lambda_{|\mathcal{H}_{RD}^W|^2} \Lambda_{P_1^W} \Lambda_{\sigma_{\mathbf{V}^{SR}}^2}^{-1} \Lambda_{\sigma_{\mathbf{V}^{SR}}^2} + \Lambda_{\sigma_{\mathbf{V}^{RD}}^2} \end{bmatrix}. \quad (2.19)$$

*Decode-and-Forward (DF)*: In this protocol, the received information on the R node is decoded and retransmitted to the D node only if the information was correctly decoded at the R node, i.e., the relay decodes the information received at first time slot and retransmits an amplified version of  $x[n]$  only when it is correctly decoded. Therefore,  $\mathbf{X}_R^q = \mathbf{X}$ . After the decoding process, the retransmission is accomplished by allocating power to the R node. In other words, the vectorial frequency domain representation of the symbol at the output of the channel associated with the *SRD* link, using DF protocol, is given by

$$\mathbf{Y}_{SRD,DF}^q = \Lambda_{\sqrt{P_1^q}} \mathcal{H}_{RD}^q \mathbf{X} + \mathbf{V}_{RD}^q. \quad (2.20)$$

Similar to AF, the ergodic achievable data rate of HSRC using DF is given by

$$C_{DF}^{\text{HSRC}} = \mathbb{E}_{\mathbf{H}_\ell^P, \mathbf{H}_\ell^W} \left\{ \max_{\Lambda_P} \frac{B_W}{N} \log_2 [\det(\mathbf{I}_{4N} + \mathbf{C}_{DF}\mathbf{D}_{DF}^{-1})] \right\} \quad (2.21)$$

subject to  $\text{Tr}(\Lambda_P) \leq P$ , in which

$$\mathbf{C}_{DF} = \begin{bmatrix} \Lambda_{P_0^P} \Lambda_{|\mathcal{H}_{SD}^P|^2} & 0 & 0 & 0 \\ 0 & \Lambda_{C^{P*}} & 0 & 0 \\ 0 & 0 & \Lambda_{P_0^W} \Lambda_{|\mathcal{H}_{SD}^W|^2} & 0 \\ 0 & 0 & 0 & \Lambda_{C^{W*}} \end{bmatrix} \quad (2.22)$$

and

$$\mathbf{D}_{DF} = \begin{bmatrix} \Lambda_{\sigma_{\mathbf{V}_{SD}^P}^2} & 0 & 0 & 0 \\ 0 & \Lambda_{D^{P*}} & 0 & 0 \\ 0 & 0 & \Lambda_{\sigma_{\mathbf{V}_{SD}^W}^2} & 0 \\ 0 & 0 & 0 & \Lambda_{D^{W*}} \end{bmatrix}, \quad (2.23)$$

where  $\Lambda_{C^{q*}}$  and  $\Lambda_{D^{q*}}$  are given by

$$\Lambda_{C^{q*}} = \begin{cases} \Lambda_{P_0^q} \Lambda_{|\mathcal{H}_{SR}^q|^2}, & \text{if } C_{SR}^q = \min\{C_{SR}^q, C_{RD}^q\}, \\ \Lambda_{P_1^q} \Lambda_{|\mathcal{H}_{RD}^q|^2}, & \text{otherwise,} \end{cases} \quad (2.24)$$

and

$$\Lambda_{D^{q*}} = \begin{cases} \Lambda_{\sigma_{\mathbf{V}_{SR}^q}^2}, & \text{if } C_{SR}^q = \min\{C_{SR}^q, C_{RD}^q\}, \\ \Lambda_{\sigma_{\mathbf{V}_{RD}^q}^2}, & \text{otherwise,} \end{cases} \quad (2.25)$$

respectively, in which

$$C_\ell^q = \frac{2B_W}{N} \log_2 [\det(\mathbf{I}_N + \Lambda_{P_t^q} \Lambda_{|\mathcal{H}_\ell^q|^2} \Lambda_{\sigma_{\mathbf{V}_\ell^q}^2}^{-1})], \quad (2.26)$$

in which  $t = 0$  for  $SR$  link and  $t = 1$  for  $RD$  link. Also, the minimum operator guarantees that the data transmission on the  $RD$  link only occurs when  $\mathbf{X}_R^q = \mathbf{X}$  and the achievable data rate of the  $SRD$  link depends on the worst channels between  $SR$  and  $RD$  links.

### 2.1.2 Limit Analyses of HSRC, PSRC, and WSRC

For carrying out these analyses, it is assumed that the complete channel state information (CSI) is available at the transmitter and OA is applied by using the water filling (WF) technique [44] at the S and R nodes. This technique optimally allocates the total transmission power among subcarriers on basis of the knowledge of the normalized signal-to-noise ratio (nSNR) matrix, which is expressed by  $\Lambda_{\bar{\zeta}_\ell^q} = \Lambda_{|\mathcal{H}_\ell^q|^2} \Lambda_{\sigma_{\mathbf{V}_\ell^q}^2}^{-1} = \mathbf{diag} \{\bar{\zeta}_\ell^q[0], \bar{\zeta}_\ell^q[1], \dots, \bar{\zeta}_\ell^q[N-1]\}$  for the  $q^{\text{th}}$  channel associated with the  $\ell^{\text{th}}$  link, in which, for a given  $q$  and  $\ell$ ,  $\bar{\zeta}_\ell^q[k]$  is the  $k^{\text{th}}$  subchannel nSNR with  $k \in \{0, 1, \dots, N-1\}$  corresponding to the frequencies  $f_k = k\Delta f$  and  $\Delta f = B_W/N$  is the subchannel bandwidth. At the S node, due to the broadcast propagation of the transmitted signal through each medium, WF is accomplished based on  $\Lambda_{\bar{\zeta}_*^q} = \mathbf{diag} \{\bar{\zeta}_*^q[0], \bar{\zeta}_*^q[1], \dots, \bar{\zeta}_*^q[N-1]\}$ , where  $\bar{\zeta}_*^q[k] = \max\{\bar{\zeta}_{SD}^q[k], \bar{\zeta}_{SR}^q[k]\}, \forall k$ . Although the WF is used, there are other resource allocation techniques with reduced computational complexity that could be used in a real-time application [45–47]. Furthermore, the achievable data rate gain, given by

$$\rho_a^b = \frac{C_a^b}{C_{SD}^P}, \quad (2.27)$$

is used as a metric of gain in relation to the achievable data rate associated with the direct  $SD^P$  link. In (2.27),  $a \in \{\text{AF}, \text{DF}\}$  denotes AF or DF and  $b \in \{\text{PSRC}, \text{WSRC}, \text{HSRC}\}$

denotes PLC SRC (PSRC), wireless SRC (WSRC) or HSRC, respectively. The choice of the  $SD^P$  link as a reference was made in order to quantify the gain or loss of achievable data rate associated with a not hybrid and non-cooperative PLC system. Moreover, the most important information is not the absolute value of achievable data rate itself, but the gain/loss associated with the use of HSRC in various different conditions. Also, to guarantee fairness in the discussed analyses, it is assumed that  $\|\mathbf{h}_\ell^P\|^2 = \|\mathbf{h}_\ell^W\|^2$  and  $P_{v,\ell}^W = P_{v,\ell}^P$ , in which  $\|\cdot\|$  denotes 2-norm,  $\|\mathbf{h}_\ell^q\|^2$  is the  $q^{\text{th}}$  channel energy for the  $\ell^{\text{th}}$  link, and  $P_{v,\ell}^q$  denotes the power of the  $q^{\text{th}}$  communication medium additive noise associated with the  $\ell^{\text{th}}$  link. In practice, the PLC and wireless additive noise powers and link energies are not equal. However, if these conditions are not adopted, a PLC or wireless link would have a great advantage against each other, resulting that this link would be dominant and it would not be possible to clearly demonstrate the benefits of a hybrid channel model. Furthermore, if there are gains when these conditions are considered, it would also appear in the situations where they are not adopted.

Past works showed that changing the R node position has a significative influence on the achievable data rate of a cooperative PLC system [24–26]. Aiming at extending this analysis to HSRC and incomplete HSRC models, the following definition applies:

$$\mu^2 \triangleq \frac{\|\mathbf{h}_{SR}^q\|^2 \|\mathbf{h}_{RD}^q\|^2}{\|\mathbf{h}_{SD}^q\|^2} \quad \text{and} \quad \beta^2 \triangleq \frac{\|\mathbf{h}_{SR}^q\|^2}{\|\mathbf{h}_{RD}^q\|^2}, \quad (2.28)$$

where  $\beta \in \mathbb{R}_+$ . Also, it is assumed that  $\mu^2 = \alpha^2 \|\mathbf{h}_{SD}^q\|^2$  and  $\alpha \in \mathbb{R}_+$ . It is important to point out that the  $SD^q$  link energy remains constant and, as  $\alpha$  grows, more energy is being given to the  $SR^q$  and  $RD^q$  links as well as the opposite occurs if  $\alpha$  decreases. Moreover, growing  $\beta$  means that more energy is being offered to the  $SR^q$  link and, proportionally, less to the  $RD^q$  link and vice-versa if  $\beta$  reduces. Note that these relations are taken into account to ensure that a balanced link energy scenario occurs when  $\alpha = \beta = 1$  (i.e.,  $SR^q$ ,  $RD^q$  and  $SD^q$  links have the same channel energy). In practice, this scenario is similar to a situation in which the nodes are equidistant to each other. Additionally, if  $\beta = 1$  and  $0 < \alpha \ll 1$ , then the R node is located at a place in the virtual line which is perpendicular to the central point of the line between S and D nodes, but far from both of them. Furthermore, when  $\alpha < 1$ , it is allowed to simulate situations in which the cooperation tends to preferably use (PLC and wireless)  $SD$  instead of the  $SRD$  link because the former will have a greater channel energy than the latter, resulting in better nSNR in its subchannels. On the opposite, if  $\alpha > 1$ , situations in which the cooperative scheme tends to use the  $SRD$  link instead of the  $SD$  one occur. Based on some calculation, limit analyses of (2.27) yield the following situations:

- (i)  $P \rightarrow \infty$ : The ergodic achievable data rate of  $SD^P$  is given by

$$C_{SD}^P = \mathbb{E}_{\mathbf{H}_{SD}^P} \left\{ \max_{\mathbf{\Lambda}_P} \frac{2B_W}{N} \log_2 [\det(\mathbf{I}_N + \mathbf{\Lambda}_P \mathbf{\Lambda}_{|\mathcal{H}_\ell^P|^2} \mathbf{\Lambda}_{\sigma_{\mathbf{V}_\ell}^P}^{-1})] \right\}. \quad (2.29)$$

Moreover, for a given  $\mathbf{H}_{SD}^P$ , the achievable data rate is obtained with

$$C_{SD}^P = \frac{2B_W}{N} \max_{\mathbf{\Lambda}_P} \log_2 [\det(\mathbf{I}_N + \mathbf{\Lambda}_P \mathbf{\Lambda}_{|\mathbf{h}_{SD}^P|^2} \mathbf{\Lambda}_{\sigma_{\mathbf{v}_{SD}^P}^2}^{-1})]. \quad (2.30)$$

Making  $K_1 = \mathbf{\Lambda}_P \mathbf{\Lambda}_{|\mathbf{h}_{SD}^P|^2} \mathbf{\Lambda}_{\sigma_{\mathbf{v}_{SD}^P}^2}^{-1}$  and for high value of  $P$ , it implies that  $\text{Tr}(\mathbf{\Lambda}_P) \gg \text{Tr}(\mathbf{I}_N)$ , thus  $\text{Tr}(K_1) \gg \text{Tr}(\mathbf{I}_N)$  and the value of  $\mathbf{I}_N$  is negligible in (2.30). Note that the use of trace operator only makes sense for extremely high or low value of  $P$ . As a consequence,  $K_2 = \log_2 [\det(\mathbf{diag}\{K_1\})]$  and

$$C_{SD}^P = 2K_2 \frac{B_W}{N}, \quad (2.31)$$

when  $\text{Tr}(K_1) \gg \text{Tr}(\mathbf{I}_N)$ . On the other hand, the ergodic achievable data rate of PSRC, for a given cooperative protocol  $a$ , is expressed by

$$C_a^{\text{PSRC}} = \mathbb{E}_{\mathbf{H}_\ell^P} \left\{ \max_{\mathbf{\Lambda}_P} \frac{B_W}{N} \log_2 [\det(\mathbf{I}_{2N} + \mathbf{C}_a \mathbf{D}_a^{-1})] \right\}. \quad (2.32)$$

Moreover, for a given  $\mathbf{H}_\ell^P, \forall \ell$ , the achievable data rate is obtained with

$$C_a^{\text{PSRC}} = \frac{B_W}{N} \max_{\mathbf{\Lambda}_P} \log_2 [\det(\mathbf{I}_{2N} + \mathbf{C}_a \mathbf{D}_a^{-1})], \quad (2.33)$$

in which

$$\mathbf{C}_a \mathbf{D}_a^{-1} = \begin{bmatrix} K_{1,SD^P} & 0 \\ 0 & K_{1,SRD^P,a} \end{bmatrix}. \quad (2.34)$$

Also for high value of  $P$ , it is had that  $\text{Tr}(\mathbf{\Lambda}_{P_0}) \gg \text{Tr}(\mathbf{I}_N)$  and  $\text{Tr}(\mathbf{\Lambda}_{P_1}) \gg \text{Tr}(\mathbf{I}_N)$ , therefore  $\text{Tr}(K_{1,SD^P}) \gg \text{Tr}(\mathbf{I}_N)$  as well as  $\text{Tr}(K_{1,SRD^P,a}) \gg \text{Tr}(\mathbf{I}_N)$ . Again, the value of  $\mathbf{I}_{2N}$  is negligible in (2.33). Then,  $K_3 = \log_2 [\det(\mathbf{diag}\{K_{1,SD^P}, K_{1,SRD^P,a}\})]$ , resulting that

$$C_a^{\text{PSRC}} = K_3 \frac{B_W}{N} \leq 2K_2 \frac{B_W}{N}, \quad (2.35)$$

when  $\text{Tr}(K_{1,SD^P}) \gg \text{Tr}(\mathbf{I}_N)$  and  $\text{Tr}(K_{1,SRD^P,a}) \gg \text{Tr}(\mathbf{I}_N)$ . Also, the same results are achieved for WSRC.

Finally, for HSRC and given  $\mathbf{H}_\ell^q, \forall \ell, q$ , the achievable data rate is given by

$$C_a^{\text{HSRC}} = \frac{B_W}{N} \max_{\mathbf{\Lambda}_P} \log_2 [\det(\mathbf{I}_{4N} + \mathbf{C}_a \mathbf{D}_a^{-1})], \quad (2.36)$$

in which

$$\mathbf{C}_a \mathbf{D}_a^{-1} = \begin{bmatrix} K_{1,SD^P} & 0 & 0 & 0 \\ 0 & K_{1,SRD^P,a} & 0 & 0 \\ 0 & 0 & K_{1,SD^W} & 0 \\ 0 & 0 & 0 & K_{1,SRD^W,a} \end{bmatrix}. \quad (2.37)$$

If  $P$  is very high, then  $\text{Tr}(\mathbf{\Lambda}_P) \gg \text{Tr}(\mathbf{I}_{4N})$ . Also  $\text{Tr}(K_{1,SD^P}) \gg \text{Tr}(\mathbf{I}_N)$  as well as  $\text{Tr}(K_{1,SRD^P,a})$ ,  $\text{Tr}(K_{1,SD^W})$ , and  $\text{Tr}(K_{1,SRD^W,a}) \gg \text{Tr}(\mathbf{I}_N)$ . Here, the value of  $\mathbf{I}_{4N}$  is negligible in (2.36). Furthermore,

$$K_4 = \log_2 [\det(\mathbf{diag}\{K_{1,SD^P}, K_{1,SRD^P,a}, K_{1,SD^W}, K_{1,SRD^W,a}\})],$$

resulting that

$$C_a^{\text{HSRC}} = K_4 \frac{B_W}{N} \leq 4K_2 \frac{B_W}{N}, \quad (2.38)$$

when  $\text{Tr}(\mathbf{\Lambda}_P) \gg \text{Tr}(\mathbf{I}_{4N})$ . Now, using the upper bound, the gain when  $P \rightarrow \infty$  is given by

$$\lim_{P \rightarrow \infty} \rho_a^{\text{PSRC}} = \lim_{P \rightarrow \infty} \frac{C_a^{\text{PSRC}}}{C_{SD}^P} = \lim_{P \rightarrow \infty} \frac{2K_2 B_W / N}{2K_2 B_W / N} = 1, \quad (2.39)$$

as well as  $\lim_{P \rightarrow \infty} \rho_a^{\text{WSRC}} = 1$ . For HSRC,

$$\lim_{P \rightarrow \infty} \rho_a^{\text{HSRC}} = \lim_{P \rightarrow \infty} \frac{C_a^{\text{HSRC}}}{C_{SD}^P} = \lim_{P \rightarrow \infty} \frac{4K_2 B_W / N}{2K_2 B_W / N} = 2. \quad (2.40)$$

In other words, if  $P \rightarrow \infty$ , the HSRC offers twice the achievable data rate of PSRC or WSRC, which are equal to the one of the  $SD^P$  link.

- (ii)  $P \rightarrow 0$ : It is assumed that  $P$  is a extremely low value. As a consequence, a very low value of  $C_{SD}^P$  will be experienced. Furthermore, a half of this value of achievable data rate will be obtained with PSRC due to the use of two time slots. This is explained due to the fact that any SRC tends to, preferably, use the  $SD$  link in order to transmit data when  $P \rightarrow 0$  because, if it uses the  $SRD$  link, then this extremely low and available total transmission power will be shared between S and R nodes and no data transmission will be possible under this condition. Therefore,

$$C_{SD}^P = 2K_0 \frac{B_W}{N}, \quad (2.41)$$

and

$$C_a^{\text{PSRC}} = K_0 \frac{B_W}{N}, \quad (2.42)$$

when  $P$  is very low, in which  $K_0 = \log_2 [\det(\mathbf{diag}\{\mathbf{I}_N + K_{1,SD^P}\})]$  and the division by two in (2.42) occurs due to the use of two time slots by PSRC. As a result,

$$\lim_{P \rightarrow 0} \rho_a^{\text{PSRC}} = \lim_{P \rightarrow 0} \frac{C_a^{\text{PSRC}}}{C_{SD}^P} = \lim_{P \rightarrow 0} \frac{K_0 B_W / N}{2K_0 B_W / N} = 0.5. \quad (2.43)$$

This result shows that the achievable data rate of PSRC is reduced to a half of the achievable data rate obtained with the  $SD^P$  link (direct link) when  $P \rightarrow 0$ . Furthermore, for WSRC, the wireless links are not so good in terms of achievable data rate as the PLC ones when  $P$  reduces. This occurs due to the PLC channel frequency selectivity, channel energy, additive power noise constraints, and OA adoption. In other words, WF can take advantage of the highest nSNR subchannels which are, in the majority, the PLC channel ones because it is known to be highly frequency selective. Also,  $C_a^{\text{WSRC}} \rightarrow \frac{1}{2}C_{SD}^W$ , in which  $C_{SD}^W$  is the achievable data rate attained with the sole use of the  $SD^W$  link. As mentioned before, the  $C_{SD}^W$  terms will have lower contribution than the  $C_{SD}^P$  ones, as  $P \rightarrow 0$ . As it is inside a  $\log_2$  operation, a non-linear relation will coordinate the relationship between  $C_a^{\text{WSRC}}$  and  $C_{SD}^P$ .

As a result, when  $P$  decreases,  $C_a^{\text{WSRC}}$  reduces in higher rate than  $C_{SD}^P$ , therefore  $\lim_{P \rightarrow 0} \rho_a^{\text{WSRC}} = 0$ .

Finally, the HSRC achievable data rate is a consequence of both PSRC and WSRC tendencies. As the dominant contribution of HSRC will be from the  $SD^P$  link, it is also evident that  $C_a^{\text{HSRC}} = C_a^{\text{PSRC}}$ , then  $\lim_{P \rightarrow 0} \rho_a^{\text{HSRC}} = \lim_{P \rightarrow 0} \rho_a^{\text{PSRC}} = 0.5$ .

(iii)  $\alpha \rightarrow \infty$ : In this situation, as  $\alpha$  grows, more energy is being given to the (PLC and wireless)  $SRD$  links. On the opposite, the  $SD$  links (including the referential  $SD^P$ ) remain with the same energy. Therefore, it is not difficult to conclude that  $\lim_{\alpha \rightarrow \infty} \rho_a^{\text{PSRC}} \rightarrow \infty$ ,  $\lim_{\alpha \rightarrow \infty} \rho_a^{\text{WSRC}} \rightarrow \infty$ , and  $\lim_{\alpha \rightarrow \infty} \rho_a^{\text{HSRC}} \rightarrow \infty$ .

(iv)  $\alpha \rightarrow 0$ : As  $\alpha$  decreases, any SRC tends to use solely the  $SD$  link as well as the HSRC tends to use both PLC and wireless  $SD$  links. As a consequence,  $C_a^{\text{PSRC}} \rightarrow \frac{1}{2}C_{SD}^P$ ,  $C_a^{\text{WSRC}} \rightarrow \frac{1}{2}C_{SD}^W$ , and  $C_a^{\text{HSRC}} \rightarrow \frac{1}{2}C_{SD}^{\text{HSRC}}$ , in which  $C_{SD}^{\text{HSRC}}$  is the achievable data rate attained with HSRC when it does not use the R node. Also, the division by two is due to the use of two time slots by PSRC, WSRC, and HSRC. As a result,  $\lim_{\alpha \rightarrow 0} \rho_a^{\text{PSRC}} = 0.5$ ,  $\lim_{\alpha \rightarrow 0} \rho_a^{\text{WSRC}} = \frac{1}{2}C_{SD}^W/C_{SD}^P$ , and  $\lim_{\alpha \rightarrow 0} \rho_a^{\text{HSRC}} = \frac{1}{2}C_{SD}^{\text{HSRC}}/C_{SD}^P$ . Finally, for the same aforementioned relation between PLC and wireless links, it is had that  $0 < \lim_{\alpha \rightarrow 0} \rho_a^{\text{WSRC}} < 0.5$  and  $0.5 < \lim_{\alpha \rightarrow 0} \rho_a^{\text{HSRC}} < 1$ .

(v)  $\beta \rightarrow 0$  and  $\beta \rightarrow \infty$ : In this situation, the R node is very close to the S ( $\beta \rightarrow \infty$ ) or D ( $\beta \rightarrow 0$ ) node resulting that the  $SRD$  link is not useful for data communication due to the bad condition of  $RD$  ( $\beta \rightarrow \infty$ ) or  $SR$  ( $\beta \rightarrow 0$ ) link, respectively. Thus, any SRC tends to use only the  $SD$  link and the same conclusion for situation (iv) can be assumed as true in this situation.

### 2.1.3 The Outage Probability

The power line and wireless channels are random process. Therefore, the diagonal matrices  $\mathbf{C}_{AF}$  and  $\mathbf{C}_{DF}$  are random process as well, resulting that the achievable data rate is also not deterministic. In this sense, outage probability is analyzed to show the probability that a target data rate is not supported by HSRC.

Basically, the outage event for a two time-slots communication system is defined as  $I(\mathbf{X}, \mathbf{Y})/2N \leq \mathcal{R}$ , in which  $\mathcal{R} \in \mathbb{R}_+$  is a given spectral efficiency value. Thus, the corresponding outage probability for the AF protocol, given realizations of the channels frequency responses  $\mathbf{H}_{SD}^P$ ,  $\mathbf{H}_{SR}^P$ ,  $\mathbf{H}_{RD}^P$ ,  $\mathbf{H}_{SD}^W$ ,  $\mathbf{H}_{SR}^W$  and  $\mathbf{H}_{RD}^W$ , is expressed by

$$\begin{aligned} P_{AF}(\mathcal{R}) &= \mathbb{P}\left\{\frac{1}{2N} \log_2 [\det(\mathbf{I}_{4N} + \mathbf{C}_{AF} \mathbf{D}_{AF}^{-1})] \leq \mathcal{R}\right\} \\ &= \mathbb{P}\left\{\det(\mathbf{I}_{4N} + \mathbf{C}_{AF} \mathbf{D}_{AF}^{-1}) \leq 2^{2\mathcal{R}N}\right\}, \end{aligned} \quad (2.44)$$

where  $\mathbb{P}\{a \leq b\}$  denotes the probability that  $a \in \mathbb{R}$  is less than or equal to  $b \in \mathbb{R}$  and  $\mathbf{C}_{AF}$  and  $\mathbf{D}_{AF}$  are given by (2.18) and (2.19), respectively. Moreover, the outage probability

for the DF protocol, given a spectral efficiency value  $\mathcal{R} \in \mathbb{R}_+$  and realizations of the channels frequency responses  $\mathbf{H}_{SD}^P, \mathbf{H}_{SR}^P, \mathbf{H}_{RD}^P, \mathbf{H}_{SD}^W, \mathbf{H}_{SR}^W$  and  $\mathbf{H}_{RD}^W$ , is given by

$$\begin{aligned} P_{DF}(\mathcal{R}) &= \mathbb{P}\left\{\frac{1}{2N} \log_2 [\det(\mathbf{I}_{4N} + \mathbf{C}_{DF} \mathbf{D}_{DF}^{-1})] \leq \mathcal{R}\right\} \\ &= \mathbb{P}\left\{\det(\mathbf{I}_{4N} + \mathbf{C}_{DF} \mathbf{D}_{DF}^{-1}) \leq 2^{2\mathcal{R}N}\right\}, \end{aligned} \quad (2.45)$$

in which  $\mathbf{C}_{DF}$  and  $\mathbf{D}_{DF}$  are given by (2.22) and (2.23), respectively.

## 2.2 The Incomplete Hybrid Single-Relay Channel

In this section, closed-form expressions of the incomplete HSRC ergodic achievable data rates and outage probabilities assuming AF and DF cooperative protocols are derived as well as limit analyses concerning the achievable data rate. The incomplete HSRC is characterized by the loss of one link or one node communication interface which can happen due to natural causes or human being influence. A summary of the most common of these issues are as follows:

- Wireless communication path interruption due to the growth of tree or construction of building.
- Wireless signal attenuation due to rain and snow events.
- The mutual interference among wireless or PLC signals from distinct users operating in the same frequency bandwidth.
- Interruption of the power line due to an automotive accident, the fall of a tree or natural events such as intense rain or wind.
- The connection/disconnection of load and a change in the electric power grid circuit design.
- A hardware failure of either power line or wireless data communication interface of any node.

### 2.2.1 The Incomplete HSRC: Achievable Data Rate

Subsection 2.2.1.1 outlines the directions to the ergodic achievable data rate for the HSRC when a link is lost, while Subsection 2.2.1.2 shows how to derive the expressions of the ergodic achievable data rate when the HSRC experiences a node communication interface loss.

### 2.2.1.1 The HSRC without a link

Figures 2 to 4 show the HSRC without  $SD^q$ ,  $SR^q$ , and  $RD^q$ , respectively, where the lost link is highlighted in the red color. The removal of a link of HSRC represents situations in which the power line is broken or the wireless channel link faces strong signal attenuation. When the  $\ell^{th}$  link associated with the  $q^{th}$  medium is missing ( $SD^q$ ,  $SR^q$  or  $RD^q$ ), it is assumed that  $\Lambda_{\sigma^2_{V_\ell}} \rightarrow \infty$  and performed (2.17) and (2.21) using  $\mathbf{I}_{3N}$  instead of  $\mathbf{I}_{4N}$ . These modified diagonal matrices will be labeled as  $\mathbf{C}'_{AF}$ ,  $\mathbf{D}'_{AF}$ ,  $\mathbf{C}'_{DF}$  and  $\mathbf{D}'_{DF}$ . Furthermore, by assuming that the respective link is a harsh medium to data communication, it will not contribute to the achievable data rate of the incomplete HSRC at all. Overall, it is not counterintuitive to assume that this link, affected by one of the issues mentioned at the beginning of this section, experiences extremely high attenuation or extremely high power noise. See Appendix A, B, and C for more details.

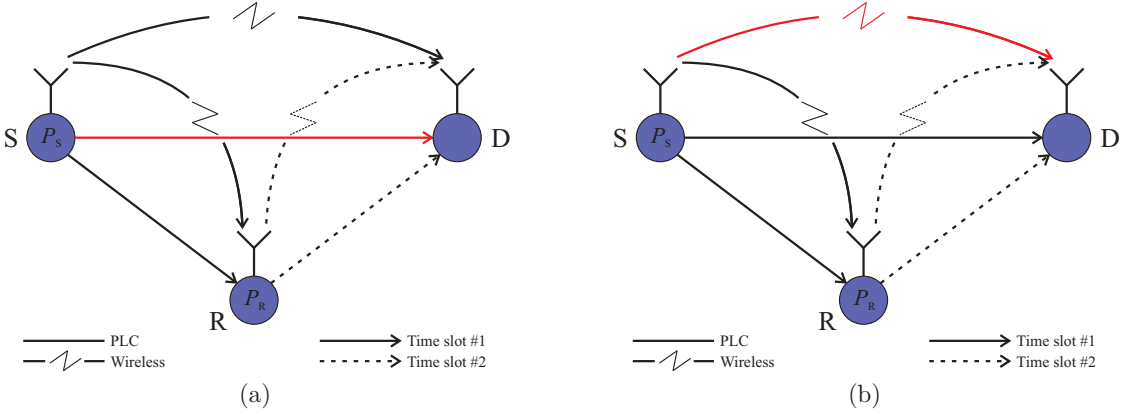


Figure 2: The HSRC without  $SD^q$ , for (a)  $q = P$  and (b)  $q = W$ .

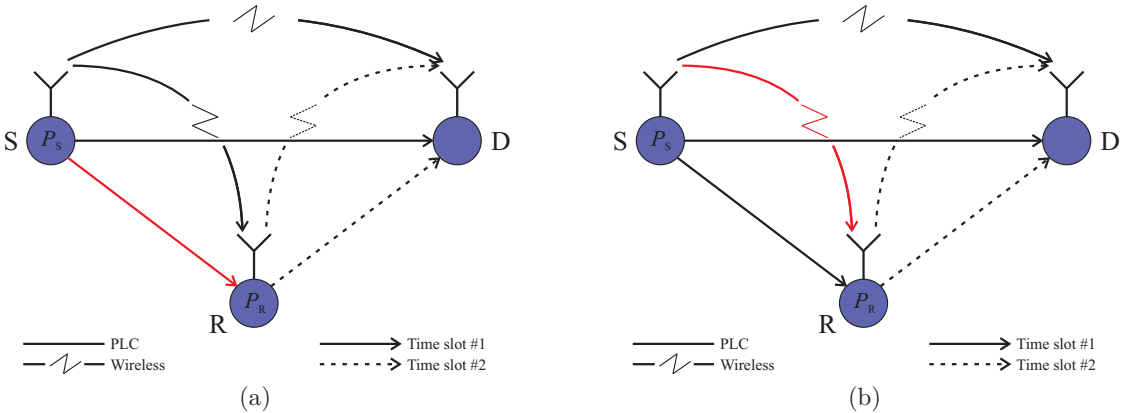


Figure 3: The HSRC without  $SR^q$ , for (a)  $q = P$  and (b)  $q = W$ .

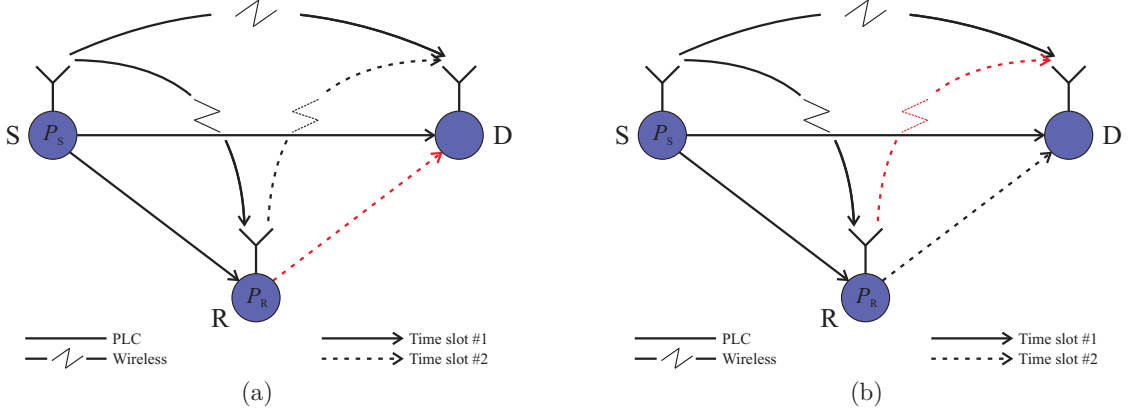


Figure 4: The HSRC without  $RD^q$ , for (a)  $q = P$  and (b)  $q = W$ .

### 2.2.1.2 The HSRC without one node communication interface

The HSRC without a node communication interface mimics situations in which one of the nodes is not hybrid. In other words, the node does not have a PLC or wireless communication interface. In this regard, a briefly explanation of how to compute the achievable data rate of such HSRC (see (2.17) and (2.21)) is presented when a PLC or wireless communication interface is missing at a given node ( $S^q$ ,  $R^q$  or  $D^q$ ). For the sake of simplicity, it is defined  $\bar{q} \triangleq P$ , if  $q = W$  and  $\bar{q} \triangleq W$ , if  $q = P$ , for further use. Here again, the modified diagonal matrices will be labeled as  $\mathbf{C}'_{AF}$ ,  $\mathbf{D}'_{AF}$ ,  $\mathbf{C}'_{DF}$  and  $\mathbf{D}'_{DF}$ . Deductions of this kind of incomplete HSRC are as follows:

*$S^q$  is lost:* If the  $q^{th}$  medium communication interface of the S node is lost, then the  $SD^q$  and  $SR^q$  links are lost (see Figure 5, the links and node communication interface lost are highlighted in red). Using the AF protocol, the achievable data rate of the incomplete HSRC can be calculated replacing  $\Lambda_{P_0^q} \Lambda_{\mathbf{Y}_{SR}^q}^{-1} \Lambda_{|\mathbf{h}_{SR}^q|^2}$  and  $\Lambda_{\mathbf{Y}_{SR}^q}^{-1} \Lambda_{\mathbf{v}_{SR}^q}$  by  $\Lambda_{P_0^{\bar{q}}} \Lambda_{\mathbf{Y}_{SR}^{\bar{q}}}^{-1} \Lambda_{|\mathbf{h}_{SR}^{\bar{q}}|^2}$  and  $\Lambda_{\mathbf{Y}_{SR}^{\bar{q}}}^{-1} \Lambda_{\mathbf{v}_{SR}^{\bar{q}}}$ , respectively, in the second (if removing  $S^P$ ) or the fourth (if removing  $S^W$ ) element of the diagonal matrices in (2.18) and (2.19). Also, it is necessary to remove the first (if removing  $S^P$ ) or the third (if removing  $S^W$ ) element in the diagonal matrices expressed in (2.18) and (2.19), and, to use  $\mathbf{I}_{3N}$  instead of  $\mathbf{I}_{4N}$  in (2.17).

Regarding the DF protocol, when a  $q^{th}$  medium communication interface of the S node is lost, the calculation of the achievable data rate is made by introducing the following changes at the second (if removing  $S^P$ ) or the fourth (if removing  $S^W$ ) element in (2.22) and (2.23), respectively,

$$\Lambda_{C^{\bar{q}*}} = \begin{cases} \Lambda_{P_0^{\bar{q}}} \Lambda_{|\mathbf{h}_{SR}^{\bar{q}}|^2}, & \text{if } C^{\bar{q}}_{SR} = \min\{C^{\bar{q}}_{SR}, C^q_{RD}\} \\ \Lambda_{P_1^q} \Lambda_{|\mathbf{h}_{RD}^q|^2}, & \text{otherwise,} \end{cases} \quad (2.46)$$

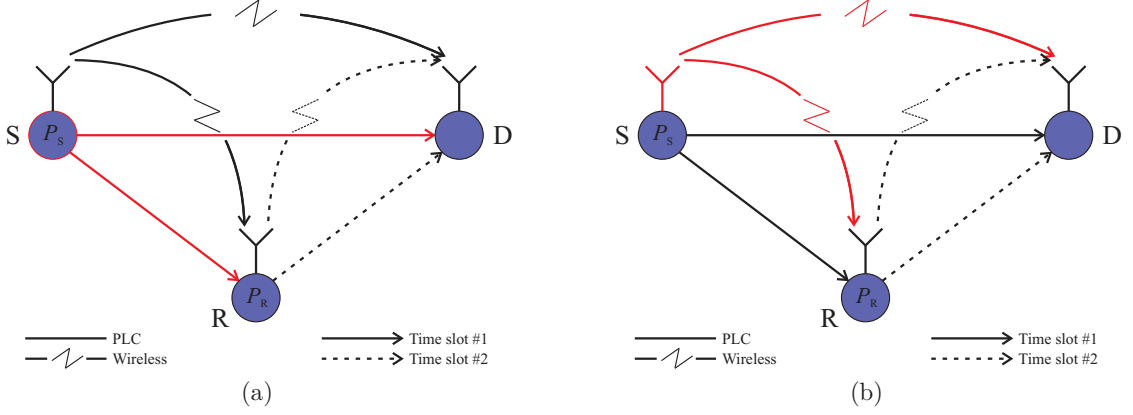


Figure 5: The HSRC without  $S^q$ , for (a)  $q = P$  and (b)  $q = W$ .

and

$$\Lambda_{D^{\bar{q}^*}} = \begin{cases} \Lambda_{\sigma_{\mathbf{v}_{SR}^{\bar{q}}}^2}, & \text{if } C_{SR}^{\bar{q}} = \min\{C_{SR}^{\bar{q}}, C_{RD}^{\bar{q}}\} \\ \Lambda_{\sigma_{\mathbf{v}_{RD}^{\bar{q}}}^2}, & \text{otherwise.} \end{cases} \quad (2.47)$$

Also, it is necessary to remove the first (if removing  $S^P$ ) or the third (if removing  $S^W$ ) element in (2.22) and (2.23), and to make use of  $\mathbf{I}_{3N}$  in (2.21). See Appendix D for more details.

$R^q$  is lost: If the  $q^{\text{th}}$  medium communication interface of the R node is missed, then it results in the loss of  $SR^q$  and  $RD^q$  links (see Figure 6, the links and node communication interface lost are highlighted in red). Adopting the AF protocol, the achievable data rate is calculated by removing the second (if removing  $R^P$ ) or the fourth (if removing  $R^W$ ) element in the diagonal of matrices given by (2.18) and (2.19) and using  $\mathbf{I}_{3N}$  in (2.17). Regarding the DF protocol, the achievable data rate is attained by removing the second (if removing  $R^P$ ) or the fourth (if removing  $R^W$ ) element in the diagonal of matrices expressed by (2.22) and (2.23) and using  $\mathbf{I}_{3N}$  in (2.21). See Appendix E for more details.

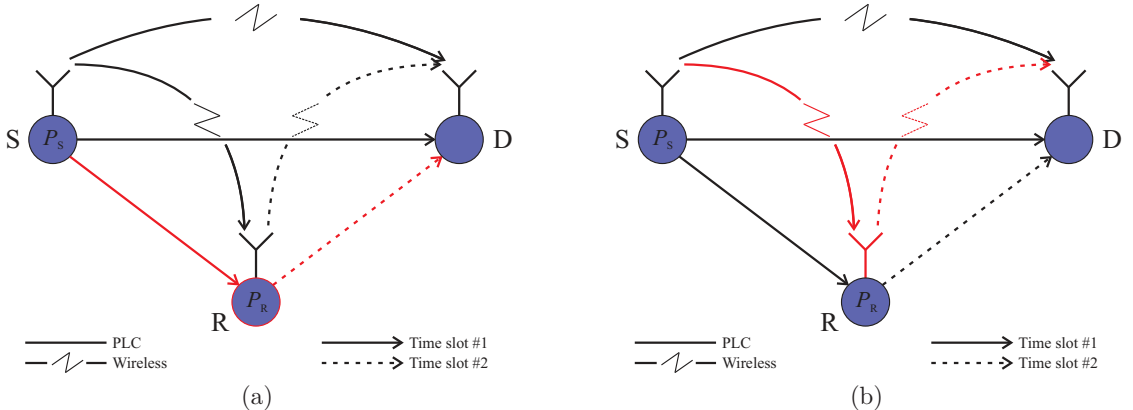


Figure 6: The HSRC without  $R^q$ , for (a)  $q = P$  and (b)  $q = W$ .

$D^q$  is lost: When  $D^q$  is missed (see Figure 7, the links and node communication interface lost are highlighted in red), HSRC turns into a PLC SRC or wireless SRC since the  $SD^q$  and  $RD^q$  links are lost and no combining technique is used at the R node to take advantage of the remaining  $SR$  links. Thus, if the  $D^q$  link is lost, the achievable data rate of the incomplete HSRC with the AF protocol is calculated by removing the first and second (if removing  $D^P$ ) or the third and fourth (if removing  $D^W$ ) elements in the diagonal of matrices given by (2.18) and (2.19) and using  $\mathbf{I}_{2N}$  in (2.17). For the DF protocol, the achievable data rate is obtained by removing the first and second (if removing  $D^P$ ) or the third and fourth (if removing  $D^W$ ) elements in the diagonal of matrices expressed by (2.22) and (2.23) and using  $\mathbf{I}_{2N}$  in (2.21). See Appendix F for more details.

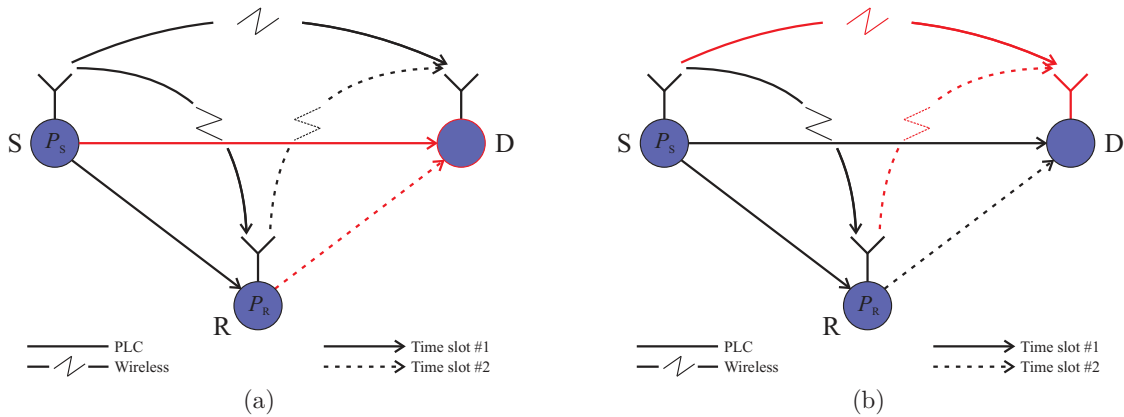


Figure 7: The HSRC without  $D^q$ , for (a)  $q = P$  and (b)  $q = W$ .

### 2.2.2 Limit Analyses of the Incomplete HSRC

Similar to Subsection 2.1.2, it is assumed that the complete CSI is available at the transmitter side and the use of OA based on the WF technique [44] at the S and R nodes. Furthermore, it is assumed that when HSRC loses the  $SR^q$  link,  $P_0^q$  is allocated only to the  $SD^q$  link and that  $P_0^q$  is allocated only to  $SR^q$  if a loss of  $SD^q$  link is experienced. Additionally, when the  $RD^q$  link is lost, it is made that  $P_1^{\bar{q}} = P_R$ .

Here, the achievable data rate ratio, given by

$$\varrho_a^b = \frac{C_a^{b*}}{C_a^{\text{HSRC}}}, \quad (2.48)$$

is used as a metric to quantify the gain or loss in relation to the achievable data rate associated with HSRC, in which  $a \in \{AF, DF\}$  denotes AF or DF protocol and  $b \in \{H, P, W\}$  denotes incomplete HSRC, PSRC, and WSRC models, respectively. Also,  $C_a^{b*}$  denotes the achievable data rate of HSRC if it loses a link or a node communication interface (the incomplete HSRC), or either one of PSRC or WSRC achievable data rate.

Concerning (2.48), the following limit analyses deserve attention:

- (I)  $P \rightarrow \infty$ : From (2.38), it is known that the achievable data rate of HSRC, when  $P$  is very high, is given by

$$C_a^{\text{HSRC}} = K_4 \frac{B_W}{N} \leq 4K_2 \frac{B_W}{N}. \quad (2.49)$$

Now, for the incomplete HSRC (except for the HSRC without  $D^q$ ) and given  $\mathbf{H}_\ell^q, \forall \ell, q$ , the achievable data rate is obtained by

$$C_a^{H^*} = \frac{B_W}{N} \max_{\mathbf{\Lambda}_P} \log_2 [\det(\mathbf{I}_{3N} + \mathbf{C}'_a \mathbf{D}'_a{}^{-1})], \quad (2.50)$$

in which

$$\mathbf{C}'_a \mathbf{D}'_a{}^{-1} = \begin{bmatrix} K_{1,SD\bar{q}} & 0 & 0 \\ 0 & K_{1,SRD\bar{q},a} & 0 \\ 0 & 0 & K_{1,\ell^q} \end{bmatrix}. \quad (2.51)$$

where  $K_{1,\ell^q}$  is the remaining  $q^{\text{th}}$  channel associated with the  $\ell^{\text{th}}$  link. Making  $P$  an extremely high value, it implies that  $\text{Tr}(\mathbf{\Lambda}_P) \gg \text{Tr}(\mathbf{I}_{3N})$ , thus  $\text{Tr}(K_{1,SD\bar{q}}) \gg \text{Tr}(\mathbf{I}_N)$  as well as  $\text{Tr}(K_{1,SRD\bar{q},a})$  and  $\text{Tr}(K_{1,\ell^q}) \gg \text{Tr}(\mathbf{I}_N)$ . Then, the value of  $\mathbf{I}_{3N}$  is negligible in (2.50). Furthermore,  $K_5 = \log_2 [\det(\mathbf{diag}\{K_{1,SD\bar{q}}, K_{1,SRD\bar{q},a}, K_{1,\ell^q}\})]$ , resulting that

$$C_a^{H^*} = K_5 \frac{B_W}{N} \leq 3K_2 \frac{B_W}{N}, \quad (2.52)$$

when  $P$  is very high. Concerning PSRC (similar to the HSRC without  $D^W$ ), it is had that, from (2.35),

$$C_a^{P^*} = K_3 \frac{B_W}{N} \leq 2K_2 \frac{B_W}{N}, \quad (2.53)$$

when  $P$  is very high and for WSRC (and the HSRC without  $D^P$ ) the same result is obtained. Consequently, using the upper bound, the ratio when  $P \rightarrow \infty$  is given by

$$\lim_{P \rightarrow \infty} \varrho_a^H = \lim_{P \rightarrow \infty} \frac{C_a^{H^*}}{C_a^{\text{HSRC}}} = \lim_{P \rightarrow \infty} \frac{3K_2 B_W / N}{4K_2 B_W / N} = 0.75 \quad (2.54)$$

and

$$\lim_{P \rightarrow \infty} \varrho_a^P = \lim_{P \rightarrow \infty} \frac{C_a^{P^*}}{C_a^{\text{HSRC}}} = \lim_{P \rightarrow \infty} \frac{2K_2 B_W / N}{4K_2 B_W / N} = 0.5 \quad (2.55)$$

as well as  $\lim_{P \rightarrow \infty} \varrho_a^W = 0.5$ .

- (II)  $P \rightarrow 0$ : Making  $P$  very low, it results that the HSRC achievable data rate will be very dependent on the  $SD^P$  link. Furthermore, the half of this value of achievable data rate will be obtained for PSRC. This is explained due to the fact that any SRC tends to, preferably, use the  $SD$  link in order to transmit data when  $P \rightarrow 0$  because, if it uses the  $SRD$  link, this extremely low available transmission power will be shared between S and R nodes. Also, as stated before, the PLC links attains higher achievable data rate for low values of  $P$  than the wireless ones, given the adopted constraints. Thus,

$$C_{SD}^P = 2K_0 \frac{B_W}{N}, \quad (2.56)$$

while

$$C_a^{P^*} = K_0 \frac{B_W}{N}, \quad (2.57)$$

and

$$C_a^{\text{HSRC}} = K_0 \frac{B_W}{N}, \quad (2.58)$$

when  $P$  is extremely low, in which  $K_0 = \log_2 [\det(\mathbf{diag}\{\mathbf{I}_N + K_{1,SD^P}\})]$ . This results in

$$\lim_{P \rightarrow 0} \rho_a^P = \lim_{P \rightarrow 0} \frac{C_a^{P^*}}{C_a^{\text{HSRC}}} = \lim_{P \rightarrow 0} \frac{K_0 B_W / N}{K_0 B_W / N} = 1. \quad (2.59)$$

Again, the loss of the  $SD^P$  link is crucial. Therefore, HSRC without  $SD^P$ ,  $S^P$  or  $D^P$ , results in  $\lim_{P \rightarrow 0} \rho_a^H = 0$  and for the same reason  $\lim_{P \rightarrow 0} \rho_a^W = 0$ . Any other incomplete HSRC that contains the  $SD^P$  link will use only it for data communication. As a consequence,  $\lim_{P \rightarrow 0} \rho_a^H = 1$ .

- (III)  $\alpha \rightarrow \infty$ : In this situation, as  $\alpha$  grows, more energy is given to (PLC and wireless)  $SRD$  links. Therefore,  $C_a^{P^*} \rightarrow C_{SRD,a}^P$ ,  $C_a^{W^*} \rightarrow C_{SRD,a}^W$ , and  $C_a^{H^*} \rightarrow C_{SRD,a}^{H^*}$  as well as  $C_a^{\text{HSRC}} \rightarrow C_{SRD,a}^{\text{HSRC}}$ , in which  $C_{SRD,a}^P$ ,  $C_{SRD,a}^W$ ,  $C_{SRD,a}^{H^*}$ , and  $C_{SRD,a}^{\text{HSRC}}$  are, respectively, the values of achievable data rate attained with the sole use of PLC  $SRD$ , wireless  $SRD$ , the incomplete HSRC using only the  $SRD$  link(s), and the HSRC using both PLC and wireless  $SRD$  links. As a result,  $\lim_{\alpha \rightarrow \infty} \rho_a^P = 0.5$ ,  $\lim_{\alpha \rightarrow \infty} \rho_a^W = 0.5$ , while  $\lim_{\alpha \rightarrow \infty} \rho_a^H = 1$  (for HSRC without  $SD^q$  or  $S^q, \forall q$ ) and  $\lim_{\alpha \rightarrow \infty} \rho_a^H = 0.5$  (for HSRCs without  $SR^q, RD^q, R^q$ , or  $D^q, \forall q$ ).
- (IV)  $\alpha \rightarrow 0$ : On the other hand, as  $\alpha$  decreases, the SRC tends to use solely the  $SD$  link as well as HSRC tends to use both PLC and wireless  $SD$  links. As a consequence,  $C_a^{P^*} \rightarrow \frac{1}{2}C_{SD}^P$ ,  $C_a^{W^*} \rightarrow \frac{1}{2}C_{SD}^W$ , and  $C_a^{H^*} \rightarrow \frac{1}{2}C_{SD}^{H^*}$  as well as  $C_a^{\text{HSRC}} \rightarrow \frac{1}{2}C_{SD}^{\text{HSRC}}$ , in which  $C_{SD}^{H^*}$  is the value of achievable data rate attained with the incomplete HSRC using the disposable(s)  $SD$  link(s). Also, the division by two is due to the use of two time slots by PSRC, WSRC, and HSRC. As a result,  $0.5 < \lim_{\alpha \rightarrow 0} \rho_a^P < 1$ ,  $0 < \lim_{\alpha \rightarrow 0} \rho_a^W < 0.5$ , while  $\lim_{\alpha \rightarrow 0} \rho_a^H = 1$  (for the HSRC without  $SR^q, RD^q$ , or  $R^q, \forall q$ ), as well as  $0 < \lim_{\alpha \rightarrow 0} \rho_a^H < 0.5$  (for the HSRC without  $SD^P, S^P$  or  $D^P$ ) and  $0.5 < \lim_{\alpha \rightarrow 0} \rho_a^H < 1$  (for the HSRC without  $SD^W, S^W$  or  $D^W$ ).
- (V)  $\beta \rightarrow 0$  and  $\beta \rightarrow \infty$ : In this situation, the R node is very close to the S ( $\beta \rightarrow \infty$ ) or D ( $\beta \rightarrow 0$ ) node, resulting that the  $SRD$  link is not good due to the bad condition of  $RD$  ( $\beta \rightarrow \infty$ ) or  $SR$  ( $\beta \rightarrow 0$ ) link, respectively. Thus, any SRC tends to use only the  $SD$  link and the same conclusion for situation (IV) can be assumed as true in this situation.

### 2.2.3 The Outage Probability

Again, the outage probability will be also used as a evaluation metric to the incomplete HSRC. The diagonal matrices  $\mathbf{C}_{AF}$  and  $\mathbf{C}_{DF}$  are random, thus  $\mathbf{C}'_{AF}$  and

$\mathbf{C}'_{DF}$  are as well. In this regard, an analysis between the probabilities of a specific data rate which is not supported by the incomplete HSRC can be performed. Furthermore, Subsection 2.2.3.1 shows the outage probability associated with HSRC when it loses a link, while Subsection 2.2.3.2 describes the outage probability of HSRC when it experiences a node communication interface loss.

### 2.2.3.1 The HSRC without a link

For situations in which HSRC loses a link, the outage probability of such incomplete HSRC with AF protocol is expressed as

$$\begin{aligned} P_{AF}(\mathcal{R}) &= \mathbb{P}\left\{\frac{1}{2N} \log_2 [\det(\mathbf{I}_{3N} + \mathbf{C}'_{AF} \mathbf{D}'_{AF}{}^{-1})] \leq \mathcal{R}\right\} \\ &= \mathbb{P}\left\{\det(\mathbf{I}_{3N} + \mathbf{C}'_{AF} \mathbf{D}'_{AF}{}^{-1}) \leq 2^{2\mathcal{R}N}\right\}, \end{aligned} \quad (2.60)$$

and, for the DF protocol, the outage probability is expressed by

$$\begin{aligned} P_{DF}(\mathcal{R}) &= \mathbb{P}\left\{\frac{1}{2N} \log_2 [\det(\mathbf{I}_{3N} + \mathbf{C}'_{DF} \mathbf{D}'_{DF}{}^{-1})] \leq \mathcal{R}\right\} \\ &= \mathbb{P}\left\{\det(\mathbf{I}_{3N} + \mathbf{C}'_{DF} \mathbf{D}'_{DF}{}^{-1}) \leq 2^{2\mathcal{R}N}\right\}. \end{aligned} \quad (2.61)$$

in which  $\mathbf{C}'_{AF}$ ,  $\mathbf{D}'_{AF}$ ,  $\mathbf{C}'_{DF}$  and  $\mathbf{D}'_{DF}$  are the modified diagonal matrices (see Appendix A, B, and C for more details about these matrices).

### 2.2.3.2 The HSRC without one communication interface

To compute the outage probability when HSRC loses a communication interface, the same changes outlined in Subsection 2.2.1.2 for the achievable data rate equations are made in (2.44) and (2.45), for AF and DF protocols, respectively. As a result, outage probabilities are evaluated as follows:

*S<sup>q</sup> is lost:* In this case, the outage probability for the AF protocol is given by

$$\begin{aligned} P_{AF}(\mathcal{R}) &= \mathbb{P}\left\{\frac{1}{2N} \log_2 [\det(\mathbf{I}_{3N} + \mathbf{C}'_{AF} \mathbf{D}'_{AF}{}^{-1})] \leq \mathcal{R}\right\} \\ &= \mathbb{P}\left\{\det(\mathbf{I}_{3N} + \mathbf{C}'_{AF} \mathbf{D}'_{AF}{}^{-1}) \leq 2^{2\mathcal{R}N}\right\}, \end{aligned} \quad (2.62)$$

and, for the DF protocol, the outage probability is expressed by

$$\begin{aligned} P_{DF}(\mathcal{R}) &= \mathbb{P}\left\{\frac{1}{2N} \log_2 [\det(\mathbf{I}_{3N} + \mathbf{C}'_{DF} \mathbf{D}'_{DF}{}^{-1})] \leq \mathcal{R}\right\} \\ &= \mathbb{P}\left\{\det(\mathbf{I}_{3N} + \mathbf{C}'_{DF} \mathbf{D}'_{DF}{}^{-1}) \leq 2^{2\mathcal{R}N}\right\}, \end{aligned} \quad (2.63)$$

in which  $\mathbf{C}'_{AF}$ ,  $\mathbf{D}'_{AF}$ ,  $\mathbf{C}'_{DF}$  and  $\mathbf{D}'_{DF}$  are the modified diagonal matrices (see Appendix D for more details about these matrices).

$R^q$  is lost: When  $R^q$  is lost, the outage probability for the AF protocol is given by

$$\begin{aligned} P_{AF}(\mathcal{R}) &= \mathbb{P}\left\{\frac{1}{2N} \log_2 [\det(\mathbf{I}_{3N} + \mathbf{C}'_{AF} \mathbf{D}'_{AF}{}^{-1})] \leq \mathcal{R}\right\} \\ &= \mathbb{P}\left\{\det(\mathbf{I}_{3N} + \mathbf{C}'_{AF} \mathbf{D}'_{AF}{}^{-1}) \leq 2^{2\mathcal{R}N}\right\}, \end{aligned} \quad (2.64)$$

and, for the DF protocol, it is expressed by

$$\begin{aligned} P_{DF}(\mathcal{R}) &= \mathbb{P}\left\{\frac{1}{2N} \log_2 [\det(\mathbf{I}_{3N} + \mathbf{C}'_{DF} \mathbf{D}'_{DF}{}^{-1})] \leq \mathcal{R}\right\} \\ &= \mathbb{P}\left\{\det(\mathbf{I}_{3N} + \mathbf{C}'_{DF} \mathbf{D}'_{DF}{}^{-1}) \leq 2^{2\mathcal{R}N}\right\}, \end{aligned} \quad (2.65)$$

in which  $\mathbf{C}'_{AF}$ ,  $\mathbf{D}'_{AF}$ ,  $\mathbf{C}'_{DF}$  and  $\mathbf{D}'_{DF}$  are the modified diagonal matrices (see Appendix E for more details about these matrices)).

$D^q$  is lost: For the AF protocol, the  $D^q$  loss results the outage probability given by

$$\begin{aligned} P_{AF}(\mathcal{R}) &= \mathbb{P}\left\{\frac{1}{2N} \log_2 [\det(\mathbf{I}_{2N} + \mathbf{C}'_{AF} \mathbf{D}'_{AF}{}^{-1})] \leq \mathcal{R}\right\} \\ &= \mathbb{P}\left\{\det(\mathbf{I}_{2N} + \mathbf{C}'_{AF} \mathbf{D}'_{AF}{}^{-1}) \leq 2^{2\mathcal{R}N}\right\}, \end{aligned} \quad (2.66)$$

and, for the DF protocol, it is expressed by

$$\begin{aligned} P_{DF}(\mathcal{R}) &= \mathbb{P}\left\{\frac{1}{2N} \log_2 [\det(\mathbf{I}_{2N} + \mathbf{C}'_{DF} \mathbf{D}'_{DF}{}^{-1})] \leq \mathcal{R}\right\} \\ &= \mathbb{P}\left\{\det(\mathbf{I}_{2N} + \mathbf{C}'_{DF} \mathbf{D}'_{DF}{}^{-1}) \leq 2^{2\mathcal{R}N}\right\}, \end{aligned} \quad (2.67)$$

in which  $\mathbf{C}'_{AF}$ ,  $\mathbf{D}'_{AF}$ ,  $\mathbf{C}'_{DF}$  and  $\mathbf{D}'_{DF}$  are the modified diagonal matrices (see Appendix F for more details about these matrices)).

### 3 Numerical Results

In order to carry out numerical simulations regarding HSRC and incomplete HSRC models, the signal transmission is assumed to occur in the industrial, scientific, and medical (ISM) frequency band (915-915.5 MHz) for wireless communication and the low-frequency band (0-500 kHz) for PLC. The occupied frequency bandwidth is 500 kHz in both media. The NB-PLC is standardized to operate in the frequencies above 500 kHz [48]. Thus, to have equality and fairness, the LP-RF wireless data transmission will occur with the same bandwidth as the one of the NB-PLC. Moreover, the choice of the center frequency of the LP-RF wireless transmission could be any of the unlicensed wireless frequencies (2.45 GHz, 5.8 GHz, etc). However, in this work, it is assumed to be at the frequency of 915.25 MHz. Furthermore, a large value of  $N$  is used such that the subchannels gains and power spectral density (PSD) of the additive noise are flat within each subchannel. This choice is useful to accomplish numerical simulations.

Brief descriptions of the adopted NB-PLC and LP-RF wireless channels models are presented as follows:

*NB-PLC channel model:* The well-known Zimmerman and Dostert [9] channel model is used, employing the parameters taken from IEEE 1901.2 standard [48, Annex D]. The frequency response of a power line channel is given by

$$H(f) = \sum_{i=1}^{N_p} g_i e^{(-a_0 + a_1 f^k) d_i} e^{-j2\pi \frac{d_i}{v_0}}, \quad (3.1)$$

where  $N_p$  is the number of propagation paths between transmitter and receiver;  $g_i$  is a weighting factor that summarizes the reflection and transmission loss along a propagation path. It is a Gaussian r.v. with zero mean and variance 1, which is scaled by 10000;  $a_0$  and  $a_1$  are attenuation parameters that depend on the characteristics of the transmission line, such as impedance;  $k$  is the slope of attenuation with respect to frequency;  $d_i$  is a Gaussian r.v. representing the length of propagation paths from transmitter to receiver (in meters) with mean  $d_a$  and standard deviation  $d_s$ , such that  $d_s < d_m$ ; and  $v_0$  is the wave propagation speed in the power line in meters/second. In accord with [48, Annex D], the values of adopted parameters for this NB-PLC channel are listed in Table 1.

The additive noise in this NB-PLC channel is modeled as a zero mean colored Gaussian random process. Adopted from [49], its PSD is expressed by

$$S^P(f) = \frac{\eta}{2} \exp(-\nu|f|), \quad (3.2)$$

where  $\nu, \eta \in \mathbb{R}_+$  are constants equal to  $1.2 \times 10^{-5}$  and  $1.0 \times 10^{-15}$ , respectively, and  $f$  is the frequency in Hertz (Hz). Given the subchannel bandwidth,  $\Delta f = B_W/N$ , thus

$$\mathbf{\Lambda}_{\mathbf{V}_\ell^P}^{\sigma^2} = \Delta f \cdot \mathbf{diag} \left\{ S^P(0), S^P(\Delta f), \dots, S^P([N-1]\Delta f) \right\}. \quad (3.3)$$

Table 1: Adopted values of the parameters used in the NB-PLC channel model.

Parameter	Value
$N_p$	50
$a_0$	$10^{-3}$
$a_1$	$2.5 \times 10^{-9}$
$k$	1
$d_a$	1000
$d_s$	400
$d_m$	100
$v_0$	$3 \times 10^{-8}/4$

*LP-RF wireless channel model:* The LP-RF wireless channel is obtained from a wideband wireless one by adopting the procedure suggested in the 802.15.4a IEEE wireless channel model report [50]. Basically, it is accomplished by filtering the wideband wireless channel model. The wideband wireless channel model is adopted from [50] and its power delay profile (PDP) is given by

$$\text{PDP}(t) = \sum_{l=0}^{\infty} \sum_{k=0}^{\infty} \beta_{kl} e^{j\theta_{kl}} \delta(n - T_l - \tau_{kl}), \quad (3.4)$$

where  $\beta_{kl}$  is a Rayleigh distribution r.v. modeling the path gains,  $\theta_{kl}$  is a r.v. with uniform distribution from 0 to  $2\pi$  modeling the randomness of phases, and,  $T_l$  and  $\tau_{kl}$  are Poisson distribution r.v. modeling the cluster (with rate  $\Gamma$ ) and ray (with rate  $\gamma$ ) arrival times, respectively.

In accord with [51], for the first cluster,  $T_0 = 0$ , and for the first ray within the  $l$ th cluster,  $\tau_{0l} = 0$ . Moreover,  $T_l$  and  $\tau_{kl}$  are described by the independent interarrival exponential probability density functions (pdfs)

$$p(T_l | T_{l-1}) = \Lambda e^{[-\Lambda(T_l - T_{l-1})]}, \quad (3.5)$$

and

$$p(\tau_{kl} | \tau_{(k-1)l}) = \lambda e^{[-\lambda(\tau_{kl} - \tau_{(k-1)l})]}, \quad (3.6)$$

respectively. Also, the path gains,  $\beta_{kl}$ , are modeled as a Rayleigh r.v. such that its pdf is given by

$$p(\beta_{kl}) = (2\beta_{kl}/\Omega_{kl}) e^{(-\beta_{kl}^2/\Omega_{kl})}, \quad (3.7)$$

where its mean-square value is

$$\Omega_{kl} = \overline{\beta^2(0,0)} e^{-\frac{T_l}{\Gamma}} e^{-\frac{\tau_{kl}}{\gamma}}, \quad (3.8)$$

and

$$\overline{\beta^2(0,0)} = (\gamma\lambda)^{-1} G(1\text{m}) r^{-\alpha}, \quad (3.9)$$

in which  $\overline{\beta^2(0,0)}$  is the average power gain of the first ray of the cluster and  $G(1\text{m})$  is the path loss at 1 meter distance,

$$G(1\text{m}) = G_t G_r \left( \frac{c}{4f\pi} \right)^2, \quad (3.10)$$

where  $c$  denotes the speed of light in meters/second, while  $G_t$  and  $G_r$  are the transmitter and receiver antenna gains, respectively.

Finally, but not the least, for each component of the cluster the small-scale realization of the amplitude,  $x$ , is computed as a Nakagami-distributed r.v.. Thus, its pdf is given by

$$p(x_{kl}) = \frac{2}{\Gamma(m)} \left( \frac{m}{\Omega_{kl}} \right)^m x^{2m-1} e^{-\frac{mx^2}{\Omega_{kl}}}, \quad (3.11)$$

where  $m \geq 1/2$  is the Nakagami  $m$ -factor,  $\Gamma(m)$  is the gamma function, and  $\Omega_{kl}$  is the mean-square value of the amplitude. The parameter  $m$  is modeled by Gaussian r.v. with mean and variance given by [50]

$$\mu(\tau_{kl}) = 3.5 - \tau_{kl}/73, \quad (3.12)$$

and

$$\sigma^2(\tau_{kl}) = 1.84 - \tau_{kl}/160, \quad (3.13)$$

respectively, in which  $\tau_{kl}$  is the  $k^{\text{th}}$  ray delay of the  $l^{\text{th}}$  cluster measured in nanoseconds.

Therefore, the wideband wireless channel continuous-time domain CIR is given by

$$h(t) = \sum_{l=0}^L \sum_{k=0}^K x_{kl} e^{j\theta_{kl}} \delta(t - T_l - \tau_{kl}). \quad (3.14)$$

According to [50] and [51], the adopted values for all parameters are displayed in Table 2. Note that  $L$  and  $K$  denote the maximum number of clusters and rays, respectively. It is important to emphasize that these values are given for a wideband wireless channel and, after the wideband channel is generated, it is filtered and its filtered CIR is of our interest.

The zero mean circularly symmetric complex Gaussian assumption is made for the wireless additive noise. Based on [37], the PSD of the additive noise in the wireless channel is considered to be

$$S^W(f) = -173.8 + NF \text{ dBm/Hz}, \quad (3.15)$$

where the receiver noise figure  $NF$  is equal to 7 dB. As a result,

$$\mathbf{\Lambda}_{\sigma_{\mathbf{v}_\ell}^2} = \Delta f \cdot \mathbf{diag} \left\{ S^W(0), S^W(\Delta f), \dots, S^W([N-1]\Delta f) \right\}. \quad (3.16)$$



and

$$\mu^2 \|\mathbf{h}_{SD}^q\|^2 = \|\mathbf{h}_{SR}^q\|^2 \|\mathbf{h}_{RD}^q\|^2$$

using  $\mu^2 = \alpha^2 \|\mathbf{h}_{SD}^q\|^2$ , thus

$$\alpha^2 \|\mathbf{h}_{SD}^q\|^4 = \|\mathbf{h}_{SR}^q\|^2 \|\mathbf{h}_{RD}^q\|^2. \quad (3.18)$$

Substituting (3.17) in (3.18),

$$\begin{aligned} \alpha^2 \|\mathbf{h}_{SD}^q\|^4 &= \alpha^2 \|\mathbf{h}_{RD}^q\|^4 \\ \|\mathbf{h}_{SD}^q\| &= \|\mathbf{h}_{RD}^q\|. \end{aligned}$$

- $\beta > \alpha$  (node D partition outer region) and  $\beta < \alpha$  (node D partition inner region): Now, suppose that  $\alpha$  is decreasing as  $\beta$  remains constant ( $\beta > \alpha$ ). Thus, the  $SR^q$  and  $RD^q$  links are having their energies reduced as  $SD^q$  remains with constant energy. As the link energy and the distance between two nodes are inversely proportional factors in this model, it means that the R node is getting far away from S and D nodes, resulting that this region is outside the node D partition. As the same region is defined for  $\beta$  increasing and  $\alpha$  fixed, it is clear that  $\alpha$  and  $\beta$  show almost opposite behavior to one another. In other words, as  $\alpha$  decreases, the R node distances from S and D nodes, as well as the increase in  $\beta$  causes the R node to approach the S node (also the decrease in  $\beta$  makes the R node to come closer to the D node). As a consequence, the node D partition is a semicircle with radius proportional to  $SD^q$  energy ( $\|\mathbf{h}_{SD}^q\|^2$ ). On the other hand, it is not difficult to assume that the  $\beta < \alpha$  region is inside this semicircle. Furthermore, suppose that there is a value of  $\beta_{\max} \gg 1$  that follows  $\beta = \alpha^{-1}$  and makes the R node to be in the same line as S and D nodes. Now, if there is a value greater than  $\beta_{\max}$  while maintaining the relation  $\beta = \alpha^{-1}$ , then the R node will be positioned above this previous line with same radius as the semicircle. As a result, it is maintained the same  $SR^q$  link energy while the  $RD^q$  link energy grows which is not true for  $\beta$  increasing. Therefore, it is not practical to assume values of  $\beta$  greater than  $\beta_{\max}$  as well as for  $\alpha_{\max}$  and the regions are defined by semicircles.

- $\beta = \alpha^{-1}$  (node S partition): Also from (2.28), it is had that

$$\mu^2 = \frac{\|\mathbf{h}_{SR}^q\|^2 \|\mathbf{h}_{RD}^q\|^2}{\|\mathbf{h}_{SD}^q\|^2} \quad \text{and} \quad \beta^2 = \frac{\|\mathbf{h}_{SR}^q\|^2}{\|\mathbf{h}_{RD}^q\|^2}.$$

Therefore,

$$\alpha^{-2} = \frac{\|\mathbf{h}_{SR}^q\|^2}{\|\mathbf{h}_{RD}^q\|^2}$$

or

$$\alpha^2 \|\mathbf{h}_{SR}^q\|^2 = \|\mathbf{h}_{RD}^q\|^2. \quad (3.19)$$

Substituting (3.19) in (3.18),

$$\begin{aligned}\alpha^2 \|\mathbf{h}_{SD}^q\|^4 &= \alpha^2 \|\mathbf{h}_{SR}^q\|^4 \\ \|\mathbf{h}_{SD}^q\| &= \|\mathbf{h}_{SR}^q\|.\end{aligned}$$

- $\beta < \alpha^{-1}$  (node S partition outer region) and  $\beta > \alpha^{-1}$  (node S partition inner region): Here, suppose that  $\alpha \ll 1$  and it is increasing as  $\beta$  remains constant ( $\beta < \alpha^{-1}$ ). Thus, the R node is getting close to S and D nodes. At a given value of  $\alpha$  that makes  $\beta = \alpha^{-1}$ , the R node touches the node S partition, as a result the  $\beta < \alpha^{-1}$  region is outside the node S partition. On the opposite, it is not difficult to assume that the  $\beta > \alpha^{-1}$  region is inside the node S partition. As well as node D partition, the inner and outer regions of the node S partition are separate by a semicircle with radius proportional to  $\|\mathbf{h}_{SD}^q\|^2$ .
- $\beta = \alpha^{-1} = \alpha$  (intersection point): Now, the only possible solution to  $\beta = \alpha^{-1} = \alpha$  is  $\beta = \alpha = 1$ . This is an important intersection point to the R node positioning, in which all links have same energy ( $\|\mathbf{h}_{SD}^q\| = \|\mathbf{h}_{SR}^q\| = \|\mathbf{h}_{RD}^q\|$ ).

The rest of this section focuses on the analyses about the ergodic achievable data rates and outage probabilities associated with HSRC. More specifically, Subsection 3.1.1 shows the achievable data rate discussion, while Subsection 3.1.2 does the same to the outage probability.

### 3.1.1 The Achievable Data Rate

In order to numerically show the behavior of HSRC, the same assumptions made in Subsection 2.1.2 with regard to link energy relation, additive noise power, and power allocation will be considered here. Additionally, it is considered the case when complete CSI is not available to the transmitter and  $P$  is uniformly allocated (UA) among all subcarriers. Note that  $P \in \{1, 100\}$  mW is adopted in order to emphasize scenarios in which the data communication faces bad and good situations. Furthermore,  $\alpha \in \{0.1, 0.5, 1, 2, 10\}$  is chosen because these values can bring a lot of information as they cover all cooperation cases. More specifically,  $\alpha = 0.1$ , simulates the case in which the R node is very far from both S and D nodes. On the other hand,  $\alpha = 10$ , means that the R node is very close to the S and D nodes. Moreover,  $\alpha = 1$  state that the R node is neither far nor close to the S and D nodes. Furthermore,  $\alpha = 0.5$  and  $\alpha = 2$  are intermediate cases among the aforementioned ones. Also, varying the parameter  $\beta$ , the analysis of four cases are introduced [24, 25]:

- case #1 ( $\beta = 1$ ): this case simulates the R node located in the middle between S and D nodes because  $\|\mathbf{h}_{SR}^q\|^2 = \|\mathbf{h}_{RD}^q\|^2$ .

- case #2 ( $\beta > 1$ ): this case simulates when the R node is closer to the S than the D node because  $\|\mathbf{h}_{SR}^q\|^2 > \|\mathbf{h}_{RD}^q\|^2$ . It is used  $\beta \in \{2, 10\}$  due to the fact that  $\beta = 10$  makes the R node very close to the S node and  $\beta = 2$  results in the R node located closer, but not so much, to the S node than the D node.
- case #3 ( $\beta < 1$ ): this case simulates when the R node is closer to the D than the S node because  $\|\mathbf{h}_{SR}^q\|^2 < \|\mathbf{h}_{RD}^q\|^2$ . It is used  $\beta \in \{1/10, 1/2\}$  due to the fact that  $\beta = 1/10$  makes the R node extremely close to the D node and  $\beta = 1/2$  results in the R node located closer, but not very, to the D node than the S node.
- case #4 ( $\alpha < \beta < \alpha^{-1}$  and  $0 < \alpha \ll 1$ ): this case simulates when the R node is far from S and D nodes because  $\|\mathbf{h}_{SR}^q\|^2 \|\mathbf{h}_{RD}^q\|^2 \ll \|\mathbf{h}_{SD}^q\|^2$ . Also,  $\|\mathbf{h}_{SD}^q\|^2 > \|\mathbf{h}_{SR}^q\|^2$  and  $\|\mathbf{h}_{SD}^q\|^2 > \|\mathbf{h}_{RD}^q\|^2$ .

A summary of position variation of the R node in function of parameters  $\alpha$  and  $\beta$  is shown in Figure 9. It is important to point out that, in practice,  $\alpha_{\max} = 1/\|\mathbf{h}_{SD}^q\|$  in terms of R node location, but theoretically it is possible to assume that  $\alpha \rightarrow \infty$ .

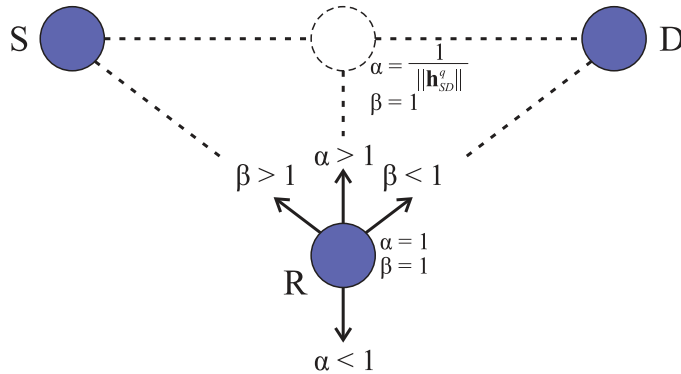


Figure 9: The R node position varying parameters  $\alpha$  and  $\beta$ .

Figure 10 shows achievable data rate gains for the case #1 when AF and DF protocols are applied. Regarding both protocols and  $P = 1$  mW, it is noticed that PSRC has a better performance than the WSRC for all adopted values of  $\alpha$ . As the WSRC has a low value of  $\rho_a^{\text{WSRC}}$ , it implies that PSRC will perform close to the HSRC. It can be seen that the frequency selectivity of PLC benefits PSRC and, consequently, HSRC when OA applies. As a result, if OA is adopted and complete CSI is available, then the WF technique will allocate, most of  $P^P$ , to the PLC subchannels with the highest nSNRs, in most cases, than the wireless subchannels nSNR for the same considered link. In other words, PSRC performs better than the WSRC when  $P$  is low,  $\|\mathbf{h}_\ell^P\|^2 = \|\mathbf{h}_\ell^W\|^2$ ,  $P_{v,\ell}^W = P_{v,\ell}^P$ , and OA is adopted. As  $P$  grows, the WF technique will distribute the power not only to the subcarriers where these peaks of nSNR are located, but also to the ones next to them. Based on that, as  $P \rightarrow \infty$ , OA tends to uniformly allocate power among the subcarriers.

Moreover, as  $\|\mathbf{h}_\ell^P\|^2 = \|\mathbf{h}_\ell^W\|^2$  and  $P_{v,\ell}^W = P_{v,\ell}^P$ , it will result in similar achievable data rate for both PLC and wireless SRCs, which is the best scenario for HSRC as it uses both media for data communication.

For instance, if  $P = 100$  mW, WSRC performs close to PSRC, looking at  $\alpha = 1$ , 22% ( $\rho_{\text{AF}}^{\text{HSRC}} \approx 1.22$ ) and 32% ( $\rho_{\text{DF}}^{\text{HSRC}} \approx 1.32$ ) of achievable data rate gains are obtained by HSRC in relation to  $SD^P$  using AF and DF protocols, respectively. Finally, with  $\alpha = 10$ , PSRC with DF achieves greater  $\rho_{\text{DF}}^{\text{PSRC}}$  for  $P = 1$  mW than for  $P = 100$  mW. This behavior is explained reminding the situation (i), in which  $\rho_a^{\text{PSRC}} \rightarrow 1$  as  $P \rightarrow \infty$ .

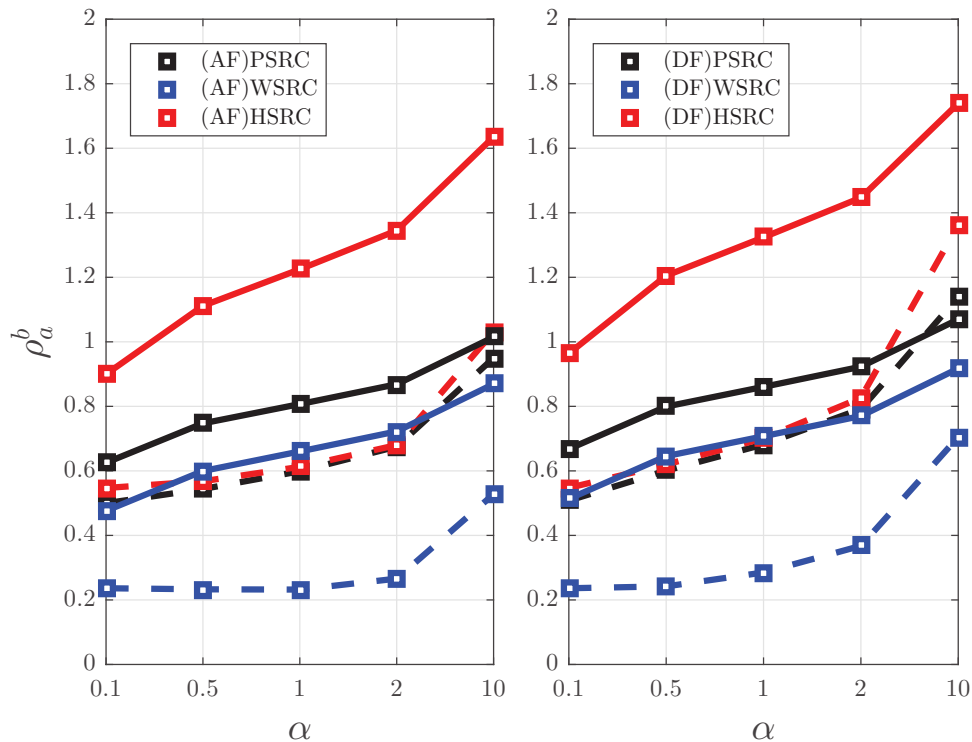


Figure 10: case #1:  $\rho_a^b$  vs  $\alpha$ , in which  $a$  and  $b$  are (a)b in the legend,  $P = 1$  mW (--) and  $P = 100$  mW (—).

For the case #2 (Figure 11), when  $\beta = 2$ , the conclusions are almost the same as those of the case #1, showing no relevant difference between both of them, except that the values of  $\rho_a^b$  are slightly smaller than those of the case #1. On the other hand, when  $\beta = 10$ , it is clearly noticed that the achievable data rate gains decrease for all values of  $P$ . Disregarding both protocols, retransmitting noisy information from the R node through the  $RD$  link ( $\beta < 1$ , the  $SR$  link is noisy but the  $RD$  link is good) or retransmitting almost noiseless information from R node through a noisy  $RD$  link ( $\beta > 1$ , the  $SR$  link is good and the  $RD$  link is noisy) are situations in which the resulting  $SRD$  link is not good at all. Therefore, varying parameter  $\beta$  will result in more energy to one of  $SR$  or  $RD$  links, obtaining a lower achievable data rate for the  $SRD$  link. Consequently, the

losses are expected for values of  $\beta \neq 1$ . Furthermore, as the R node remains closer to the S node as  $\beta$  grows (case #2), it implies that SRC (PSRC, WSRC, and HSRC) will lose cooperation gains since it is in favor of the  $SR$  link in exchange of the  $RD$  one. As a consequence, if AF,  $\alpha = 1$ , and  $P = 100$  mW are considered, then 11% ( $\rho_{AF}^{HSRC} \approx 1.11$ ) gain and 9% ( $\rho_{AF}^{HSRC} \approx 0.91$ ) loss of achievable data rate are obtained for HSRC in relation to  $SD^P$  when  $\beta = 2$  and  $\beta = 10$ , respectively. Similarly, for the DF protocol and under same considerations, a 15% ( $\rho_{DF}^{HSRC} \approx 1.15$ ) gain and 8% ( $\rho_{DF}^{HSRC} \approx 0.92$ ) loss of achievable data rate are obtained by HSRC in relation to  $SD^P$  when  $\beta = 2$  and  $\beta = 10$ , respectively.

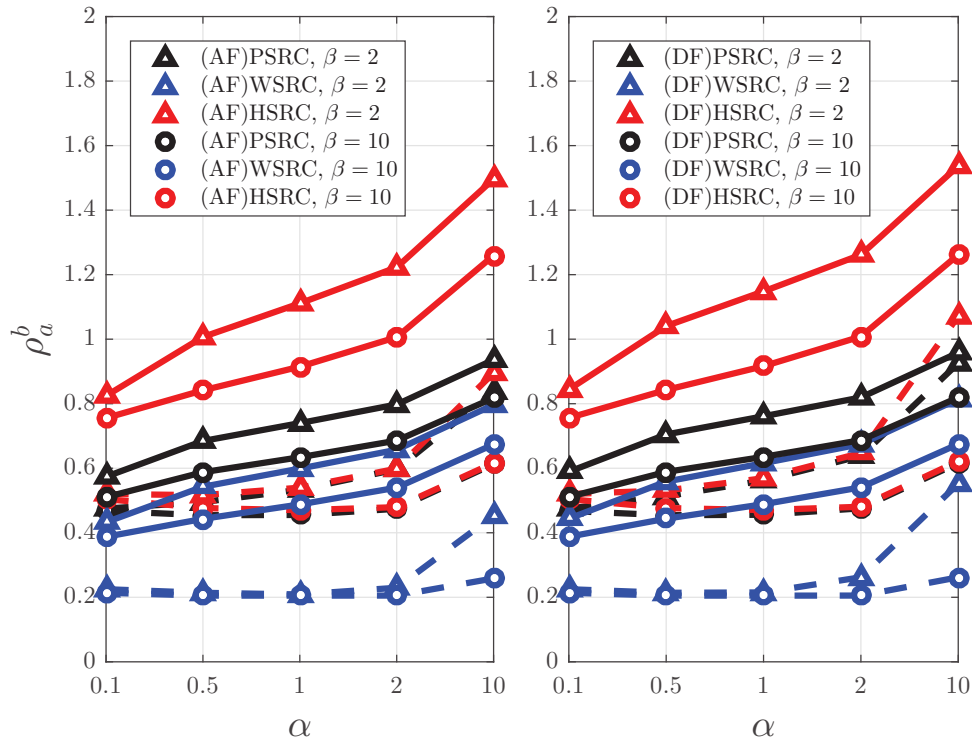


Figure 11: case #2:  $\rho_a^b$  vs  $\alpha$ , in which  $a$  and  $b$  are  $(a)b$  in the legend,  $P = 1$  mW (--) and  $P = 100$  mW (—).

Now, for the case #3 (Figure 12), when  $\beta = 1/2$ , the behaviors are almost those of the case #1, showing no relevant difference between both of them, except for the small reduction on values of  $\rho_a^b$  for all values of  $P$ . Differently, when  $\beta = 1/10$  and for all values of  $P$ , it is clearly noticed that the achievable data rate gains face more reduction. As stated before, this is an expected behavior since the  $SR$  link offers more signal attenuation than the  $RD$  one, resulting in a worse  $SRD$  link and, as a consequence, a worse SRC achievable data rate. Note that, if AF applies,  $\alpha = 1$  and  $P = 100$  mW, then a 18% ( $\rho_{AF}^{HSRC} \approx 1.18$ ) and 9% ( $\rho_{AF}^{HSRC} \approx 1.09$ ) gains of achievable data rate are reached with HSRC in relation to the  $SD^P$  when  $\beta = 1/2$  and  $\beta = 1/10$ , respectively. Similarly, for the DF protocol,  $\alpha = 1$ , and  $P = 100$  mW, a 30% ( $\rho_{DF}^{HSRC} \approx 1.30$ ) and 13% ( $\rho_{DF}^{HSRC} \approx 1.13$ ) gains of achievable

data rate are obtained with HSRC in relation to the  $SD^P$  when  $\beta = 1/2$  and  $\beta = 1/10$ , respectively.

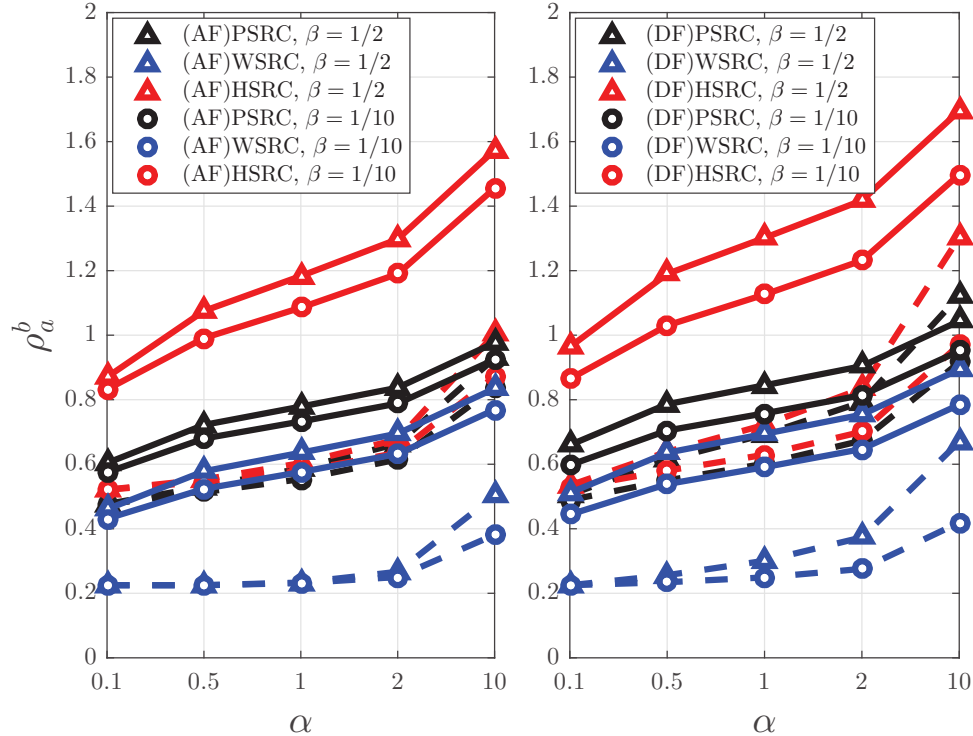


Figure 12: case #3:  $\rho_a^b$  vs  $\alpha$ , in which  $a$  and  $b$  are (a)b in the legend,  $P = 1$  mW (--) and  $P = 100$  mW (—).

Finally, it can be seen that for the case #4 (for example, see Figure 10 at  $\alpha = 0.1$ ), the three SRCs have low values of  $\rho_a^b$  because the achievable data rate gain reduces as  $\alpha$  decreases. Therefore, the case #4 is the worst scenario for cooperation, resulting in low values of achievable data rate gain for both AF and DF protocols. This behavior agrees with [24, 25].

In general, the SRCs using DF performs better than its counterpart using AF. Also, it can be seen that HSRC outperforms PSRC and WSRC for all chosen values of  $P$  and cooperative protocols. Furthermore, based on the presented results, it is pointed out that the best performance in terms of achievable data rate gain, for the situation in which the R node is neither far nor close to S and D nodes ( $\alpha = 1$ ), is observed in case #1 ( $\beta = 1$ ), where the R node is located in the middle between S and D nodes, agreeing with [24, 25]. Furthermore, HSRC achieves a higher achievable data rate gain in the case #3 than in the case #2 for both considered cooperative protocols. It occurs because, in case #2, the R node is close to the S node, making the cooperative protocols retransmit a good estimation of  $\mathbf{X}$  through a noisy  $RD$  link. On the other hand, for case #3, most of the subchannels saw by the R node are quite noisy, but the ones who are not, receive

a greater portion of  $P_R$  (due to the OA), which results in a better use of the *SRD* link.

Finally, Figure 13 shows, for all cases, the achievable data rate gain comparisons between HSRC and the two LP-RF wireless SRC (2WSRC) in parallel (with acronym 2W) operating at center frequencies of  $f_{c,1} = 905$  MHz and  $f_{c,2} = 915$  MHz, respectively. To obtain these curves,  $\|\mathbf{h}_\ell^q\|^2 = \|\mathbf{h}_\ell^{W_1}\|^2 = \|\mathbf{h}_\ell^{W_2}\|^2$  is assumed, where  $\|\mathbf{h}_\ell^{W_1}\|^2$  and  $\|\mathbf{h}_\ell^{W_2}\|^2$  denote the channel energy of 2WSRC with center frequencies of  $f_{c,1}$  and  $f_{c,2}$  associated with the  $\ell^{th}$  link, respectively. Also,  $P_{v,\ell}^q = P_{v,\ell}^{W_1} = P_{v,\ell}^{W_2}$ , in which  $P_{v,\ell}^{W_1}$  and  $P_{v,\ell}^{W_2}$  denote the power of the additive noises of 2WSRC with center frequencies of  $f_{c,1}$  and  $f_{c,2}$  associated with the  $\ell^{th}$  link, respectively. In addition, for the sake of fair comparison, it is adopted  $\rho_a^{2W} = C_a^{2W}/C_{SD}^P$ , where  $C_a^{2W}$  is the achievable data rate for 2WSRC. Furthermore,  $P = \{1, 10, 100, 1000\}$  mW, OA, AF and DF protocols are considered. Here,  $P = 1000$  mW is adopted in order to give a more comprehensive view on the HSRC and 2WSRC behaviors because it was stated that as  $P$  grows, the wireless and PLC links performances come close to each other due to the fact that OA tends to uniform power allocation (UA). Also, Figure 13 shows performance curves for cases #1 ( $\alpha = \beta = 1$ ), #2 ( $\alpha = 1, \beta = 10$ ), #3 ( $\alpha = 1, \beta = 1/10$ ), and #4 ( $\alpha = 0.1, \beta = 1$ ). These values of  $\alpha$  and  $\beta$  are chosen to show HSRC and 2WSRC performances in a balanced link energy scenario (case #1) and highly non-balanced link energy scenarios (cases #2, #3, and #4).

Concerning Figure 13, it can be seen that HSRC outperforms 2WSRC for all values of  $P$  and for all cases. Also, it confirms that 2WSRC tends to perform similar to HSRC as  $P \rightarrow \infty$ . Moreover, HSRC attains higher achievable data rate gain than 2WSRC for low values of  $P$  because the PLC portion of HSRC achieves higher data rates than the wireless ones of 2WSRC. Furthermore, in cases #1 and #4, 2WSRC using DF protocol almost achieves the same value of  $\rho_a^b$  in comparison to HSRC using AF and  $P = 1000$  mW, which is not true for cases #2 and #3. These behaviors are explained due to the fact that, in cases #1 and #4, the PLC and wireless *SR* and *RD* links have same link energy, which offers a better performance on the *SRD* link usage than in the other cases. Although in case #4 the R node is far from both S and D nodes, the high value of  $P$  makes the use of the *SRD* link to be realizable. As the difference between the two cooperative protocols are only observed when the *SRD* link is used for data communication, the curves of  $\rho_a^b$  for the both cooperative protocols separate from each other as  $P$  grows (and *SRD* link is usable) because DF acts better in the *SRD* link than AF. Again, the highest values of  $\rho_a^b$  are attained in case #1, followed by cases #3, #2, and #4, respectively. Moreover, it shows that for very low or very high  $P$ , this behavior can be changed because there is a balance between  $\alpha, \beta$  and  $P$ , which can make the difference between links energy less notice. For example, HSRC in case #4 with  $P \rightarrow \infty$  can act similar to in case #1 because the high and available  $P$  does not make the distance between the S-R and R-D nodes an impediment to reliable perform communication among them.

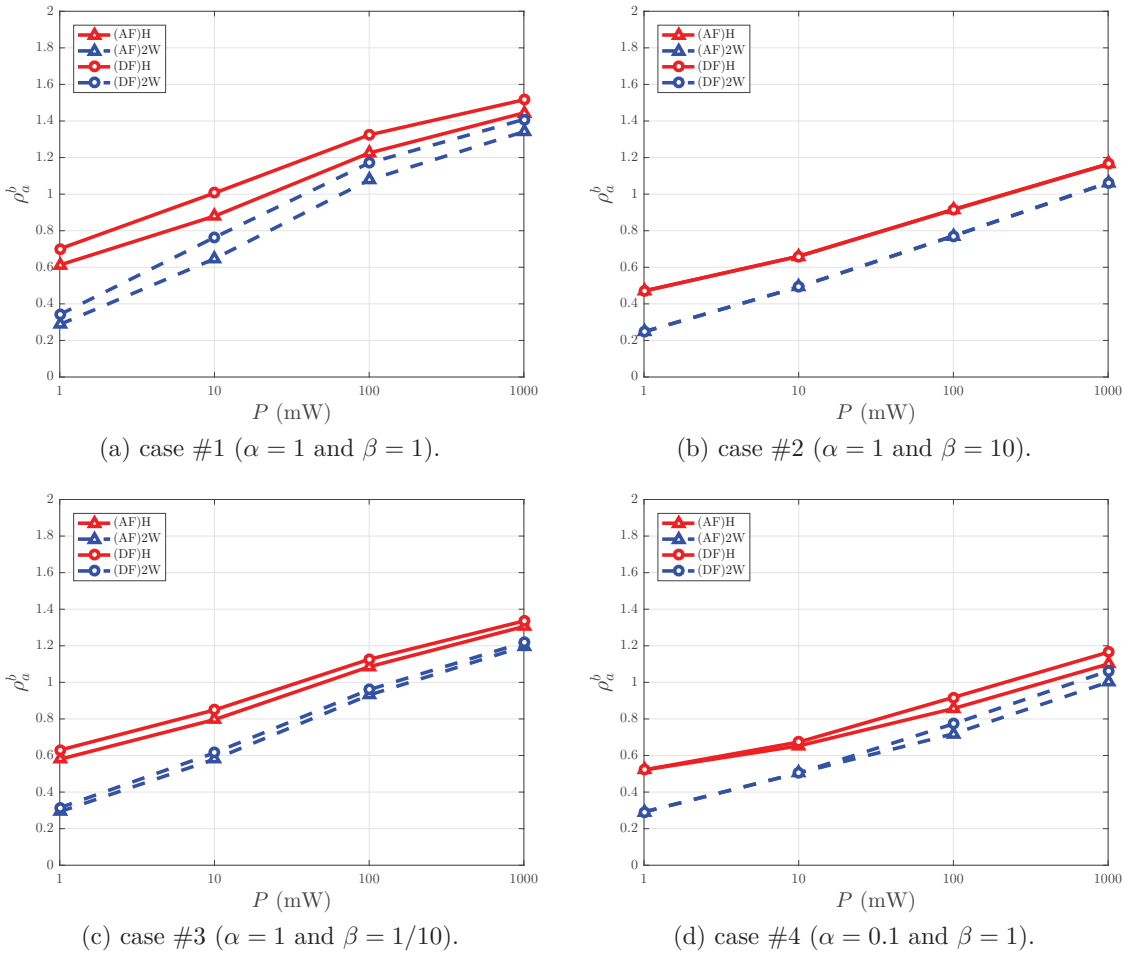


Figure 13:  $\rho_a^b$  vs  $P$ , in which  $a$  and  $b$  are (a) $b$  in the legend, when assuming OA.

### 3.1.2 The Outage Probability

Figures 14 to 16 show the outage probability of HSRC when UA and OA are used for cases #1 ( $\beta = 1$  and  $\alpha = 1$ ), #2 ( $\beta = 10$  and  $\alpha = 1$ ) and #3 ( $\beta = 1/10$  and  $\alpha = 1$ ), respectively. For case #1 (see Figure 14), it can be noticed that the outage probability gap between AF and DF protocols is slightly smaller when using OA than UA. It occurs because the difference between both protocols is that the DF retransmits the correctly decoded information received by the R node, eliminating the residual noise from the  $SR$  link, whereas AF does not. Thus, AF and DF protocols perform close to each other when adopting OA. For instance, if  $P = 10$  mW, then the use of UA in HSRC results in 2.4 and 3.1 bps/Hz of spectral efficiencies for AF and DF protocols, respectively, if  $P_{AF}(\mathcal{R}) = P_{DF}(\mathcal{R}) = 0.1$ . Under the same outage probability, OA achieves  $\mathcal{R} = 2.8$  and 3.3 bps/Hz for AF and DF protocols, respectively.

In case #2 (see Figure 15), for a given spectral efficiency threshold ( $\mathcal{R}_{th}$ ), the outage probability is slightly smaller when OA is assumed than UA for all values of  $P$ .

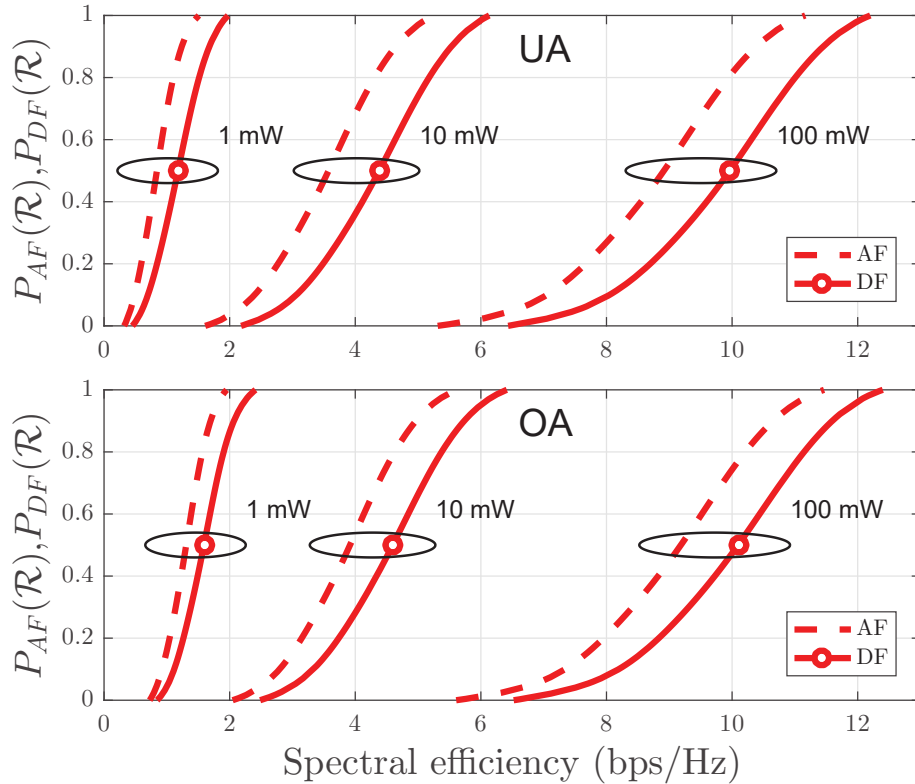


Figure 14: Outage probability for the HSRC when  $\alpha = 1$ , case #1 ( $\beta = 1$ ). UA (top) and OA (bottom) are adopted. Also, the values of total transmission power ( $P$ ) are highlighted.

Actually, there is a very small difference between both of them. Also, AF and DF protocols perform similarly to each other when using both OA and UA. For instance, if  $\beta = 10$ , then the R node is close to the S node. Therefore,  $SR$  is a good link as it has a high link energy, causing the R node to retransmit an almost noiseless version of the received information from the S node with AF protocol, which is similar to the use of DF protocol that correctly decodes  $\mathbf{X}_R^q$  to obtain  $\mathbf{X}$  at the R node. For instance, for  $P = 10$  mW and  $P_{AF}(\mathcal{R}) = P_{DF}(\mathcal{R}) = 0.1$ , HSRC offers 2.0 and 2.4 bps/Hz of spectral efficiencies for both AF and DF protocols assuming UA and OA, respectively.

Addressing case #3 (see Figure 16) and UA, AF and DF protocols perform similarly to each other. This behavior is caused by the proximity of the R node to the D node. In fact, in this circumstance, the R node does not provide a gain of achievable data rate on the  $SRD$  link. On the other hand, when OA applies, transmission power allocated at the R node is quite efficient to exploit the high nSNR subchannels, resulting that an identical copy of  $\mathbf{X}$  (when it can correctly decode  $\mathbf{X}_R^q$ , for DF protocol) or a less noisy  $\mathbf{X}_R^q$  (for AF protocol) is detected at the R node. Therefore, for the DF protocol, an almost noiseless retransmission (the  $RD$  link has a high energy) of  $\mathbf{X}$  from R to D node is accomplished, which is not true for the AF protocol. As a result, DF outperforms

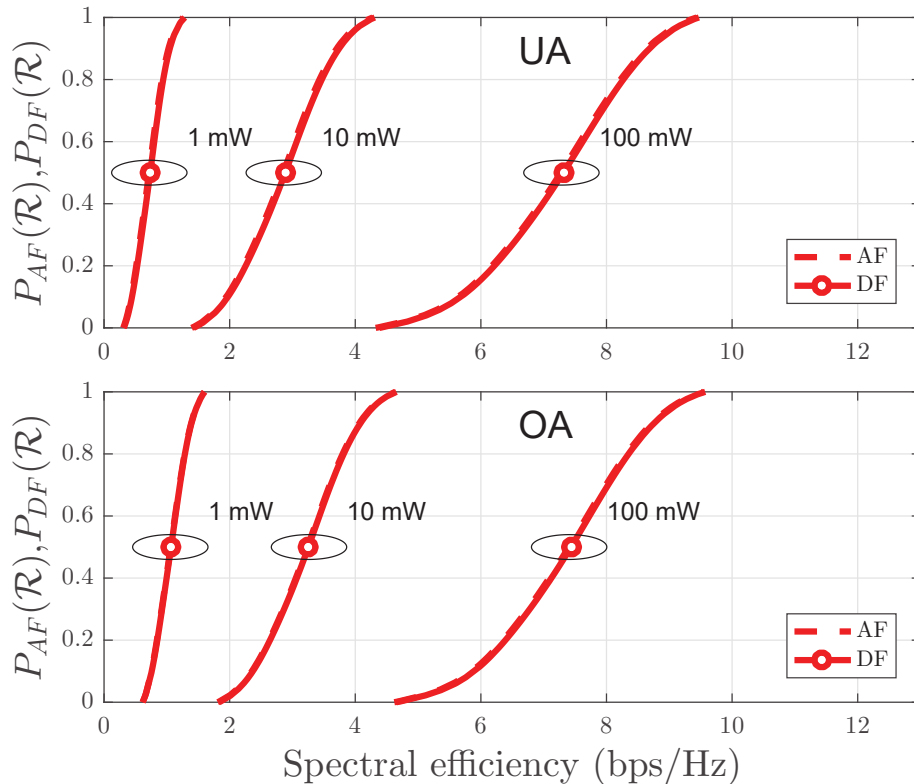


Figure 15: Outage probability for the HSRC when  $\alpha = 1$ , case #2 ( $\beta = 10$ ). UA (top) and OA (bottom) are adopted. Also, the values of total transmission power ( $P$ ) are highlighted.

AF. Simulations with  $P = 10$  mW, UA and for values of outage probability equal to 0.1, shows that HSRC achieves around 2.0 bps/Hz of spectral efficiency for both AF and DF protocols. On the other hand, for the same values of outage probability,  $P$  and using OA, 2.7 and 2.9 bps/Hz are achieved for AF and DF protocols, respectively.

Overall, the outage probability for OA is lower than for UA for any value of  $\mathcal{R}_{th}$  and  $P$ . Also, DF performs better than or almost equal to AF in all cases. Furthermore, when UA is adopted, cases #2 and #3 show very similar outage probability behavior, which is not true regarding OA.

### 3.2 The Incomplete HSRC

This section is organized as follows: Subsection 3.2.1 addresses the power allocation assumptions when HSRC loses a link or node communication interface as well as the achievable data rate analyses; Subsection 3.2.2 offers a discussion about the outage probability curves of the incomplete HSRC.

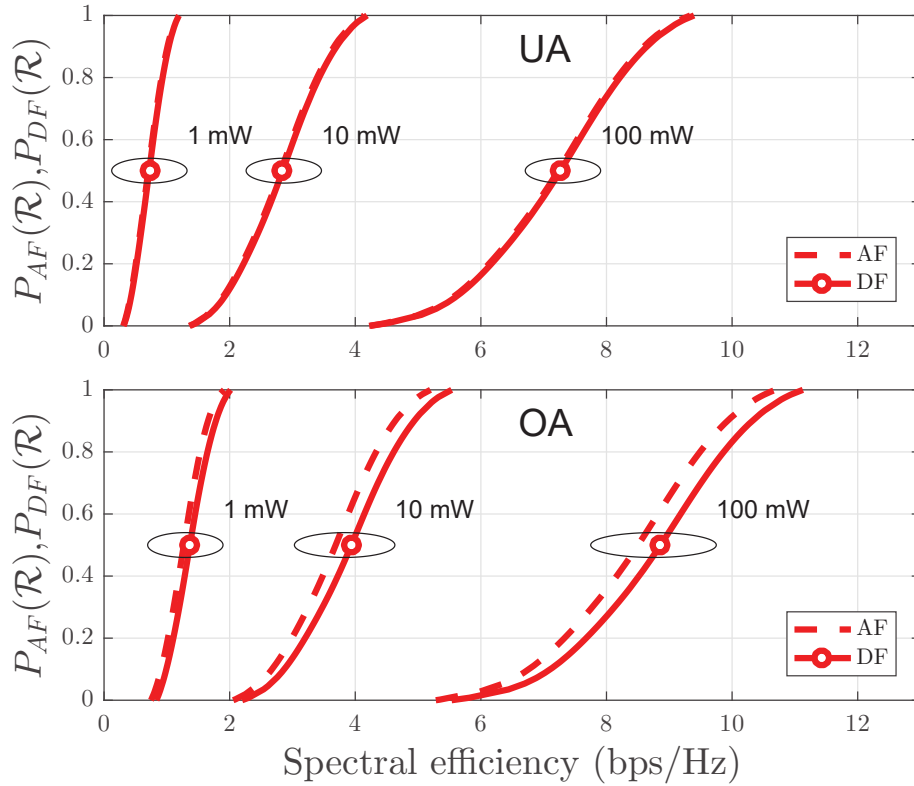


Figure 16: Outage probability for the HSRC when  $\alpha = 1$ , case #3 ( $\beta = 1/10$ ). UA (top) and OA (bottom) are adopted. Also, the values of total transmission power ( $P$ ) are highlighted.

### 3.2.1 The Achievable Data Rate

In the numerical simulations and analyses, if a link is lost, the achievable data rate ratio, see (2.48), is labeled using the following acronyms:

- The HSRC without  $q^{th}$  channel associated with the  $SD$  link - w/o( $SD^q$ ).
- The HSRC without  $q^{th}$  channel associated with the  $SR$  link - w/o( $SR^q$ ).
- The HSRC without  $q^{th}$  channel associated with the  $RD$  link - w/o( $RD^q$ ).

Also, when one node communication interface is lost, it is used:

- The HSRC without  $q^{th}$  channel communication interface on the S node - w/o( $S^q$ ).
- The HSRC without  $q^{th}$  channel communication interface on the R node - w/o( $R^q$ ).
- The HSRC without  $q^{th}$  channel communication interface on the D node - w/o( $D^q$ ).

Moreover, for comparison purposes, the achievable data rate ratio associated with PSRC and WSRC makes use of the acronyms PSRC and WSRC, respectively. Furthermore,

$\beta = \{1, 10, 1/10\}$  is assumed for cases #1, #2 and #3, respectively, while case #4 occurs for  $\beta = 1$  and  $\alpha = 0.1$ . These values of  $\beta$  are chosen to quantify the incomplete HSRC gain/loss in relation to the HSRC when a balanced links energy scenario (case #1) and highly unbalanced links energy scenario (cases #2, #3, and #4) occur. Furthermore, the intermediate values of  $\beta$  will result in a performance between the chosen values of  $\beta$ .

### 3.2.1.1 The Incomplete HSRC: The HSRC without a link

Adopting OA together with AF and DF protocols, Figures 17 and 18 show the achievable data rate ratio for cases #1, #2 and #3, respectively. Looking at Figure 17(a) to 17(c) and  $\forall \alpha$ , it is noticed that the incomplete HSRC has  $\varrho_{AF}^H > 0.9$  when the missed link is wireless and lower than or equal to the values of  $\varrho_{AF}^H$  when the missed link is PLC. As the magnitude of the PLC channel frequency response shows more intense peaks and valleys than the wireless ones and  $P_{v,\ell}^W = P_{v,\ell}^P$ , the highest values of nSNR will be experienced in the PLC subchannels in comparison to the wireless ones and, since OA is adopted,  $P$  is allocated to the subcarriers in which their respective subchannel nSNRs are the highest, which explains the greater loss of  $\varrho_{AF}^H$  when a PLC link is lost. Remember that the gap between PLC and wireless performance decays as  $P$  grows, as previously discussed in situation (I). Furthermore, it is stated that PSRC acts as a lower bound for the HSRC without any wireless link as well as the HSRC without any PLC link is lower bounded by the WSRC.

Without loss of generality, as the HSRC misses a wireless link, the performance curves overlap each other for  $P = 1$  mW, therefore the focus of our discussion will be on the HSRC without PLC link. Looking at Figure 17(a), it can be noticed that, as  $\alpha$  grows from 1,  $\varrho_{AF}^H$  increases when the missed link is  $SD^P$  and decreases when the  $SR^P$  or  $RD^P$  link is missed. It occurs due to the fact that the resulting  $SRD$  link is being favored (for both PSRC and WSRC) in relation to the  $SD$  link, if  $\alpha \gg 1$ . On the other hand, if  $\alpha \ll 1$ , then the  $SD$  (PLC and wireless) link has a higher link energy than the  $SRD$  one, resulting in the opposite behavior of  $\varrho_{AF}^H$ ; however, this behavior is not noted in the HSRC without  $SD^P$  and  $\alpha \ll 1$ , see Figure 17(a), because WSRC yields the most significant contribution and ignores the remaining  $SR^P$  and  $RD^P$  links availability. More specifically, case #1 shows that the wireless links contribution is lower than the PLC ones when there is a balance between the links energy (see WSRC curve with  $\alpha = 1$ ). Moreover, the WSRC contribution increases as  $\alpha$  moves away from 1. As  $P = 1$  mW,  $P_{v,\ell}^W = P_{v,\ell}^P$ , and OA are considered, the wireless links are not as good as the PLC ones, but when there is a substantial increase or decrease of  $\alpha$  away from 1, the wireless  $SRD$  or  $SD$  link can offers more contribution to increase achievable data rate ratio.

Now, for case #2 and  $P = 1$  mW (see Figure 17(b)), the R node is closer to the S than the D node. Therefore, the  $SR$  (PLC and wireless) link has higher energy in case

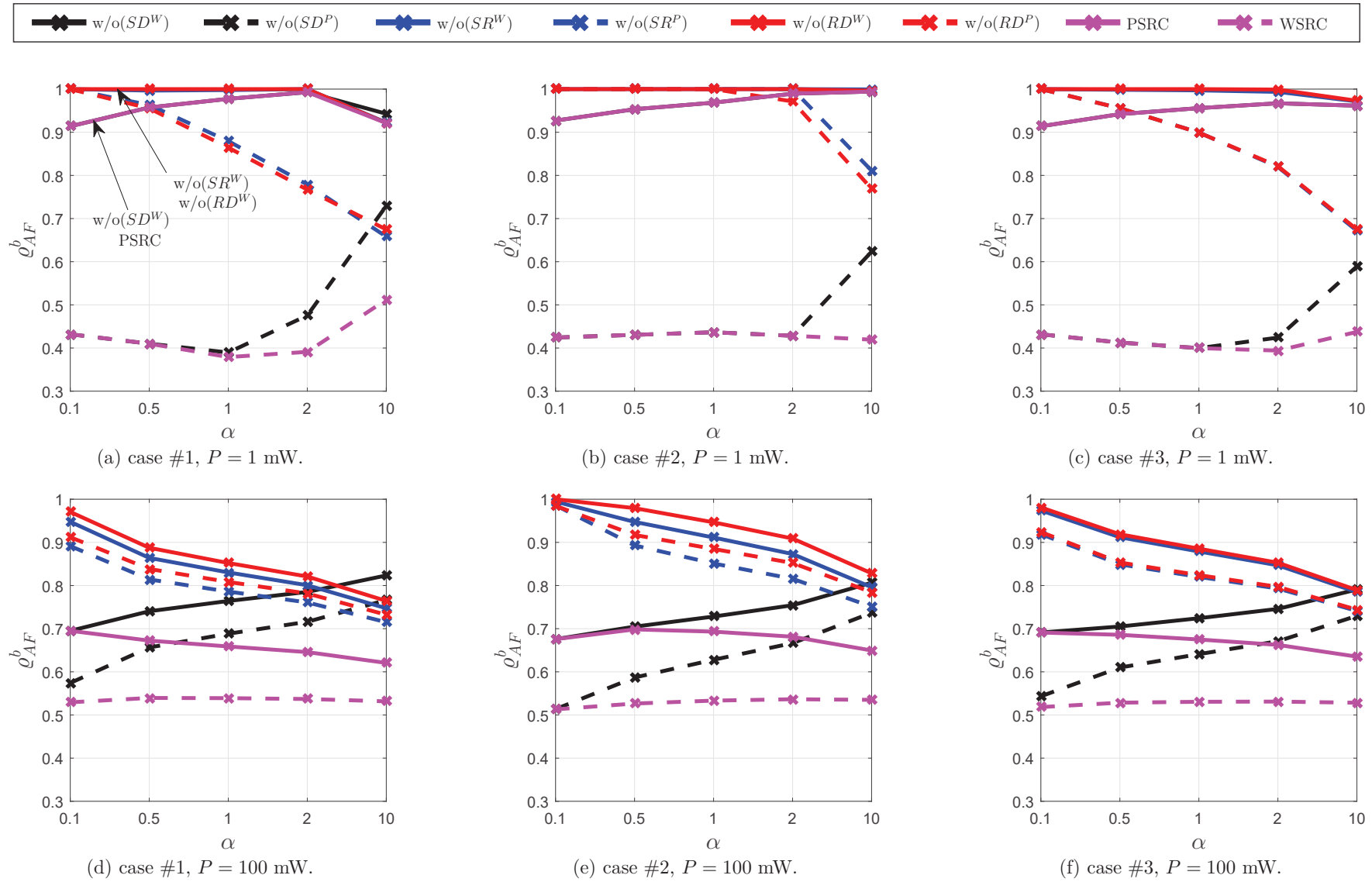


Figure 17:  $Q_{AF}^b$  vs  $\alpha$  for the HSRC without a link, PSRC, and WSRC.

#2 than in case #1 and the opposite occurs with respect to the  $RD$  link, because the  $SRD$  link has the same link energy in both cases. Moreover, it can be seen that a loss of the  $SD^P$  link is worse in case #2 than in case #1 due to the fact that is better to have a balance in the energy of  $SR$  and  $RD$  links (i.e., similar achievable data rate) than a  $SRD$  link composed of the cascade of low and high energy links, which limits the  $SRD$  link achievable data rate to the worse of  $SR$  and  $RD$  links. Thus, the  $SD$  (PLC and wireless) link contribution is more relevant when  $SRD$  link is not so good (case #2). Similarly, the (PLC and wireless)  $SR$  or  $RD$  link loss is worse in case #1 than in case #2, for the same aforementioned reason. Furthermore, as case #2 has a good  $SR^P$  link, the  $P_0^P$  is well shared between  $SD^P$  and  $SR^P$  links, but the  $RD^P$  link has low energy and, as a consequence, the transmission power spent with the  $SR^P$  link data communication is not well used, which explains the gap of performance when losing  $SR^P$  or  $RD^P$  link.

Looking at case #3 and  $P = 1$  mW, see Figure 17(c), it can be seen a similar performance to case #2 for the HSRC without the  $SD^P$  link, i.e., the (PLC and wireless)  $SRD$  link is not so good because  $\beta = 1/10$  makes the  $SR$  link to be worse in case #3 than in case #1. Moreover, in case #3, the HSRC without  $SR^P$  or  $RD^P$  link performs similar to the case #1 and worse than in the case #2. Since OA is adopted, the remaining wireless  $SRD$  link performs better when the R node is closer to the D than to the S node (case #3) because the retransmitted information from the R node can take advantage of high subchannel nSNRs, which is not true for case #2. Regarding case #2, the (PLC and wireless)  $SR$  link is good but it does not make the information travel a long path from S node to R node without remarkable signal degradation. As a result, for case #2 ( $\beta = 10$ ), the PSRC and WSRC behave similar to a system that transmits the same information from two nearby nodes direct to the D node. Therefore, it is more prejudicial to lose a (PLC or wireless)  $SR$  or  $RD$  link at case #3 than at case #2. Additionally, the gap of performance experienced in case #2 by using the HSRC without the  $SR^P$  or  $RD^P$  link is not seen in case #3. This occurs because, in case #3, the  $SR^P$  link is already a bad link and, as a consequence, a low portion of  $P_0^P$  is allocated to it. It means that losing  $SR^P$  or  $RD^P$  link does not result in relevant performance differences among them. Also, for  $P = 1$  mW, it is slightly better to lose the  $SR^P$  than the  $RD^P$  link in case #2, which is not true for other cases or  $P = 100$  mW. In fact, for high values of  $P$ , the WSRC contribution yields significative and positive impact on the achievable data rate, resulting that the HSRC without the  $RD^P$  link has a better performance than the HSRC without  $SR^P$  link due to the fact that  $P_1^W = P_R$  is considered in the former and  $P_0^P$  is allocated only to the  $SD^P$  link in the latter. In other words, it is better to the transmission power of R node to be totally allocated to transmit information through  $RD^W$  link than to allocate  $P_0^P$  solely to the  $SD^P$  link, except for case #2 and  $P = 1$  mW whereas, at the same time, the  $RD^W$  link is bad and the total available transmission power is low ( $SD^P$  is much better than  $SD^W$ ).

In general, with the increase of  $P$  (see Figures 17(d)-17(f)), the achievable data rate ratios tend to the values previously discussed in situations (I), (III), (IV), and (V). It is important to emphasize that, with  $P = 100$  mW, PSRC and WSRC perform close to each other. Again, for all cases, it is seen that greater  $\varrho_{AF}^H$  is experienced when HSRC loses a wireless link rather than a PLC one. Furthermore, the PSRC performance keeps acting as a lower bound for the HSRC without a wireless link as well as the WSRC performance works as a lower bound for the HSRC without a PLC link. Overall, it is showed that the HSRC without a link has a higher  $\varrho_{AF}^H$  than individual PSRC or WSRC. Finally, but not the least, when  $\alpha \ll 1$ , the loss of a (PLC or wireless)  $SD$  link shows more significant losses than the lost of  $SR$  or  $RD$  link and the opposite occurs for  $\alpha \gg 1$ .

For case #4 and  $\forall P$  (see Figures 17(a) and 17(d), at  $\alpha = 0.1$ ), the incomplete HSRC yields the highest achievable data rate ratio ( $\varrho_{AF}^H > 0.87$ ) when the  $SR^P$  or  $RD^P$  link is missed and the lowest  $\varrho_{AF}^H$  when the  $SD^P$  link is lost. These are expected behaviors since the R node is far from both S and D nodes, resulting that  $\varrho_{AF}^H$  remarkably depends on both PLC and wireless  $SD$  links.

Figure 18 shows, for all cases, the achievable data rate ratio of the incomplete HSRC when a link is missed and DF protocol is applied. In general, the curves in Figures 18(a) to 18(f) show some similarities with those curves associated with the incomplete HSRC using AF protocol, which have already been discussed. In fact, these similarities are addressed to the HSRC flexibility to deal with the loss of one link due to its multiple available data communication paths. It means that losing a link, out of six, is not so prejudicial as the HSRC can keep a reliable communicating through the other five remaining links. Also, the curves in Figure 17 are normalized by the HSRC using AF as well as the curves in Figure 18 are normalized by the HSRC using DF. Thus, the focus of our analyses will be on the  $\varrho_a^b$  differences among cooperative protocols curves.

In this regard, looking at Figures 18(a) to 18(c) and  $\alpha = 10$ , it can be notice that the incomplete HSRC yields greater values of  $\varrho_a^H$  for DF protocol than AF protocol (Figures 17(a) to 17(c)) when the  $SD^P$  link is lost. This happens due to the fact that the DF protocol performs better in the  $SRD$  (PLC and wireless) link than the AF protocol. Thus, losing the  $SR$  or  $RD$  link is more significant when using DF than AF. On the other hand, removing a  $SD$  link is less meaningful as the  $SRD$  link has a greater impact on the achievable data rate ratio for the use of the DF protocol. More specifically, the case #1 with  $P = 1$  mW (see Figure 18(a)) shows that the lowest WSRC contribution occurs at  $\alpha = 0.5$  (see WSRC curve) due to the fact that, using the DF protocol, the (PLC and wireless)  $SRD$  link performs better than using the AF protocol and the minimum WSRC contribution occurs when  $\alpha = 1$ . Also, the small difference between the use of AF and DF protocols is addressed to the fact that HSRC with OA offers high robustness against frequency selectivity due to its multiplicity of available links and also because WF

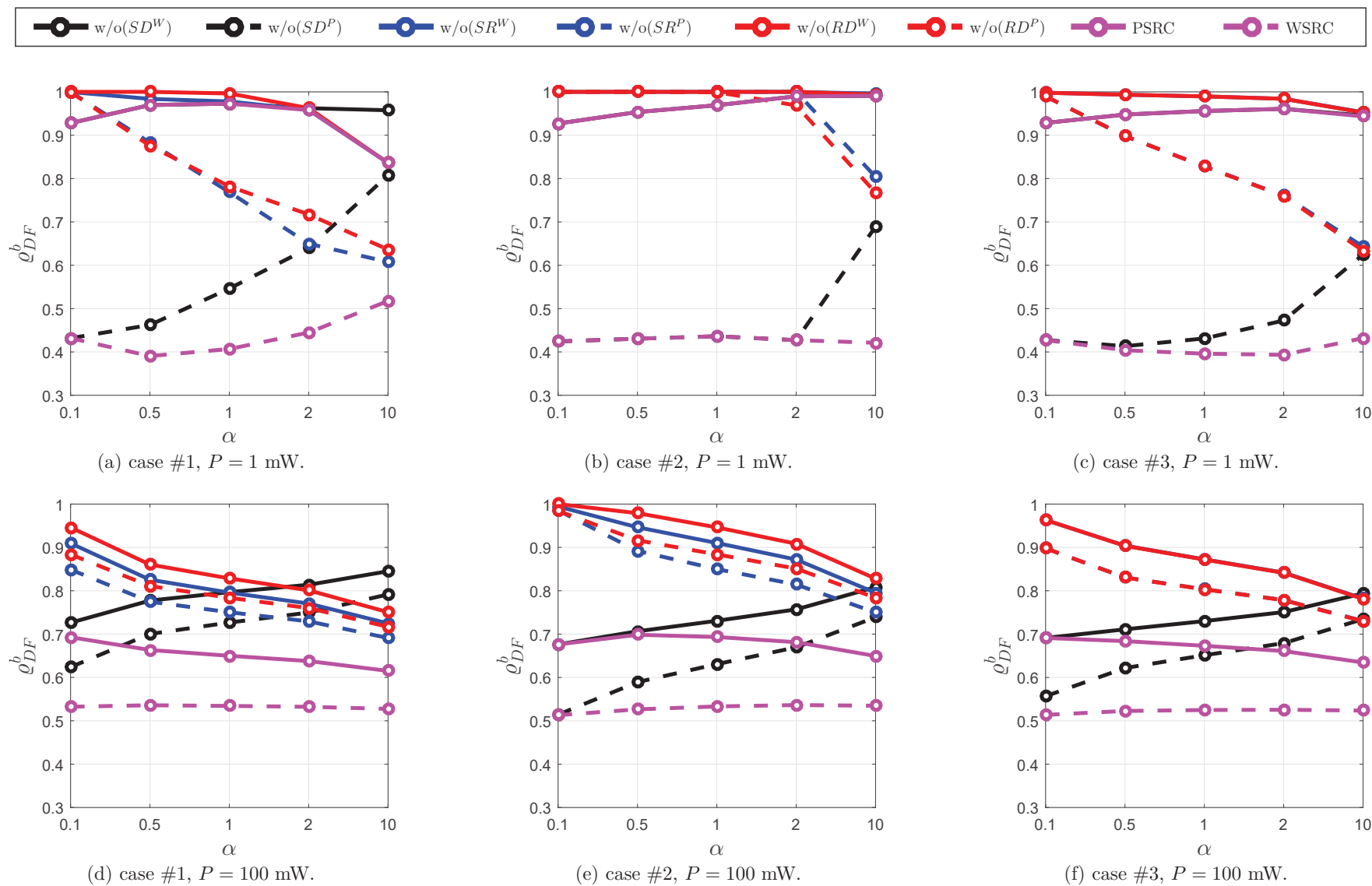


Figure 18:  $\varrho_{DF}^b$  vs  $\alpha$  for the HSRC without a link, PSRC, and WSRC.

avoid high attenuation subchannels, i.e., the HSRC model with OA offers flexibility to compensate differences between both protocols.

For all cases, considering  $P = 100$  mW and the DF protocol (Figures 18(d) to 18(f)), it can be seen similar behavior of  $\varrho_a^H$  to the AF protocol (Figures 17(d) to 17(f)) for the same aforementioned reason, except for the small differences of achievable data rate ratio mentioned in the previous paragraph.

### 3.2.1.2 The Incomplete HSRC: The HSRC without one node communication interface

From now on, the HSRC without a node communication interface will be analyzed, for both AF (see Figure 19) and DF (see Figure 20) protocols. Overall, looking at Figure 19, the first thing to note is that the curves associated with the HSRC without one D node communication interface, whether PLC or wireless, performs similar to the opposite SRC, i.e., the HSRC without  $D^P$  performs equal to the WSRC as well as the HSRC without  $D^W$  performs equal to the PSRC. This holds true for all considered cases and cooperative protocols since a loss of the  $D^q$  node communication interface results in losing both  $SD^q$  and  $RD^q$  links and, as a consequence, the remaining  $SR^q$  link is not useful as no combining technique is applied at the R node. Furthermore, similar to previous subsection, the loss of any PLC node communication interface is lower bounded by the WSRC and the loss of any wireless node communication interface is lower bounded by the PSRC.

Again and without loss of generality, as the HSRC without a wireless node communication interface curves overlap each other due to its low contribution to the HSRC in relation to the PLC one for  $P = 1$  mW, the focus of our discussion will be on the HSRC without PLC node communication interface. Regarding the case #1 with  $P = 1$  mW and  $\alpha = 0.1$ , see Figure 19(a), it is showed that the (PLC and wireless)  $SD$  link yields the most significant contribution (the lowest values of  $\varrho_{AF}^H$  occurs when  $S^q$  is lost). Thus, removing S node communication interface results in removing  $SR$  and  $SD$  links as well and, as a consequence, a greater loss of  $\varrho_{AF}^H$  is experienced. On the other hand, for  $\alpha = 10$ , removing the  $SR$  or  $RD$  link has a greater impact on  $\varrho_{AF}^H$ , whereas a loss of R node communication interface introduces a loss of both  $SR$  and  $RD$  links.

For case #2, see Figure 19(b), and  $\alpha = 10$ , it is seen that losing the  $S^P$  is worse in case #2 than in case #1. This happens due to the fact that the remaining  $RD^P$  link contribution is greater in case #1 than in case #2. In fact,  $RD^P$  link is not good in case #2, as mentioned before. On the other hand, for  $\alpha = 10$ , the opposite occurs ( $\varrho_{AF}^H$  in case #1 is lower than in case #2) when removing the  $R^P$  for the same reason.

Now, for case #3 with  $P = 1$  mW, see Figure 19(c), the removal of  $S^P$  acts similar to case #2 in terms of achievable data rate ratio. However, removing the  $R^P$  in case #3 results in greater performance degradation than in case #2 and it is similar to case #1.

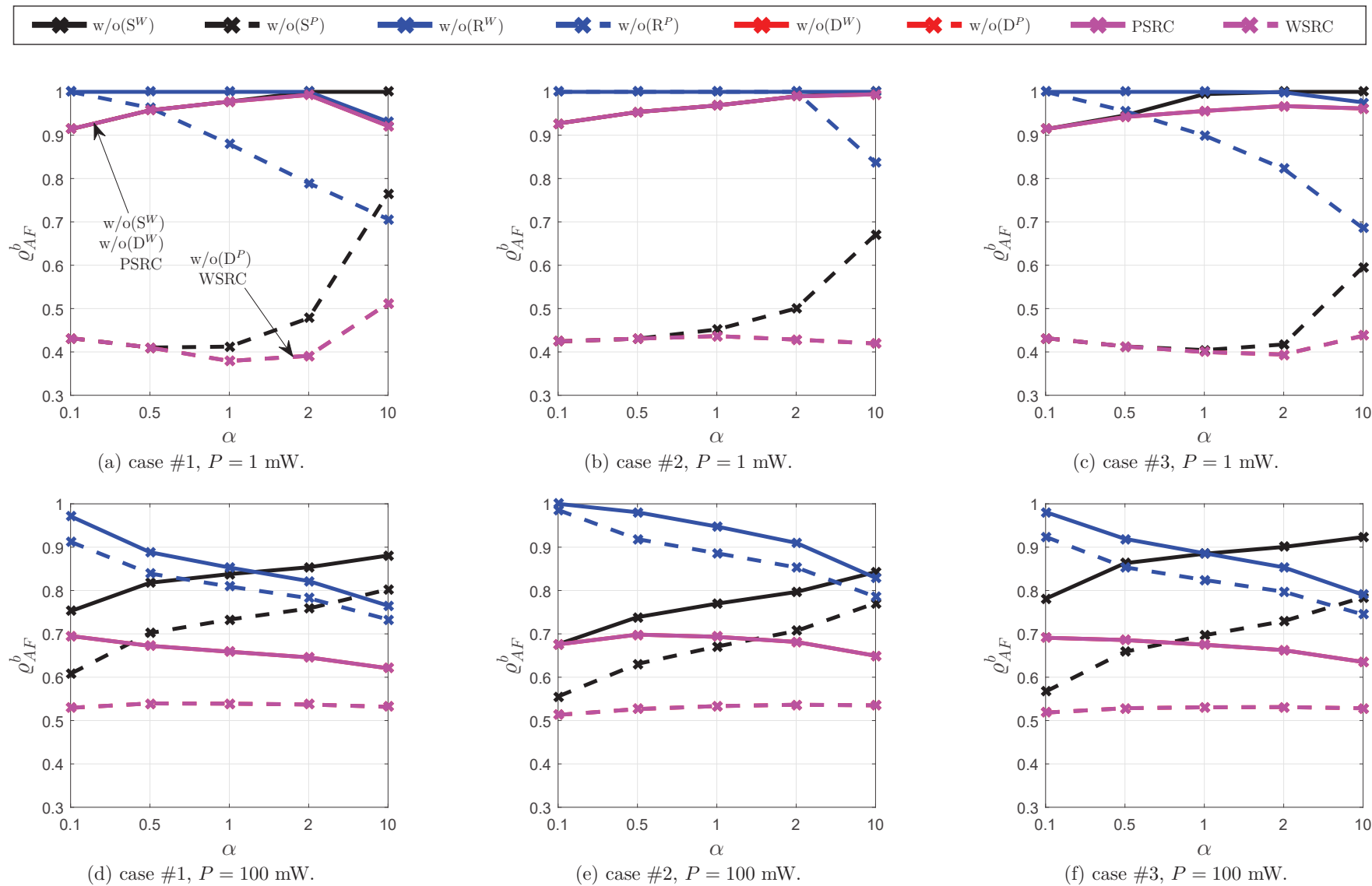


Figure 19:  $Q_{AF}^b$  vs  $\alpha$  for the HSRC without a node communication interface, PSRC, and WSRC.

It occurs because, in case #2, the R node is close to the S node, making the cooperative protocols to retransmit a good estimate of  $\mathbf{X}$  through a low energy (PLC and wireless)  $RD$  link. On the other hand, for case #3, most of the  $SR$  link subchannels have low nSNR, but the ones with high values of nSNR can be exploited by applying OA, resulting in a better usage of the  $SRD$  link.

Figures 19(d) to 19(f) show, for all cases, the achievable data rate ratio when  $P = 100$  mW and the AF protocol are adopted. Overall, for  $\forall\alpha$ , the worst is to lose a D node communication interface. Also, for  $\alpha \ll 1$ , the loss of a (PLC or wireless) S node communication interface has similar  $\varrho_{AF}^H$  to the loss of the D node communication interface. On the other hand, for  $\alpha \gg 1$ , the best achievable data rate ratio occurs when the HSRC loses one S node communication interface. Although, a loss of PLC node communication interface is still worse, the performance difference due to the loss of PLC or wireless node communication interface decreases when  $P$  increases.

Finally, but not the least, case #4 (see Figures 19(a) and 19(d), at  $\alpha = 0.1$ ) shows higher  $\varrho_{AF}^H$  values when a (PLC or wireless) R node communication interface is missed because, in this case, the R node is far from both S and D nodes ( $SRD$  link is not useful). On the other hand, losing a S or D node communication interface significantly impacts performance as it will make the incomplete HSRC to work with a single  $SD$  link – the loss of S node communication interface is still better than the lost of D node communication interface for  $P = 100$  mW, because, in the former situation, the HSRC can take advantage of the remaining  $RD$  link to retransmit the information of the R node to the D node.

One important point is that the HSRC without the  $SD$  link (PLC or wireless) performs similar to the HSRC without one S node communication interface. Also, the HSRC without  $SR$  or  $RD$  link performs similar to the HSRC without one R node communication interface. Furthermore, the performance of the HSRC without one D node communication interface is the same as the ones obtained with independent PSRC or WSRC.

The performance of the HSRC without one node communication interface when the DF protocol applies is shown in Figure 20. As it can be seen,  $\varrho_a^H$  is similar to those ones obtained with the AF protocol (see Figure 19). The difference noticed between AF and DF performance curves is that the HSRC without any S node communication interface, for all cases and  $\forall P$ , offers  $\varrho_{DF}^H \geq \varrho_{AF}^H, \forall\alpha$ . For instance, the HSRC without a  $S^P$ , case #1,  $\alpha = 1$ , and  $P = 1$  mW, results in  $\varrho_{DF}^H = 0.58$  and  $\varrho_{AF}^H = 0.41$  (see Figures 19(a) and 20(a)). This is expected due to the fact that the remaining  $RD^P$  link is still cooperating with the incomplete HSRC, whereas DF acts better at the (PLC and wireless)  $SRD$  link than AF. Also, the opposite occurs when HSRC misses any R node communication interface.

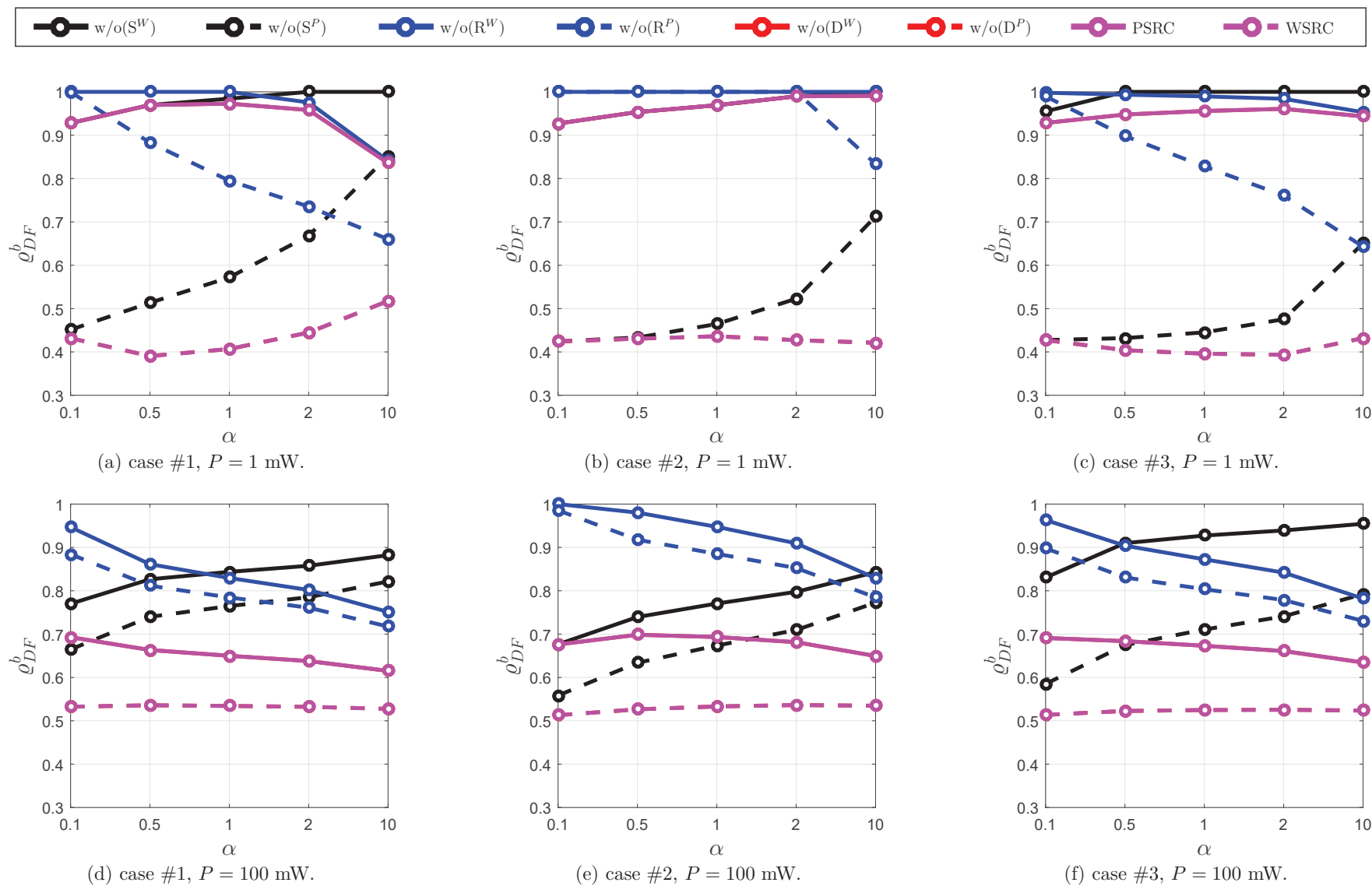


Figure 20:  $\varrho_{DF}^b$  vs  $\alpha$  for the HSRC without a node communication interface, PSRC, and WSRC.

### 3.2.2 The Outage Probability

This subsection discusses the outage probability of the HSRC without one link or a node communication interface. This analysis is carried for cases #1, #2 and #3, assuming  $\alpha = 1$  and  $\beta = 1, 10$  and  $1/10$ , respectively. The analysis of case #4 is not carried out because, from now on, it is clear that no relevant information can be extracted in this case as it will be the worst one when HSRC loses a  $S^q$  or  $D^q$  node communication interface and the best one when HSRC loses a  $R^q$  node communication interface due to its high dependency of both PLC and wireless  $SD$  links.

#### 3.2.2.1 The Incomplete HSRC: The HSRC without a link

Figure 21 shows outage probability curves of the HSRC without a link, PSRC and WSRC, with  $\alpha = 1$  and  $P = 100$  mW, for cases: (a) #1, (b) #2, and (c) #3. In this plot and for any given  $\mathcal{R}_{th}$ , it can be seen that the DF protocol always achieves a lower outage probability than the AF protocol. Moreover, for a given link loss, case #1 shows the lowest outage probabilities at any  $\mathcal{R}_{th}$ , followed by cases #3 and #2, which is explained due to the fact that in case #3 the (PLC and wireless)  $SRD$  link usage is better than in case #2 as mentioned in the previous section. Furthermore, the loss of any link in case #1 is less prejudicial than in other cases because, in case #1, the balanced link energy scenario ( $\alpha = \beta = 1$ ) occurs, resulting that all links can have a significant contribution to HSRC, for both cooperative protocols. Therefore, a loss of any of these links will be well covered by the other links. For example, given  $\mathcal{R}_{th} = 6$  bps/Hz, a  $P_{AF}(\mathcal{R}_{th}) = 0.2$  is obtained for the HSRC without  $SD^W$  in case #1, whereas the same  $\mathcal{R}_{th}$  results in  $P_{AF}(\mathcal{R}_{th}) = 0.8$  and  $P_{AF}(\mathcal{R}_{th}) = 0.5$  for cases #2 and #3, respectively. Also, these results reaffirm that even when HSRC loses any link, it remains better than or equal to the PSRC or WSRC.

#### 3.2.2.2 The Incomplete HSRC: The HSRC without one node communication interface

Figure 22(a) to (c) show outage probability curves of the HSRC without a node communication interface, PSRC, and WSRC with  $\alpha = 1$  and  $P = 100$  mW, for cases #1, #2, and #3, respectively. Regarding these figures and the AF protocol, it is shown that the highest outage probabilities are attained by the WSRC and HSRC without  $D^P$ . On the other hand, the lowest outage probabilities are obtained by the HSRC without  $R^W$ . Furthermore, for the AF protocol, the HSRC without  $S^W$  almost achieves the lowest outage probabilities in cases #1 and #3. This occurs because, at these cases, the loss of  $S^W$  does not result in substantial losses as the remaining  $RD^W$  link can alleviate the loss of  $S^W$ . For the DF protocol and cases #1 and #3, the  $S^W$  communication interface loss achieves the lowest outage probabilities in comparison to the HSRC without any other node communication interface, PSRC and WSRC. In fact, the loss of any S communication interface is less significant when assuming DF rather than AF because

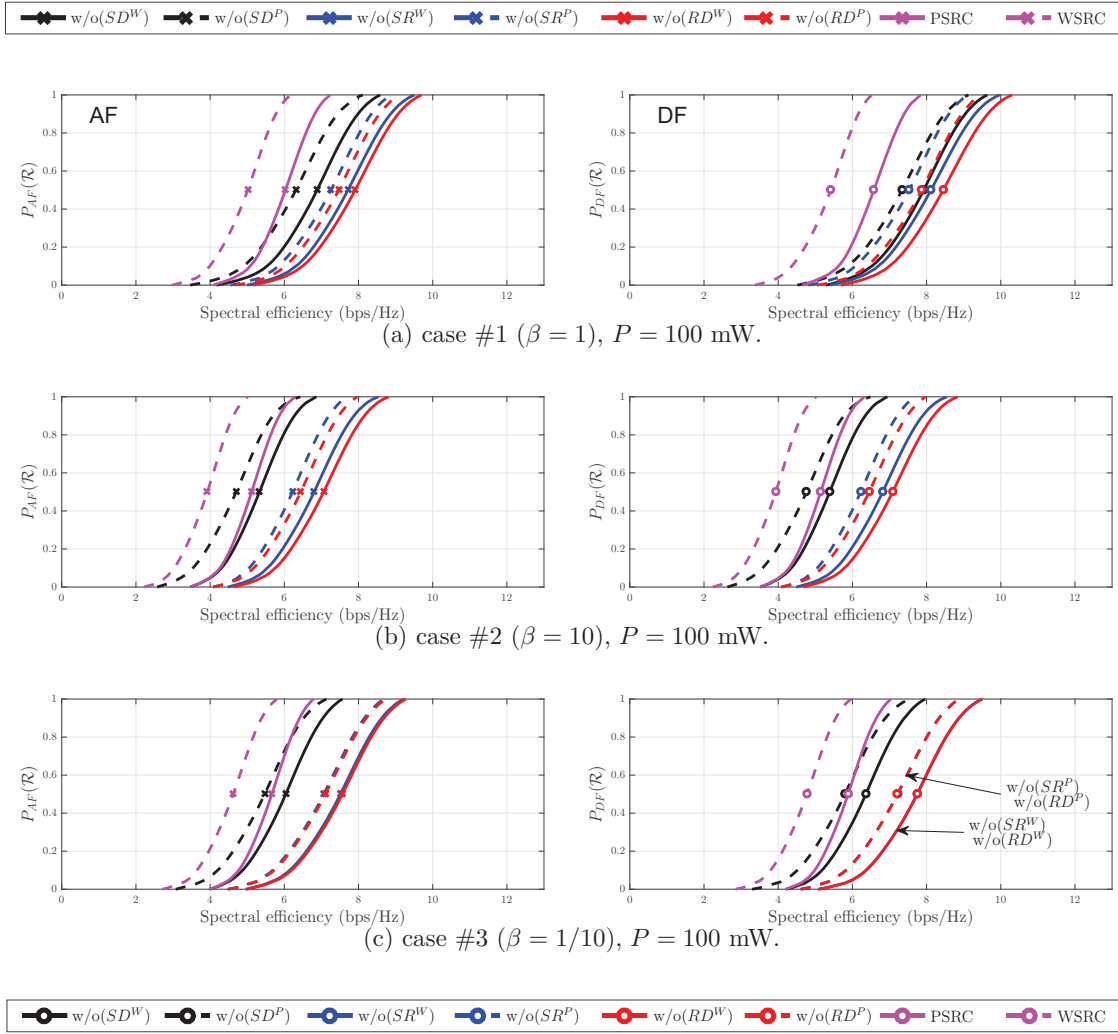


Figure 21: Outage probability for the HSRC without a link when  $\alpha = 1$ .

the former protocol can attain a better performance at the remaining  $RD$  link. Finally, in case #2, the HSRC without (PLC or wireless) S communication interface has higher values of outage probability than in the other cases, for a given  $\mathcal{R}_{th}$ , due to the summed effect of the loss of a (PLC or wireless)  $SD$  and  $SR$  links, in which the impact is most significant and negative in this case than in the others (check Figure 21, HSRC without  $SD^q$  and  $SR^q$  curves).

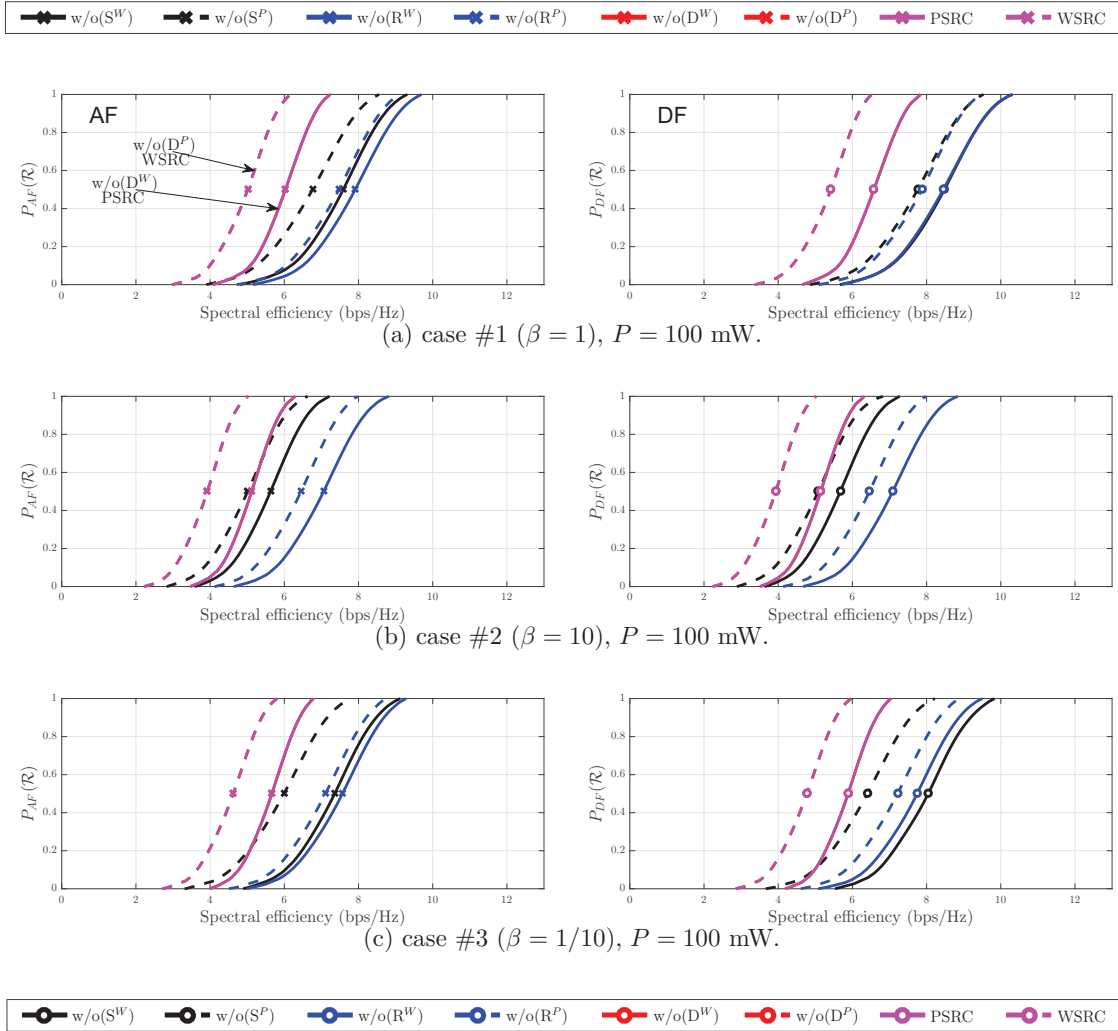


Figure 22: Outage probability for the HSRC without a node communication interface when  $\alpha = 1$ .

## 4 Conclusion

In this work, the HSRC and the incomplete HSRC models were formulated and their achievable data rates and outage probabilities analyzed. Numerical results based on achievable data rate gain in relation to  $SD^P$  and comparison to PSRC and WSRC was investigated for the cases where the R node is located in the middle between the S and D nodes (case #1), closer to the S than the D node (case #2), closer to the D than the S node (case #3), and far from both S and D nodes (case #4). In the sequel, it showed that HSRC offers higher achievable data rate gains than PSRC and WSRC for all variation of  $P$ ,  $\alpha$  and  $\beta$ . Additionally, for  $\alpha = 1$ , the highest achievable data rate gain of HSRC is obtained in case #1 ( $\beta = 1$ , the R node is in the middle between S and D nodes). On the other hand, HSRC performs worst for case #4 ( $\alpha = 0.1$ ,  $\beta < \alpha^{-1}$  and  $\beta > \alpha$ ), in which the R node is far from both S and D nodes.

Furthermore, it was discussed the outage probabilities related to HSRC. Based on the numerical results and a given spectral efficiency threshold  $\mathcal{R}_{th}$ , the attained results show that the HSRC with OA always yields lower outage probabilities than the HSRC with UA. Regarding the cooperative protocols, DF achieves lower outage probability than AF. Moreover, the case #1 results in the lowest outage probabilities and DF outperforms AF in all cases. Additionally, it was shown, for all cases, that HSRC performs better than 2WSRC when OA together with the chosen cooperative protocols, constraints on channel energy, and additive noise power apply.

In general, the HSRC without a wireless link (or node communication interface) performs better than or, at least, equal to the HSRC missing a PLC link (or node communication interface) for both AF and DF protocols, if  $P_{v,\ell}^W = P_{v,\ell}^P$ ,  $\|\mathbf{h}_\ell^P\|^2 = \|\mathbf{h}_\ell^W\|^2$ , and OA is adopted,  $\forall P, \alpha, \beta$ . Overall, for all cases, the incomplete HSRC performs better than or equal to PSRC or WSRC. Also, the limit analysis when  $P \rightarrow \infty$  (I) and  $P \rightarrow 0$  (II) confirmed this behavior. Moreover, PSRC acts as a lower bound for the HSRC when a wireless link (or node communication interface) is missed as well as the HSRC missing a PLC link (or node communication interface) is lower bounded by the WSRC. Additionally, the importance on the achievable data rate ratio of (PLC and wireless)  $SD$  link (or S node communication interface) when  $\alpha \ll 1$  (R node is far from both S and D nodes) and  $SR$  and  $RD$  links (or R node communication interface) if  $\alpha \gg 1$  (R node is close to the S and D nodes) was shown.

Moreover, HSRC is similar to the single SRC (PSRC or WSRC) when it misses one D node communication interface. Besides, the wireless links contribution to HSRC are low when  $P = 1$  mW, therefore when a wireless link (or node communication interface) is missed, high values of achievable data rate ratio are observed and the opposite occurs when a PLC link (or node communication interface) is lost. As  $P$  increases, the gap of

performance between PLC and wireless links reduces and the aforementioned behavior is less noticed. Finally, but not the least, when HSRC misses a *SR* or *RD* link (or R node communication interface) more significant losses are experienced with the use of DF than AF because the former has a better performance on the *SRD* link. The opposite situation occurs for the *SD* link (or S node communication interface) loss due to the lower contribution of the *SD* link when applying DF rather than AF. Now, and most important, HSRC presents a small difference of performance between the use of AF and DF protocols due to the fact that HSRC is more flexible to compensate differences between both protocols.

Concerning case #1 and  $P = 1$  mW, it was shown that the wireless contribution is lower as  $\alpha$  is closer to 1 or 0.5 for AF and DF protocols, respectively, because the wireless links do not have a significant impact on the achievable data rate ratio. Furthermore, case #2 has a greater loss than case #1 when HSRC misses a *SD* link (or S node communication interface). On the other hand, case #2 has a lower loss than case #1 when misses the *SR* or *RD* link (or R node communication interface). Also, case #3 has similar performance to case #2 when HSRC misses a *SD* link (or S node communication interface) and it is similar to case #1 when a *SR* or *RD* link (or R node interface) is lost. Also, in comparison to the other cases, case #4 showed high achievable data rate ratios for the incomplete HSRC when a *SR* or *RD* link (or R node communication interface) is lost and low values of such ratio when a *SD* link (or S/D node communication interface) is missed due to its great dependence on the PLC and wireless *SD* links.

Finally, the outage probability curves related to the incomplete HSRC showed that the loss of any link or node communication interface results in less significant losses in case #1, followed by cases #3 and #2, respectively, if  $\alpha = 1$ ,  $P = 100$  mW, and one of the cooperative protocol is adopted because, in case #1, the balanced link energy scenario occurs and, as a consequence, all links can offer a significant contribution to the spectral efficiency. As a result, HSRC becomes more robust against a link or node communication interface loss in case #1 than in cases #2 and #3.

#### 4.1 Future Works

A list of future works are as follows:

- To consider the wireless frequency band of transmission occurs in other unlicensed wireless bandwidths (e.g., 2.4-2.5 GHz or 5.725-5.875 GHz).
- To analyze the same metrics to HSRC and 2WSRC based on measured channels and noises instead of mathematical models.

- To analyze the HSRC achievable data rates and outage probabilities for different system compositions, e.g., multiple relay [23] and multi-hop [52] models.
- To discuss the bit error rate performance of HSRC and aforementioned models in comparison to the not hybrid ones.
- To introduce and to check the energy harvesting technique [53] benefits on the HSRC model.
- To expand these analyses to the hybrid system composed of PLC-wireless communication and visible light communication (VLC) [54].

## REFERENCES

- [1] N. Shlezinger and R. Dabora, "On the capacity of narrowband PLC channels," *IEEE Trans. Commun.*, vol. 63, no. 4, pp. 1191–1201, Apr. 2015.
- [2] S. Galli, A. Scaglione, and Z. Wang, "For the grid and through the grid: The role of power line communications in the smart grid," *Proc. IEEE*, vol. 99, no. 6, pp. 998–1027, Jun. 2011.
- [3] M. Sayed and N. Al-Dhahir, "Narrowband-PLC/wireless diversity for smart grid communications," in *Proc. IEEE Global Commun. Conf.*, Dec. 2014, pp. 2966–2971.
- [4] Z. Lin, P. I. Mak, and R. P. Martins, "A sub-ghz multi-ISM-band zigbee receiver using function-reuse and gain-boosted n-path techniques for IoT applications," *IEEE J. Solid-State Circuits*, vol. 49, no. 12, pp. 2990–3004, Dec. 2014.
- [5] M. V. Ribeiro, "Técnicas de processamento de sinais aplicadas a transmissão de dados via rede elétrica e ao monitoramento da qualidade de energia," Ph.D. dissertation, State University of Campinas, 2005.
- [6] M. Nassar *et al.*, "Local utility power line communications in the 3-500 khz band: Channel impairments, noise, and standards," *IEEE Signal Process. Mag.*, vol. 29, no. 5, pp. 116–127, Sep. 2012.
- [7] J. Anatory, N. Theethayi, R. Thottappillil, M. Kissaka, and N. Mvungi, "The effects of load impedance, line length, and branches in typical low-voltage channels of the BPLC systems of developing countries: Transmission-line analyses," *IEEE Trans. Power Del.*, vol. 24, no. 2, pp. 621–629, Apr. 2009.
- [8] S. Güzelgöz, H. B. Celebi, and H. Arslan, "Statistical characterization of the paths in multipath PLC channels," *IEEE Trans. Power Del.*, vol. 26, no. 1, pp. 181–187, Jan. 2011.
- [9] M. Zimmerman and K. Dostert, "A multipath model for the power line channel," *IEEE Trans. Commun.*, vol. 50, no. 4, pp. 553–559, Apr. 2002.
- [10] M. V. Ribeiro *et al.*, "Clustered-orthogonal frequency division multiplexing for power line communication: When is it beneficial?" *IET Commun.*, vol. 8, no. 13, pp. 2336–2347, Sep. 2014.
- [11] M. Tlich, A. Zeddami, F. Moulin, and F. Gauthier, "Indoor power-line communications channel characterization up to 100 mhz - part ii: Time frequency analysis," *IEEE Trans. Power Del.*, vol. 23, no. 3, pp. 1402–1409, Jul. 2008.
- [12] J. A. Cortés, F. J. Cañete, L. Díez, and J. L. G. Moreno, "On the statistical properties of indoor power line channels: Measurements and models," in *Proc. IEEE Int. Symp. on Power Line Commun. Appl.*, Apr. 2011, pp. 271–276.
- [13] G. R. Colen *et al.*, "Measurement setup for characterizing low-voltage and outdoor electric distribution grids for PLC systems," in *Proc. PES Conf. Innov. Smart Grid Technol. Latin Amer.*, Apr. 2013, pp. 1–5.

- [14] T. R. Oliveira *et al.*, “A methodology for estimating frequency responses of electric power grids,” *J. Control Autom. Elec. Syst.*, vol. 25, no. 6, pp. 720–731, Dec. 2014.
- [15] A. M. Tonello, F. Versolatto, and A. Pittolo, “In-home power line communication channel: Statistical characterization,” *IEEE Trans. Commun.*, vol. 62, no. 6, pp. 2096–2106, Jun. 2014.
- [16] A. A. M. Picorone, T. R. Oliveira, and M. V. Ribeiro, “PLC channel estimation based on pilots signal for OFDM modulation: A review,” *IEEE Latin Amer. Trans.*, vol. 12, no. 4, pp. 580–589, Jun. 2014.
- [17] V. Fernandes, S. Angelova, W. A. Finamore, and M. V. Ribeiro, “On modeling power-line communication noise,” in *Proc. XXXIII Simpósio Brasileiro de Telecomunicações*, Sep. 2015.
- [18] S. Güzelgöz, “Characterizing wireless and powerline communication channels with applications to smart grid networks,” Ph.D. dissertation, University of South Florida, Apr. 2011.
- [19] M. Sayed, G. Sebaali, E. B. L., and N. Al-Dhahir, “Efficient diversity technique for hybrid narrowband-powerline/wireless smart grid communications,” in *Proc. IEEE Int. Conf. Smart Grid Commun.*, Nov. 2015, pp. 1–6.
- [20] A. Nosratinia, T. E. Hunter, and A. Hedayat, “Cooperative communication in wireless networks,” *IEEE Commun. Mag.*, vol. 42, no. 10, pp. 74–80, Oct. 2004.
- [21] J. N. Laneman, D. N. C. Tse, and G. W. Wornell, “Cooperative diversity in wireless networks: Efficient protocols and outage behavior,” *IEEE Trans. Inf. Theory*, vol. 50, no. 12, pp. 3062–3080, Dec. 2004.
- [22] P. Herhold, E. Zimmermann, and G. Fettweis, “On the performance of cooperative amplify-and-forward relay networks,” in *Proc. Int. ITG Conf. Source and Channel Coding*, Jan. 2004, pp. 451–458.
- [23] G. Farhadi and N. C. Beaulieu, “Ergodic capacity analysis of wireless relaying systems in rayleigh fading,” in *Proc. IEEE Int. Conf. Commun.*, May 2008, pp. 3730–3735.
- [24] M. S. P. Facina, H. A. Latchman, H. V. Poor, and M. V. Ribeiro, “Cooperative in-home power line communication: Analyses based on a measurement campaign,” *IEEE Trans. Commun.*, vol. 64, no. 2, pp. 778–789, Feb. 2016.
- [25] M. S. P. Facina, “Cooperative in-home power line communication: Analyses based on a measurement campaign,” Master’s thesis, Federal University of Juiz de Fora, 2015.
- [26] S. D’Alessandro and A. M. Tonello, “On rate improvements and power saving with opportunistic relaying in home power line networks,” *EURASIP J. Adv. Signal Process.*, vol. 2012, no. 1, pp. 1–17, Sep. 2012.
- [27] J. Valencia, T. R. Oliveira, and M. V. Ribeiro, “Cooperative power line communication: Analysis of brazilian in-home channels,” in *Proc. IEEE Int. Symp. Power Line Commun. Appl.*, Mar. 2014, pp. 301–305.

- [28] R. M. Oliveira, M. S. P. Facina, M. V. Ribeiro, and A. B. Vieira, "Performance evaluation of in-home broadband PLC systems using a cooperative MAC protocol," *Comput. Netw.*, vol. 95, pp. 62–76, Dec. 2015.
- [29] M. Dohler and Y. Li, *Cooperative Communications: Hardware, Channel & PHY*. Wiley, 2010.
- [30] G. Sebaali and B. L. Evans, "Design tradeoffs in joint powerline and wireless transmission for smart grid communications," in *Proc. IEEE Int. Symp. on Power Line Commun. Appl.*, Mar. 2015, pp. 83–88.
- [31] L. M. B. A. Dib, V. Fernandes, and M. V. Ribeiro, "A discussion about hybrid PLC-wireless communication for smart grids," in *Proc. XXXIV Simpósio Brasileiro de Telecomunicações*, Sep. 2016, pp. 848–852.
- [32] M. Kuhn and A. Wittneben, "PLC enhanced wireless access networks: A link level capacity consideration," in *Proc. IEEE Veh. Technol. Conf.*, May 2002, pp. 125–129.
- [33] M. Kuhn, S. Berger, I. Hammerström, and A. Wittneben, "Power line enhanced cooperative wireless communications," *IEEE J. Sel. Areas in Commun.*, vol. 24, no. 7, pp. 1401–1410, Jul. 2006.
- [34] S. Güzelgöz, H. B. Celebi, and H. Arsian, "Analysis of a multi-channel receiver: Wireless and PLC reception," in *Proc. Signal Process. Conf.*, Aug. 2010, pp. 1106–1110.
- [35] S. W. Lai and G. G. Messier, "Using the wireless and PLC channels for diversity," *IEEE Trans. Commun.*, vol. 60, no. 12, pp. 3865–3875, Dec. 2012.
- [36] S. W. Lai, N. Shabehpour, G. G. Messier, and L. Lampe, "Performance of wireless/power line media diversity in the office environment," in *Proc. IEEE Global Commun. Conf.*, Dec. 2014, pp. 2972–2976.
- [37] J. Lee and Y. Kim, "Diversity relaying for parallel use of power-line and wireless communication networks," *IEEE Trans. Power Del.*, vol. 29, no. 3, pp. 1301–1310, Jun. 2014.
- [38] V. Fernandes, M. L. Filomeno, W. A. Finamore, and M. V. Ribeiro, "An investigation on narrow band PLC-wireless parallel channel capacity," in *Proc. XXXIV Simpósio Brasileiro de Telecomunicações*, Sep. 2016, pp. 834–838.
- [39] T. R. Oliveira, C. A. G. Marques, M. S. Pereira, S. L. Netto, and M. V. Ribeiro, "The characterization of hybrid PLC-wireless channels: A preliminary analysis," in *Proc. IEEE Int. Symp. on Power Line Commun. Appl.*, Mar. 2013, pp. 98–102.
- [40] T. R. Oliveira, F. J. A. Andrade, A. A. M. Picorone, H. A. Latchman, S. L. Netto, and M. V. Ribeiro, "Characterization of hybrid communication channel in indoor scenario," *Journal of Commun. and Inf. Systems*, vol. 31, no. 1, pp. 224–235, 2016.
- [41] C. Choudhuri and U. Mitra, "Capacity bounds for relay channels with intersymbol interference and colored gaussian noise," *IEEE Trans. Inf. Theory*, vol. 60, no. 9, pp. 5639–5652, Sep. 2014.

- [42] A. J. Goldsmith and M. Effros, "The capacity region of broadcast channels with intersymbol interference and colored gaussian noise," *IEEE Trans. Inf. Theory*, vol. 47, no. 1, pp. 219–240, Jan. 2001.
- [43] T. M. Cover and J. A. Thomas, *Elements of Information Theory*. Wiley, 1991.
- [44] J. M. Cioffi, *Chapter 4: Multi-channel modulation*, accessed in May 2016. [Online]. Available: <http://web.stanford.edu/group/cioffi/book/chap4.pdf>
- [45] G. R. Colen *et al.*, "A temporal compressive resource allocation technique for complexity reduction in PLC transceivers," *Trans. Emerging Telecommun. Technol.*, May 2015.
- [46] G. R. Colen, L. G. de Oliveira, A. J. Han Vinck, and M. V. Ribeiro, "A spectral compressive resource allocation technique for PLC systems," *IEEE Trans. Commun.*, 2016, to be published.
- [47] G. R. Colen, "Resource allocation and time-frequency modulation for power line communication," Ph.D. dissertation, Federal University of Juiz de Fora, 2016.
- [48] *IEEE Standard for Low Frequency (less than 500 kHz) Narrow Band Power Line Communications for Smart Grid Application*, IEEE Std. 1901.2, 2013.
- [49] M. Katayama, T. Yamazato, and H. Okada, "A mathematical model of noise in narrowband power line communication systems," *IEEE J. Sel. Areas Commun.*, vol. 24, no. 7, pp. 1267–1276, Jul. 2006.
- [50] A. F. Molisch *et al.*, "IEEE 802.15.4a channel model - final report," IEEE 802.15 WPAN Low Rate Alternative PHY Task Group, Tech. Rep., Nov. 2004.
- [51] A. A. M. Saleh and R. A. Valenzuela, "A statistical model for indoor multipath propagation," *IEEE J. Sel. Areas Commun.*, vol. 5, no. 2, pp. 128–137, Feb. 1987.
- [52] A. Dubey and R. K. Mallik, "PLC system performance with AF relaying," *IEEE Trans. Commun.*, vol. 63, no. 6, pp. 2337–2345, Jun. 2015.
- [53] N. T. Do, D. B. da Costa, and B. An, "Performance analysis of multirelay RF energy harvesting cooperative networks with hardware impairments," *IET Commun.*, vol. 10, no. 18, pp. 2551–2558, Dec. 2016.
- [54] M. Kashef, A. Torky, M. Abdallah, N. Al-Dhahir, and K. Qaraqe, "On the achievable rate of a hybrid PLC/VLC/RF communication system," in *Proc. IEEE Global Commun. Conf.*, Dec. 2015, pp. 1–6.

## Appendix A – Achievable Data Rate: The HSRC without $SD^q$

Figure 23 shows the HSRC without  $SD^q$  in which the missed link is highlighted in the red color. The  $\mathbf{D}_{AF}$  matrix is the denominator term in (2.17) and it contains the matrix  $\Lambda_{\mathbf{v}_{SD}^q}^{\sigma^2}$  which tends to infinity when the  $SD^q$  link is lost. As a consequence, this change is introduced by the removal of the first element (if removing  $SD^P$ ) or third element (if removing  $SD^W$ ) of the diagonal matrices  $\mathbf{C}_{AF}$  and  $\mathbf{D}_{AF}$  given by (2.18) and (2.19), respectively. As a result, the new matrices  $\mathbf{C}'_{AF}$  and  $\mathbf{D}'_{AF}$  will be given by (A.1) and (A.2). Furthermore, the loss of the  $SD^q$  link implies that  $P_0^q$  is allocated only to the  $SR^q$  link.

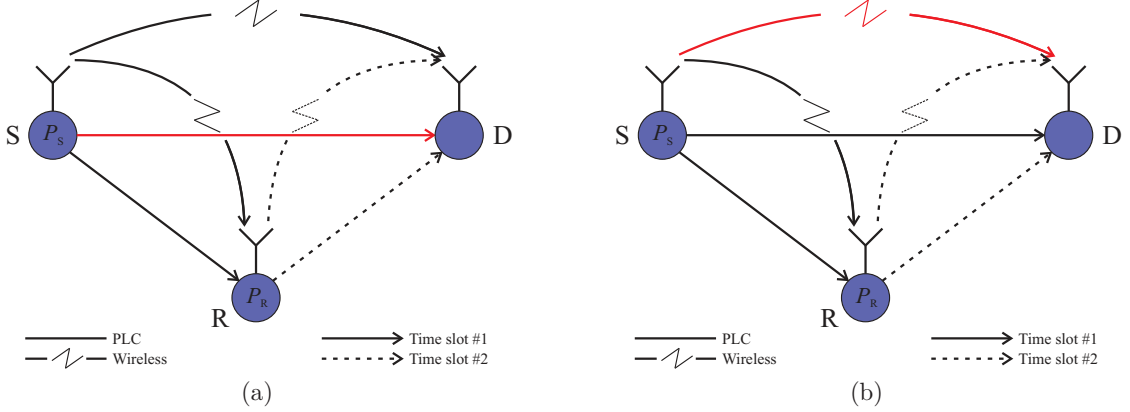


Figure 23: The HSRC without  $SD^q$ , for (a)  $q = P$  and (b)  $q = W$ .

$$\mathbf{C}'_{AF} = \begin{bmatrix} \Lambda_{P_0^q} \Lambda_{|\mathcal{H}_{SD}^q|^2} & 0 & 0 \\ 0 & \Lambda_{P_0^q} \Lambda_{P_1^q} \Lambda_{\sigma_{Y_{SR}}^q}^{-1} \Lambda_{|\mathcal{H}_{SR}^q|^2} \Lambda_{|\mathcal{H}_{RD}^q|^2} & 0 \\ 0 & 0 & \Lambda_{P_0^q} \Lambda_{P_1^q} \Lambda_{\sigma_{Y_{SR}}^q}^{-1} \Lambda_{|\mathcal{H}_{SR}^q|^2} \Lambda_{|\mathcal{H}_{RD}^q|^2} \end{bmatrix} \quad (\text{A.1})$$

$$\mathbf{D}'_{AF} = \begin{bmatrix} \Lambda_{\mathbf{v}_{SD}^q}^{\sigma^2} & 0 & 0 \\ 0 & \Lambda_{|\mathcal{H}_{RD}^q|^2} \Lambda_{P_1^q} \Lambda_{\sigma_{Y_{SR}}^q}^{-1} \Lambda_{\sigma_{Y_{SR}}^q}^2 + \Lambda_{\sigma_{Y_{RD}}^q}^2 & 0 \\ 0 & 0 & \Lambda_{|\mathcal{H}_{RD}^q|^2} \Lambda_{P_1^q} \Lambda_{\sigma_{Y_{SR}}^q}^{-1} \Lambda_{\sigma_{Y_{SR}}^q}^2 + \Lambda_{\sigma_{Y_{RD}}^q}^2 \end{bmatrix} \quad (\text{A.2})$$

Thus, if the AF protocol is adopted, then the achievable data rate of this incomplete HSRC is expressed as

$$C_{AF} = \mathbb{E}_{\mathbf{H}_\ell^P, \mathbf{H}_\ell^W} \left\{ \max_{\Lambda_P} \frac{B_W}{N} \log_2 [\det(\mathbf{I}_{3N} + \mathbf{C}'_{AF} \mathbf{D}'_{AF}^{-1})] \right\} \quad (\text{A.3})$$

subject to  $\text{Tr}(\mathbf{\Lambda}_P) \leq P$ . Similarly, for the DF protocol, the achievable data rate of the HSRC without  $SD^q$  is given by

$$C_{DF} = \mathbb{E}_{\mathbf{H}_\ell^P, \mathbf{H}_\ell^W} \left\{ \max_{\mathbf{\Lambda}_P} \frac{B_W}{N} \log_2 [\det(\mathbf{I}_{3N} + \mathbf{C}'_{DF} \mathbf{D}'_{DF})] \right\} \quad (\text{A.4})$$

subject to  $\text{Tr}(\mathbf{\Lambda}_P) \leq P$ , in which

$$\mathbf{C}'_{DF} = \begin{bmatrix} \mathbf{\Lambda}_{P_0^{\bar{q}}} \mathbf{\Lambda}_{|\mathcal{H}_{SD}^{\bar{q}}|^2} & 0 & 0 \\ 0 & \mathbf{\Lambda}_{C^{\bar{q}*}} & 0 \\ 0 & 0 & \mathbf{\Lambda}_{C^{q*}} \end{bmatrix}, \quad (\text{A.5})$$

and

$$\mathbf{D}'_{DF} = \begin{bmatrix} \mathbf{\Lambda}_{\sigma^2 \mathbf{v}_{SD}^{\bar{q}}} & 0 & 0 \\ 0 & \mathbf{\Lambda}_{D^{\bar{q}*}} & 0 \\ 0 & 0 & \mathbf{\Lambda}_{D^{q*}} \end{bmatrix}, \quad (\text{A.6})$$

where  $\mathbf{\Lambda}_{C^{\bar{q}*}}$  and  $\mathbf{\Lambda}_{C^{q*}}$  are given by (2.24) as well as  $\mathbf{\Lambda}_{D^{\bar{q}*}}$  and  $\mathbf{\Lambda}_{D^{q*}}$  are given by (2.25).

## Appendix B – Achievable Data Rate: The HSRC without $SR^q$

Figure 24 shows the HSRC without  $SR^q$  in which the missed link is highlighted in red. The  $\mathbf{D}_{AF}$  matrix is the denominator term in (2.17) and it contains the term  $\Lambda_{\sigma_{\mathbf{v}_{SR}^q}^2}$  which tends to infinity when the  $SR^q$  link is lost. Similarly, to the same end, it can be removed the second element (if removing  $SR^P$ ) or fourth element (if removing  $SR^W$ ) of the diagonal matrices  $\mathbf{C}_{AF}$  and  $\mathbf{D}_{AF}$  given by (2.18) and (2.19), respectively, resulting in the new matrices  $\mathbf{C}'_{AF}$  and  $\mathbf{D}'_{AF}$  given by (B.1) and (B.2). Furthermore, it is considered that  $P_0^q$  is allocated only to the  $SD^q$  link when the  $SR^q$  link is lost.

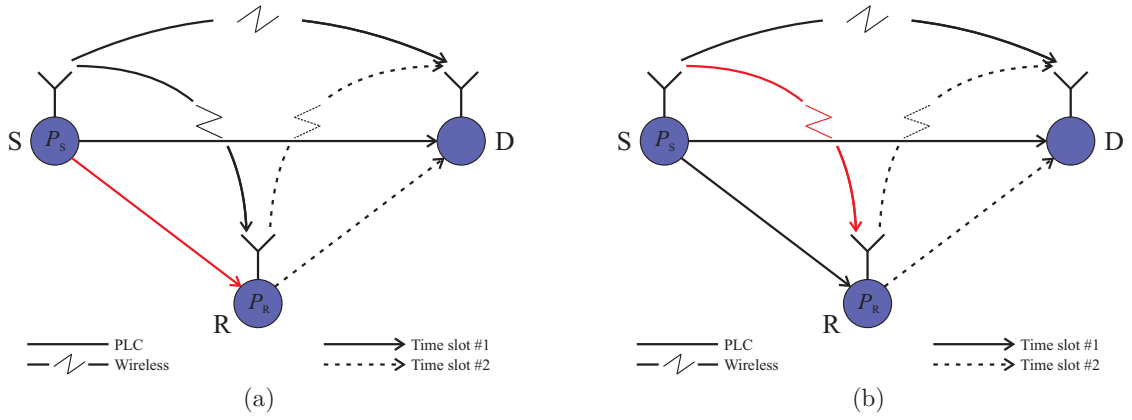


Figure 24: The HSRC without  $SR^q$ , for (a)  $q = P$  and (b)  $q = W$ .

$$\mathbf{C}'_{AF} = \begin{bmatrix} \Lambda_{P_0^q} \Lambda_{|\mathcal{H}_{SD}^q|^2} & 0 & 0 \\ 0 & \Lambda_{P_0^q} \Lambda_{P_1^q} \Lambda_{\sigma_{\mathbf{Y}_{SR}^q}^2}^{-1} \Lambda_{|\mathcal{H}_{SR}^q|^2} \Lambda_{|\mathcal{H}_{RD}^q|^2} & 0 \\ 0 & 0 & \Lambda_{P_0^q} \Lambda_{|\mathcal{H}_{SD}^q|^2} \end{bmatrix} \quad (\text{B.1})$$

$$\mathbf{D}'_{AF} = \begin{bmatrix} \Lambda_{\sigma_{\mathbf{v}_{SD}^q}^2} & 0 & 0 \\ 0 & \Lambda_{|\mathcal{H}_{RD}^q|^2} \Lambda_{P_1^q} \Lambda_{\sigma_{\mathbf{Y}_{SR}^q}^2}^{-1} \Lambda_{\sigma_{\mathbf{v}_{SR}^q}^2} + \Lambda_{\sigma_{\mathbf{v}_{RD}^q}^2} & 0 \\ 0 & 0 & \Lambda_{\sigma_{\mathbf{v}_{SD}^q}^2} \end{bmatrix} \quad (\text{B.2})$$

Thus, if the AF protocol is adopted, then the achievable data rate of this kind of incomplete HSRC is expressed as

$$C_{AF} = \mathbb{E}_{\mathbf{H}_\ell^P, \mathbf{H}_\ell^W} \left\{ \max_{\Lambda_P} \frac{B_W}{N} \log_2 [\det(\mathbf{I}_{3N} + \mathbf{C}'_{AF} \mathbf{D}'_{AF}^{-1})] \right\} \quad (\text{B.3})$$

subject to  $\text{Tr}(\Lambda_P) \leq P$ . Similarly, for the DF protocol, the achievable data rate of the incomplete HSRC is given by

$$C_{DF} = \mathbb{E}_{\mathbf{H}_\ell^P, \mathbf{H}_\ell^W} \left\{ \max_{\Lambda_P} \frac{B_W}{N} \log_2 [\det(\mathbf{I}_{3N} + \mathbf{C}'_{DF} \mathbf{D}'_{DF}^{-1})] \right\} \quad (\text{B.4})$$

subject to  $\text{Tr}(\mathbf{\Lambda}_P) \leq P$ , in which

$$\mathbf{C}'_{DF} = \begin{bmatrix} \mathbf{\Lambda}_{P_0^q} \mathbf{\Lambda}_{|\mathbf{r}_{SD}^q|^2} & 0 & 0 \\ 0 & \mathbf{\Lambda}_{C\bar{q}^*} & 0 \\ 0 & 0 & \mathbf{\Lambda}_{P_0^q} \mathbf{\Lambda}_{|\mathbf{r}_{SD}^q|^2} \end{bmatrix}, \quad (\text{B.5})$$

and

$$\mathbf{D}'_{DF} = \begin{bmatrix} \mathbf{\Lambda}_{\sigma_{\mathbf{v}_{SD}^q}^2} & 0 & 0 \\ 0 & \mathbf{\Lambda}_{D\bar{q}^*} & 0 \\ 0 & 0 & \mathbf{\Lambda}_{\sigma_{\mathbf{v}_{SD}^q}^2} \end{bmatrix}, \quad (\text{B.6})$$

where  $\mathbf{\Lambda}_{C\bar{q}^*}$  and  $\mathbf{\Lambda}_{D\bar{q}^*}$  are given by (2.24) and (2.25), respectively.

### Appendix C – Achievable Data Rate: The HSRC without $RD^q$

Figure 25 shows the HSRC without  $RD^q$  in which the missed link is highlighted in the red color. The  $\mathbf{D}_{AF}$  matrix is the denominator term in (2.17) and it contains the matrix  $\Lambda_{\sigma^2 \mathbf{v}_{RD}^q}$  which tends to infinity when the  $RD^q$  link is lost. Therefore, it can be, similarly, removed the second element (if removing  $RD^P$ ) or fourth element (if removing  $RD^W$ ) of the diagonal matrices  $\mathbf{C}_{AF}$  and  $\mathbf{D}_{AF}$  given by (2.18) and (2.19), respectively. As a result, the new matrices  $\mathbf{C}'_{AF}$  and  $\mathbf{D}'_{AF}$  are given by (C.1) and (C.2). Furthermore, it is considered that the power available to the R node transmission is allocated only to the  $RD^{\bar{q}}$  link ( $P_1^{\bar{q}} = P_R$ ). Note that, for the HSRC without  $RD^q$ , the same matrices  $\mathbf{C}'_{AF}$  and  $\mathbf{D}'_{AF}$  are obtained as for the HSRC without  $SR^q$  because the matrices  $\Lambda_{\sigma^2 \mathbf{v}_{SR}^q}$  and  $\Lambda_{\sigma^2 \mathbf{v}_{RD}^q}$  appear at the same positions in  $\mathbf{D}_{AF}$ . Thus, the difference among them is the power allocation.

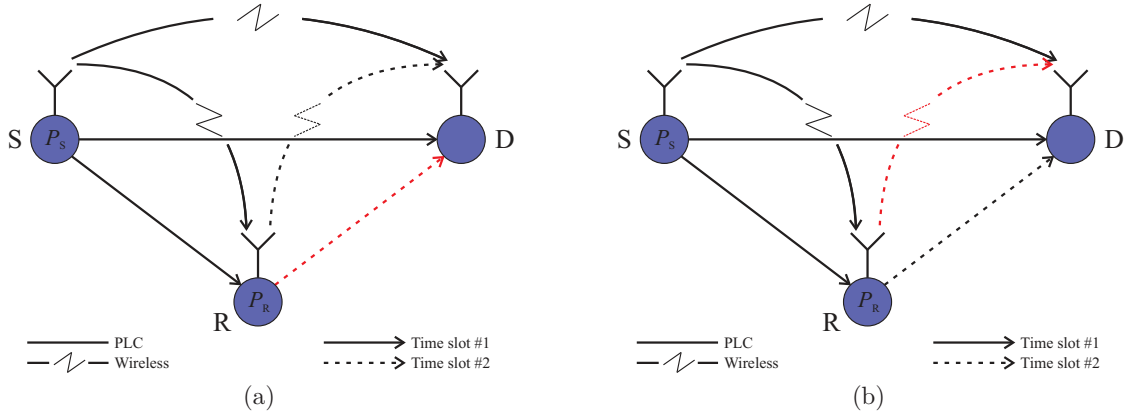


Figure 25: The HSRC without  $RD^q$ , for (a)  $q = P$  and (b)  $q = W$ .

$$\mathbf{C}'_{AF} = \begin{bmatrix} \Lambda_{P_0^{\bar{q}}} \Lambda_{|\mathcal{H}_{SD}^{\bar{q}}|^2} & 0 & 0 \\ 0 & \Lambda_{P_0^{\bar{q}}} \Lambda_{P_1^{\bar{q}}} \Lambda_{\sigma^2 \mathbf{y}_{SR}^{\bar{q}}}^{-1} \Lambda_{|\mathcal{H}_{SR}^{\bar{q}}|^2} \Lambda_{|\mathcal{H}_{RD}^{\bar{q}}|^2} & 0 \\ 0 & 0 & \Lambda_{P_0^q} \Lambda_{|\mathcal{H}_{SD}^q|^2} \end{bmatrix} \quad (\text{C.1})$$

$$\mathbf{D}'_{AF} = \begin{bmatrix} \Lambda_{\sigma^2 \mathbf{v}_{SD}^{\bar{q}}} & 0 & 0 \\ 0 & \Lambda_{|\mathcal{H}_{RD}^{\bar{q}}|^2} \Lambda_{P_1^{\bar{q}}} \Lambda_{\sigma^2 \mathbf{y}_{SR}^{\bar{q}}}^{-1} \Lambda_{\sigma^2 \mathbf{v}_{SR}^{\bar{q}}} + \Lambda_{\sigma^2 \mathbf{v}_{RD}^{\bar{q}}} & 0 \\ 0 & 0 & \Lambda_{\sigma^2 \mathbf{v}_{SD}^q} \end{bmatrix} \quad (\text{C.2})$$

Thus, if the AF protocol is adopted, then the achievable data rate of this incomplete HSRC is expressed as

$$C_{AF} = \mathbb{E}_{\mathbf{H}_\ell^P, \mathbf{H}_\ell^W} \left\{ \max_{\Lambda_P} \frac{B_W}{N} \log_2 [\det(\mathbf{I}_{3N} + \mathbf{C}'_{AF} \mathbf{D}'_{AF}^{-1})] \right\} \quad (\text{C.3})$$

subject to  $\text{Tr}(\mathbf{\Lambda}_{P_0^q}) + \text{Tr}(\mathbf{\Lambda}_{P_0^{\bar{q}}}) + \text{Tr}(\mathbf{\Lambda}_{P_1^{\bar{q}}}) \leq P$ . Similarly, for the DF protocol, the achievable data rate of the incomplete HSRC is given by

$$C_{DF} = \mathbb{E}_{\mathbf{H}_\ell^P, \mathbf{H}_\ell^W} \left\{ \max_{\mathbf{\Lambda}_P} \frac{B_W}{N} \log_2 [\det(\mathbf{I}_{3N} + \mathbf{C}'_{DF} \mathbf{D}'_{DF}{}^{-1})] \right\} \quad (\text{C.4})$$

subject to  $\text{Tr}(\mathbf{\Lambda}_{P_0^q}) + \text{Tr}(\mathbf{\Lambda}_{P_0^{\bar{q}}}) + \text{Tr}(\mathbf{\Lambda}_{P_1^{\bar{q}}}) \leq P$ , in which

$$\mathbf{C}'_{DF} = \begin{bmatrix} \mathbf{\Lambda}_{P_0^{\bar{q}}} \mathbf{\Lambda}_{|\mathbf{h}_{SD}^{\bar{q}}|^2} & 0 & 0 \\ 0 & \mathbf{\Lambda}_{C^{\bar{q}*}} & 0 \\ 0 & 0 & \mathbf{\Lambda}_{P_0^q} \mathbf{\Lambda}_{|\mathbf{h}_{SD}^q|^2} \end{bmatrix}, \quad (\text{C.5})$$

and

$$\mathbf{D}'_{DF} = \begin{bmatrix} \mathbf{\Lambda}_{\sigma_{\mathbf{v}_{SD}^{\bar{q}}}^2} & 0 & 0 \\ 0 & \mathbf{\Lambda}_{D^{\bar{q}*}} & 0 \\ 0 & 0 & \mathbf{\Lambda}_{\sigma_{\mathbf{v}_{SD}^q}^2} \end{bmatrix}, \quad (\text{C.6})$$

where  $\mathbf{\Lambda}_{C^{\bar{q}*}}$  and  $\mathbf{\Lambda}_{D^{\bar{q}*}}$  are given by (2.24) and (2.25), respectively.

### Appendix D – Achievable Data Rate: The HSRC without $S^q$

Figure 26 shows the HSRC without the  $S^q$  link in which the missed links due to the  $S^q$  loss are highlighted in red as well as the respective communication interface. Using (2.8) and (2.10), the received symbol of this incomplete HSRC assuming AF is expressed as (D.1). Furthermore, it is considered that  $P_S$  is allocated solely to the  $\bar{q}^{th}$  communication medium transmission by the S node ( $P_0^{\bar{q}} = P_S$ ).

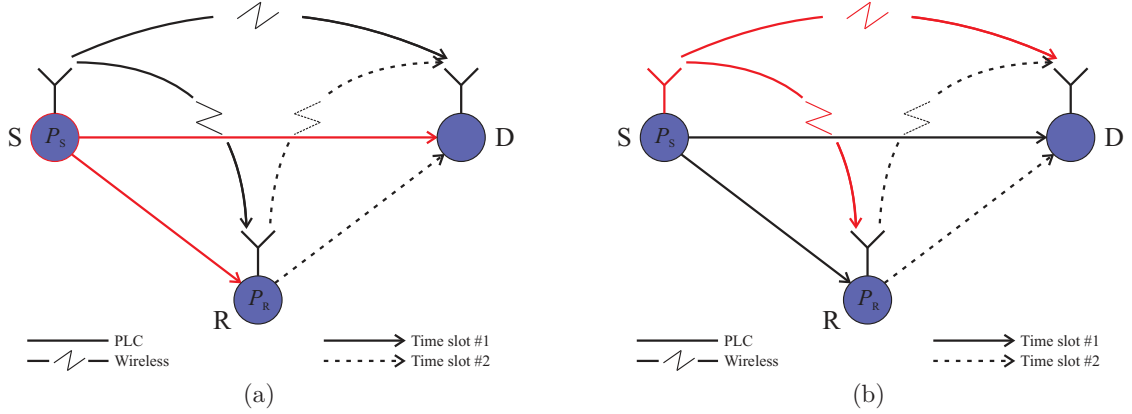


Figure 26: The HSRC without  $S^q$ , for (a)  $q = P$  and (b)  $q = W$ .

$$\begin{aligned}
\mathbf{Y} &= \begin{bmatrix} \mathbf{Y}_{SD}^{\bar{q}} \\ \mathbf{Y}_{SRD,AF}^{\bar{q}} \\ \mathbf{Y}_{SRD,AF}^q \end{bmatrix} \\
&= \begin{bmatrix} \mathcal{H}_{SD}^{\bar{q}} & 0 & 0 \\ 0 & \mathcal{H}_{SR}^{\bar{q}} \mathcal{H}_{RD}^{\bar{q}} & 0 \\ 0 & 0 & \mathcal{H}_{SR}^{\bar{q}} \mathcal{H}_{RD}^q \end{bmatrix} \begin{bmatrix} \Lambda \sqrt{P_0^{\bar{q}}} \mathbf{X} \\ \Lambda \sqrt{P_0^{\bar{q}}} \Lambda \sqrt{P_1^{\bar{q}}} \Lambda_{\sigma_{\mathbf{Y}_{SR}^{\bar{q}}}}^{-1} \mathbf{X} \\ \Lambda \sqrt{P_0^{\bar{q}}} \Lambda \sqrt{P_1^q} \Lambda_{\sigma_{\mathbf{Y}_{SR}^q}}^{-1} \mathbf{X} \end{bmatrix} + \begin{bmatrix} \mathbf{V}_{SD}^{\bar{q}} \\ \Lambda \sqrt{P_1^{\bar{q}}} \mathcal{H}_{RD}^{\bar{q}} \Lambda_{\sigma_{\mathbf{Y}_{SR}^{\bar{q}}}}^{-1} \mathbf{V}_{SR}^{\bar{q}} + \mathbf{V}_{RD}^{\bar{q}} \\ \Lambda \sqrt{P_1^q} \mathcal{H}_{RD}^q \Lambda_{\sigma_{\mathbf{Y}_{SR}^q}}^{-1} \mathbf{V}_{SR}^{\bar{q}} + \mathbf{V}_{RD}^q \end{bmatrix} \\
&= \begin{bmatrix} \mathcal{H}_{SD}^{\bar{q}} \Lambda \sqrt{P_0^{\bar{q}}} \\ \mathcal{H}_{SR}^{\bar{q}} \mathcal{H}_{RD}^{\bar{q}} \Lambda \sqrt{P_0^{\bar{q}}} \Lambda \sqrt{P_1^{\bar{q}}} \Lambda_{\sigma_{\mathbf{Y}_{SR}^{\bar{q}}}}^{-1} \\ \mathcal{H}_{SR}^{\bar{q}} \mathcal{H}_{RD}^q \Lambda \sqrt{P_0^{\bar{q}}} \Lambda \sqrt{P_1^q} \Lambda_{\sigma_{\mathbf{Y}_{SR}^q}}^{-1} \end{bmatrix} \mathbf{X} + \begin{bmatrix} \mathbf{I}_N & 0 & 0 & 0 \\ 0 & \Lambda \sqrt{P_1^{\bar{q}}} \mathcal{H}_{RD}^{\bar{q}} \Lambda_{\sigma_{\mathbf{Y}_{SR}^{\bar{q}}}}^{-1} & \mathbf{I}_N & 0 \\ 0 & \Lambda \sqrt{P_1^q} \mathcal{H}_{RD}^q \Lambda_{\sigma_{\mathbf{Y}_{SR}^q}}^{-1} & 0 & \mathbf{I}_N \end{bmatrix} \mathbf{V} \\
&= \mathbf{A}' \mathbf{X} + \mathbf{B}' \mathbf{V},
\end{aligned} \tag{D.1}$$

where  $\mathbf{V} = \left[ \mathbf{V}_{SD}^{\bar{q}T} \mathbf{V}_{SR}^{\bar{q}T} \mathbf{V}_{RD}^{\bar{q}T} \mathbf{V}_{RD}^qT \right]^T$ . Making  $\mathbf{C}'_{AF} = \mathbf{A}' \mathbf{R}_{\mathbf{X}\mathbf{X}} \mathbf{A}'^\dagger$  and  $\mathbf{D}'_{AF} = \mathbf{B}' \mathbf{R}_{\mathbf{V}\mathbf{V}} \mathbf{B}'^\dagger$ . Thus, from (2.13), it results that

$$I(\mathbf{X}, \mathbf{Y}) = \log_2 \left[ \det(\mathbf{I}_{3N} + \mathbf{C}'_{AF} \mathbf{D}'_{AF}{}^{-1}) \right], \tag{D.2}$$

in which

$$\mathbf{C}'_{AF} = \begin{bmatrix} \Lambda_{P_0^{\bar{q}}}\Lambda_{|\mathcal{H}_{SD}^{\bar{q}}|^2} & 0 & 0 \\ 0 & \Lambda_{P_0^{\bar{q}}}\Lambda_{P_1^{\bar{q}}}\Lambda_{\sigma_{Y_{SR}^{\bar{q}}}^2}^{-1} \Lambda_{|\mathcal{H}_{SR}^{\bar{q}}|^2}\Lambda_{|\mathcal{H}_{RD}^{\bar{q}}|^2} & 0 \\ 0 & 0 & \Lambda_{P_0^{\bar{q}}}\Lambda_{P_1^q}\Lambda_{\sigma_{Y_{SR}^{\bar{q}}}^2}^{-1} \Lambda_{|\mathcal{H}_{SR}^{\bar{q}}|^2}\Lambda_{|\mathcal{H}_{RD}^q|^2} \end{bmatrix} \quad (\text{D.3})$$

$$\mathbf{D}'_{AF} = \begin{bmatrix} \Lambda_{\sigma_{\mathbf{v}_{SD}^{\bar{q}}}^2} & 0 & 0 \\ 0 & \Lambda_{|\mathcal{H}_{RD}^{\bar{q}}|^2}\Lambda_{P_1^{\bar{q}}}\Lambda_{\sigma_{Y_{SR}^{\bar{q}}}^2}^{-1} \Lambda_{\sigma_{\mathbf{v}_{SR}^{\bar{q}}}^2} + \Lambda_{\sigma_{\mathbf{v}_{RD}^{\bar{q}}}^2} & 0 \\ 0 & 0 & \Lambda_{|\mathcal{H}_{RD}^q|^2}\Lambda_{P_1^q}\Lambda_{\sigma_{Y_{SR}^{\bar{q}}}^2}^{-1} \Lambda_{\sigma_{\mathbf{v}_{SR}^{\bar{q}}}^2} + \Lambda_{\sigma_{\mathbf{v}_{RD}^q}^2} \end{bmatrix} \quad (\text{D.4})$$

Finally, for the AF protocol, the achievable data rate of this incomplete HSRC is expressed as

$$C_{AF} = \mathbb{E}_{\mathbf{H}_\ell^P, \mathbf{H}_\ell^W} \left\{ \max_{\Lambda_P} \frac{B_W}{N} \log_2 [\det(\mathbf{I}_{3N} + \mathbf{C}'_{AF}\mathbf{D}'_{AF}^{-1})] \right\} \quad (\text{D.5})$$

subject to  $\text{Tr}(\Lambda_{P_0^{\bar{q}}}) + \text{Tr}(\Lambda_{P_1^q}) + \text{Tr}(\Lambda_{P_1^{\bar{q}}}) \leq P$ . Similarly, for the DF protocol, the achievable data rate is given by

$$C_{DF} = \mathbb{E}_{\mathbf{H}_\ell^P, \mathbf{H}_\ell^W} \left\{ \max_{\Lambda_P} \frac{B_W}{N} \log_2 [\det(\mathbf{I}_{3N} + \mathbf{C}'_{DF}\mathbf{D}'_{DF}^{-1})] \right\} \quad (\text{D.6})$$

subject to  $\text{Tr}(\Lambda_{P_0^{\bar{q}}}) + \text{Tr}(\Lambda_{P_1^q}) + \text{Tr}(\Lambda_{P_1^{\bar{q}}}) \leq P$ , in which

$$\mathbf{C}'_{DF} = \begin{bmatrix} \Lambda_{P_0^{\bar{q}}}\Lambda_{|\mathcal{H}_{SD}^{\bar{q}}|^2} & 0 & 0 \\ 0 & \Lambda_{C^{\bar{q}*}} & 0 \\ 0 & 0 & \Lambda_{C^{\bar{q}*}} \end{bmatrix}, \quad (\text{D.7})$$

and

$$\mathbf{D}'_{DF} = \begin{bmatrix} \Lambda_{\sigma_{\mathbf{v}_{SD}^{\bar{q}}}^2} & 0 & 0 \\ 0 & \Lambda_{D^{\bar{q}*}} & 0 \\ 0 & 0 & \Lambda_{D^{\bar{q}*}} \end{bmatrix}, \quad (\text{D.8})$$

where  $\Lambda_{C^{\bar{q}*}}$ ,  $\Lambda_{D^{\bar{q}*}}$ ,  $\Lambda_{C^{\bar{q}*}}$ , and  $\Lambda_{D^{\bar{q}*}}$  are given by (2.24), (2.25), (2.46), and (2.47), respectively.

### Appendix E – Achievable Data Rate: The HSRC without $R^q$

Figure 27 shows the HSRC without  $R^q$  in which the missed links due to the  $R^q$  loss are highlighted in red as well as the respective communication interface. Using (2.8) and (2.10), the received symbol of this kind of incomplete HSRC assuming AF can be expressed as (E.1). Furthermore, it is considered that  $P_0^q$  is allocated only to the  $SD^q$  link and  $P_1^{\bar{q}} = P_R$ .

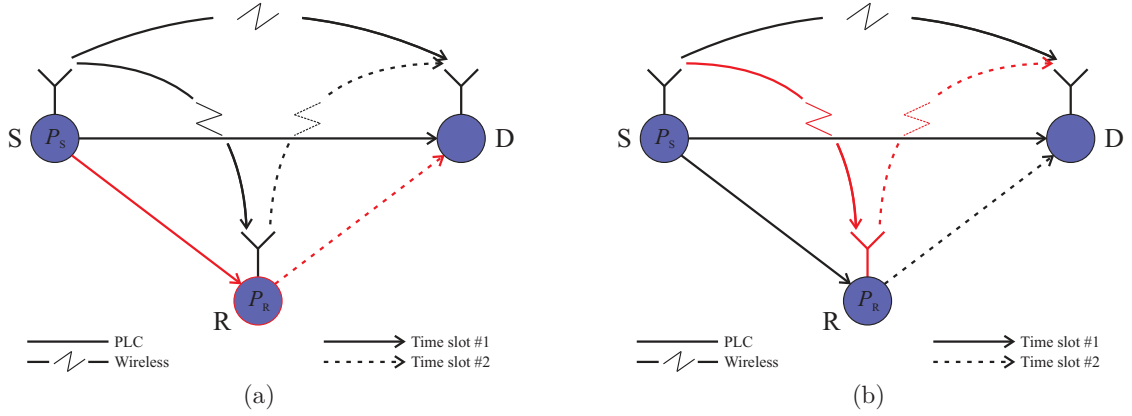


Figure 27: The HSRC without  $R^q$ , for (a)  $q = P$  and (b)  $q = W$ .

$$\begin{aligned}
\mathbf{Y} &= \begin{bmatrix} \mathbf{Y}_{SD}^{\bar{q}} \\ \mathbf{Y}_{SRD,AF}^{\bar{q}} \\ \mathbf{Y}_{SD}^q \end{bmatrix} \\
&= \begin{bmatrix} \mathcal{H}_{SD}^{\bar{q}} & 0 & 0 \\ 0 & \mathcal{H}_{SR}^{\bar{q}} \mathcal{H}_{RD}^{\bar{q}} & 0 \\ 0 & 0 & \mathcal{H}_{SD}^q \end{bmatrix} \begin{bmatrix} \Lambda \sqrt{P_0^{\bar{q}}} \mathbf{X} \\ \Lambda \sqrt{P_0^{\bar{q}}} \Lambda \sqrt{P_1^{\bar{q}}} \Lambda_{\sigma_{\mathbf{Y}_{SR}^{\bar{q}}}}^{-1} \mathbf{X} \\ \Lambda \sqrt{P_0^q} \mathbf{X} \end{bmatrix} + \begin{bmatrix} \mathbf{V}_{SD}^{\bar{q}} \\ \Lambda \sqrt{P_1^{\bar{q}}} \mathcal{H}_{RD}^{\bar{q}} \Lambda_{\sigma_{\mathbf{Y}_{SR}^{\bar{q}}}}^{-1} \mathbf{V}_{SR}^{\bar{q}} + \mathbf{V}_{RD}^{\bar{q}} \\ \mathbf{V}_{SD}^q \end{bmatrix} \\
&= \begin{bmatrix} \mathcal{H}_{SD}^{\bar{q}} \Lambda \sqrt{P_0^{\bar{q}}} \\ \mathcal{H}_{SR}^{\bar{q}} \mathcal{H}_{RD}^{\bar{q}} \Lambda \sqrt{P_0^{\bar{q}}} \Lambda \sqrt{P_1^{\bar{q}}} \Lambda_{\sigma_{\mathbf{Y}_{SR}^{\bar{q}}}}^{-1} \\ \mathcal{H}_{SD}^q \Lambda \sqrt{P_0^q} \end{bmatrix} \mathbf{X} + \begin{bmatrix} \mathbf{I}_N & 0 & 0 & 0 \\ 0 & \Lambda \sqrt{P_1^{\bar{q}}} \mathcal{H}_{RD}^{\bar{q}} \Lambda_{\sigma_{\mathbf{Y}_{SR}^{\bar{q}}}}^{-1} & \mathbf{I}_N & 0 \\ 0 & 0 & 0 & \mathbf{I}_N \end{bmatrix} \mathbf{V} \\
&= \mathbf{A}' \mathbf{X} + \mathbf{B}' \mathbf{V},
\end{aligned} \tag{E.1}$$

where  $\mathbf{V} = [\mathbf{V}_{SD}^{\bar{q}T} \mathbf{V}_{SR}^{\bar{q}T} \mathbf{V}_{RD}^{\bar{q}T} \mathbf{V}_{SD}^{qT}]^T$ . Making  $\mathbf{C}'_{AF} = \mathbf{A}' \mathbf{R}_{\mathbf{X}\mathbf{X}} \mathbf{A}'^\dagger$  and  $\mathbf{D}'_{AF} = \mathbf{B}' \mathbf{R}_{\mathbf{V}\mathbf{V}} \mathbf{B}'^\dagger$ . Thus, from (2.13), it results that

$$I(\mathbf{X}, \mathbf{Y}) = \log_2 \left[ \det(\mathbf{I}_{3N} + \mathbf{C}'_{AF} \mathbf{D}'_{AF}^{-1}) \right], \tag{E.2}$$

in which

$$\mathbf{C}'_{AF} = \begin{bmatrix} \Lambda_{P_0^q} \Lambda_{|\mathcal{H}_{SD}^q|}^2 & 0 & 0 \\ 0 & \Lambda_{P_0^q} \Lambda_{P_1^q} \Lambda_{\sigma_{\mathbf{Y}_{SR}^q}}^{-1} \Lambda_{|\mathcal{H}_{SR}^q|}^2 \Lambda_{|\mathcal{H}_{RD}^q|}^2 & 0 \\ 0 & 0 & \Lambda_{P_0^q} \Lambda_{|\mathcal{H}_{SD}^q|}^2 \end{bmatrix} \quad (\text{E.3})$$

$$\mathbf{D}'_{AF} = \begin{bmatrix} \Lambda_{\sigma_{\mathbf{V}_{SD}^q}}^2 & 0 & 0 \\ 0 & \Lambda_{|\mathcal{H}_{RD}^q|}^2 \Lambda_{P_1^q} \Lambda_{\sigma_{\mathbf{Y}_{SR}^q}}^{-1} \Lambda_{\sigma_{\mathbf{V}_{SR}^q}}^2 + \Lambda_{\sigma_{\mathbf{V}_{RD}^q}}^2 & 0 \\ 0 & 0 & \Lambda_{\sigma_{\mathbf{V}_{SD}^q}}^2 \end{bmatrix} \quad (\text{E.4})$$

It is important to point out that for the HSRC without  $SR^q$  and  $RD^q$ , the same matrices  $\mathbf{C}'_{AF}$  and  $\mathbf{D}'_{AF}$  are obtained as for the HSRC without  $R^q$  because the matrices  $\Lambda_{\sigma_{\mathbf{V}_{SR}^q}}^2$  and  $\Lambda_{\sigma_{\mathbf{V}_{RD}^q}}^2$  appear at the same positions in  $\mathbf{D}_{AF}$ , canceling the same elements. Thus, the difference among the loss of  $R^q$  and the loss of  $SR^q$  and  $RD^q$  is the power allocation assumption.

Finally, for the AF protocol, the achievable data rate of this incomplete HSRC is expressed as

$$C_{AF} = \mathbb{E}_{\mathbf{H}_\ell^P, \mathbf{H}_\ell^W} \left\{ \max_{\Lambda_P} \frac{B_W}{N} \log_2 [\det(\mathbf{I}_{3N} + \mathbf{C}'_{AF} \mathbf{D}'_{AF}^{-1})] \right\} \quad (\text{E.5})$$

subject to  $\text{Tr}(\Lambda_{P_0^q}) + \text{Tr}(\Lambda_{P_0^q}) + \text{Tr}(\Lambda_{P_1^q}) \leq P$ . Similarly, for the DF protocol, the achievable data rate is given by

$$C_{DF} = \mathbb{E}_{\mathbf{H}_\ell^P, \mathbf{H}_\ell^W} \left\{ \max_{\Lambda_P} \frac{B_W}{N} \log_2 [\det(\mathbf{I}_{3N} + \mathbf{C}'_{DF} \mathbf{D}'_{DF}^{-1})] \right\} \quad (\text{E.6})$$

subject to  $\text{Tr}(\Lambda_{P_0^q}) + \text{Tr}(\Lambda_{P_0^q}) + \text{Tr}(\Lambda_{P_1^q}) \leq P$ , in which

$$\mathbf{C}'_{DF} = \begin{bmatrix} \Lambda_{P_0^q} \Lambda_{|\mathcal{H}_{SD}^q|}^2 & 0 & 0 \\ 0 & \Lambda_{C^q} & 0 \\ 0 & 0 & \Lambda_{P_0^q} \Lambda_{|\mathcal{H}_{SD}^q|}^2 \end{bmatrix}, \quad (\text{E.7})$$

and

$$\mathbf{D}'_{DF} = \begin{bmatrix} \Lambda_{\sigma_{\mathbf{V}_{SD}^q}}^2 & 0 & 0 \\ 0 & \Lambda_{D^q} & 0 \\ 0 & 0 & \Lambda_{\sigma_{\mathbf{V}_{SD}^q}}^2 \end{bmatrix}, \quad (\text{E.8})$$

where  $\Lambda_{C^q}$  and  $\Lambda_{D^q}$  are given by (2.24) and (2.25), respectively.

### Appendix F – Achievable Data Rate: The HSRC without $D^q$

Figure 28 shows the HSRC without  $D^q$  in which the missed links due to the  $D^q$  loss are highlighted as well as the respective communication interface. Using (2.8) and (2.10), the received symbol of this incomplete HSRC assuming the AF protocol can be expressed as (F.1).

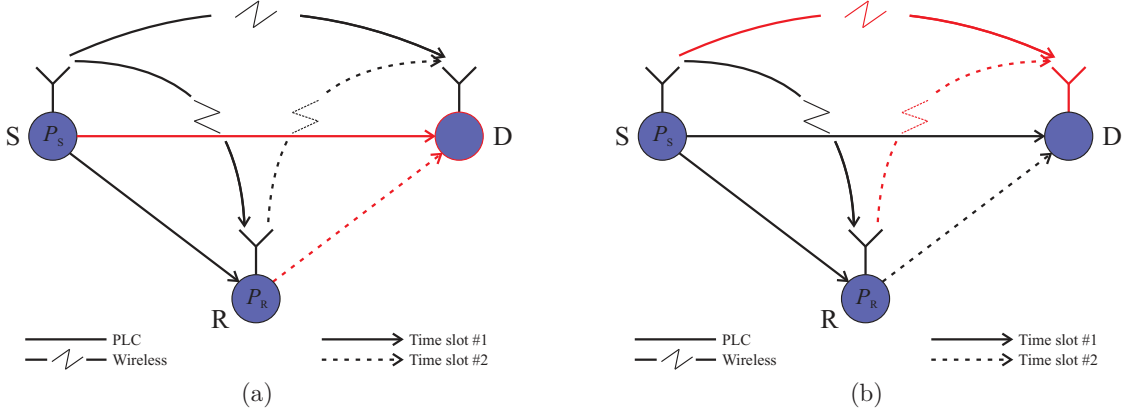


Figure 28: The HSRC without  $D^q$ , for (a)  $q = P$  and (b)  $q = W$ .

$$\begin{aligned}
 \mathbf{Y} &= \begin{bmatrix} \mathbf{Y}_{SD}^{\bar{q}} \\ \mathbf{Y}_{SRD,AF}^{\bar{q}} \end{bmatrix} \\
 &= \begin{bmatrix} \mathcal{H}_{SD}^{\bar{q}} & 0 \\ 0 & \mathcal{H}_{SR}^{\bar{q}} \mathcal{H}_{RD}^{\bar{q}} \end{bmatrix} \begin{bmatrix} \Lambda \sqrt{P_0^{\bar{q}}} \mathbf{X} \\ \Lambda \sqrt{P_0^{\bar{q}}} \Lambda \sqrt{P_1^{\bar{q}}} \Lambda_{\sigma_{\mathbf{Y}_{SR}^{\bar{q}}}}^{-1} \mathbf{X} \end{bmatrix} + \begin{bmatrix} \mathbf{V}_{SD}^{\bar{q}} \\ \Lambda \sqrt{P_1^{\bar{q}}} \mathcal{H}_{RD}^{\bar{q}} \Lambda_{\sigma_{\mathbf{Y}_{SR}^{\bar{q}}}}^{-1} \mathbf{V}_{SR}^{\bar{q}} + \mathbf{V}_{RD}^{\bar{q}} \end{bmatrix} \\
 &= \begin{bmatrix} \mathcal{H}_{SD}^{\bar{q}} \Lambda \sqrt{P_0^{\bar{q}}} \\ \mathcal{H}_{SR}^{\bar{q}} \mathcal{H}_{RD}^{\bar{q}} \Lambda \sqrt{P_0^{\bar{q}}} \Lambda \sqrt{P_1^{\bar{q}}} \Lambda_{\sigma_{\mathbf{Y}_{SR}^{\bar{q}}}}^{-1} \end{bmatrix} \mathbf{X} + \begin{bmatrix} \mathbf{I}_N & 0 & 0 \\ 0 & \Lambda \sqrt{P_1^{\bar{q}}} \mathcal{H}_{RD}^{\bar{q}} \Lambda_{\sigma_{\mathbf{Y}_{SR}^{\bar{q}}}}^{-1} & \mathbf{I}_N \end{bmatrix} \mathbf{V} \\
 &= \mathbf{A}' \mathbf{X} + \mathbf{B}' \mathbf{V},
 \end{aligned} \tag{F.1}$$

where  $\mathbf{V} = [\mathbf{V}_{SD}^{\bar{q}T} \mathbf{V}_{SR}^{\bar{q}T} \mathbf{V}_{RD}^{\bar{q}T}]^T$ . Making  $\mathbf{C}'_{AF} = \mathbf{A}' \mathbf{R}_{\mathbf{X}\mathbf{X}} \mathbf{A}'^\dagger$  and  $\mathbf{D}'_{AF} = \mathbf{B}' \mathbf{R}_{\mathbf{V}\mathbf{V}} \mathbf{B}'^\dagger$ . Thus, from (2.13), it results that

$$I(\mathbf{X}, \mathbf{Y}) = \log_2 \left[ \det(\mathbf{I}_{2N} + \mathbf{C}'_{AF} \mathbf{D}'_{AF}{}^{-1}) \right], \tag{F.2}$$

in which

$$\mathbf{C}'_{AF} = \begin{bmatrix} \Lambda_{P_0^{\bar{q}}} \Lambda_{|\mathcal{H}_{SD}^{\bar{q}}|^2} & 0 \\ 0 & \Lambda_{P_0^{\bar{q}}} \Lambda_{P_1^{\bar{q}}} \Lambda_{\sigma_{\mathbf{Y}_{SR}^{\bar{q}}}^2}^{-1} \Lambda_{|\mathcal{H}_{SR}^{\bar{q}}|^2} \Lambda_{|\mathcal{H}_{RD}^{\bar{q}}|^2} \end{bmatrix} \tag{F.3}$$

$$\mathbf{D}'_{AF} = \begin{bmatrix} \Lambda_{\mathbf{v}_{SD}^{\bar{q}}} \sigma^2 & 0 \\ 0 & \Lambda_{|\mathcal{H}_{RD}^{\bar{q}}|^2} \Lambda_{P_1^{\bar{q}}} \Lambda_{\mathbf{y}_{SR}^{\bar{q}}}^{-1} \Lambda_{\mathbf{v}_{SR}^{\bar{q}}} \sigma^2 + \Lambda_{\mathbf{v}_{RD}^{\bar{q}}} \sigma^2 \end{bmatrix} \quad (\text{F.4})$$

Finally, for the AF protocol, the achievable data rate of this incomplete HSRC is expressed as

$$C_{AF} = \mathbb{E}_{\mathbf{H}_\ell^{\bar{q}}} \left\{ \max_{\Lambda_P} \frac{B_W}{N} \log_2 [\det(\mathbf{I}_{2N} + \mathbf{C}'_{AF} \mathbf{D}'_{AF}{}^{-1})] \right\} \quad (\text{F.5})$$

subject to  $\text{Tr}(\Lambda_{P_0^{\bar{q}}}) + \text{Tr}(\Lambda_{P_1^{\bar{q}}}) \leq P$ . On the other hand, for the DF protocol, the achievable data rate is given by

$$C_{DF} = \mathbb{E}_{\mathbf{H}_\ell^{\bar{q}}} \left\{ \max_{\Lambda_P} \frac{B_W}{N} \log_2 [\det(\mathbf{I}_{2N} + \mathbf{C}'_{DF} \mathbf{D}'_{DF}{}^{-1})] \right\} \quad (\text{F.6})$$

subject to  $\text{Tr}(\Lambda_{P_0^{\bar{q}}}) + \text{Tr}(\Lambda_{P_1^{\bar{q}}}) \leq P$ , in which

$$\mathbf{C}'_{DF} = \begin{bmatrix} \Lambda_{P_0^{\bar{q}}} \Lambda_{|\mathcal{H}_{SD}^{\bar{q}}|^2} & 0 \\ 0 & \Lambda_{C^{\bar{q}*}} \end{bmatrix}, \quad (\text{F.7})$$

and

$$\mathbf{D}'_{DF} = \begin{bmatrix} \Lambda_{\mathbf{v}_{SD}^{\bar{q}}} \sigma^2 & 0 \\ 0 & \Lambda_{D^{\bar{q}*}} \end{bmatrix}, \quad (\text{F.8})$$

where  $\Lambda_{C^{\bar{q}*}}$  and  $\Lambda_{D^{\bar{q}*}}$  are given by (2.24) and (2.25), respectively.

## Appendix G – Publications

The list of journal papers under preparation, written, or submitted during the graduate period is as follows:

- V. Fernandes, W. A. Finamore, H. Vincent Poor, and M. V. Ribeiro, “Low-bit rate hybrid PLC-wireless single-relay channel: Achievable data rate and outage behavior,” *IEEE Transactions on Communications*, 2016, under review.
- V. Fernandes, H. Vincent Poor, and M. V. Ribeiro, “Incomplete low-bit rate hybrid PLC-wireless single-relay channel: Achievable data rate,” *IEEE Transactions on Communications*, 2016, under review.
- L. M. B. A. Dib, V. Fernandes, M. L. Filomeno and M. V. Ribeiro, “Hybrid PLC-wireless communication for smart grids and internet of things applications,” *IEEE Internet of Things Journal*, 2016, under review.
- V. Fernandes, H. Vincent Poor, and M. V. Ribeiro, “Incomplete low-bit rate hybrid PLC-wireless single-relay channel: Outage analysis,” *IEEE Transactions on Communications*, under preparation.

The list of conference papers published during the graduate period is as follows:

- V. Fernandes, M. L. Filomeno, W. A. Finamore, and M. V. Ribeiro, “An investigation on narrow band PLC-wireless parallel channel capacity,” in *Proc. XXXIV Simpósio Brasileiro de Telecomunicações*, Sep. 2016, pp. 834-838.
- L. M. B. A. Dib, V. Fernandes, and M. V. Ribeiro, “A discussion about hybrid PLC-wireless communication for smart grids,” in *Proc. XXXIV Simpósio Brasileiro de Telecomunicações*, Sep. 2016, pp. 848-852.
- M. L. Filomenos, V. Fernandes, and M. V. Ribeiro, “Análise estatística da capacidade de canais PLC residenciais cooperativos baseada no modelo single relay channel,” in *Proc. XXXIV Simpósio Brasileiro de Telecomunicações*, Sep. 2016, pp. 843-847.
- V. Fernandes, S. Angelova, W. A. Finamore, and M. V. Ribeiro, “On modeling power-line communication noise,” in *Proc. XXXIII Simpósio Brasileiro de Telecomunicações*, Sep. 2015.
- G. R. Colen, T. M. Peixoto, V. Fernandes, and M. V. Ribeiro, “A frequency domain resource allocation technique with reduced complexity for PLC system,” in *Proc. XXXIII Simpósio Brasileiro de Telecomunicações*, Sep. 2015.